

1 **Impact of dust addition on Mediterranean plankton**

Formatted: Indent: First line: 1.27 cm

Deleted: enrichment

2 **communities under present and future conditions of pH and**

3 **temperature: an experimental overview**

4 Frédéric Gazeau<sup>1</sup>, Céline Ridame<sup>2</sup>, France Van Wambeke<sup>3</sup>, Samir Alliouane<sup>1</sup>, Christian Stolpe<sup>1</sup>,

5 Jean-Olivier Irisson<sup>1</sup>, Sophie Marro<sup>1</sup>, Jean-Michel Grisoni<sup>4</sup>, Guillaume De Liège<sup>4</sup>, Sandra

6 Nunige<sup>3</sup>, Kahina Djaoudi<sup>3</sup>, Elvira Pulido-Villena<sup>3</sup>, Julie Dinasquet<sup>5,6</sup>, Ingrid Obernosterer<sup>6</sup>,

7 Philippe Catala<sup>6</sup>, Cécile Guieu<sup>1</sup>

8 <sup>1</sup> Sorbonne Université, CNRS, Laboratoire d'Océanographie de Villefranche, LOV, 06230

9 Villefranche-sur-Mer, France

10 <sup>2</sup> CNRS-INSU/IRD/MNHN/UPMC, LOCEAN: Laboratoire d'Océanographie et du Climat:

11 Expérimentation et Approches Numériques, UMR 7159, 75252 Paris Cedex 05, France

12 <sup>3</sup> Aix-Marseille Université, Université de Toulon, CNRS/INSU, IRD, MIO, UM 110, 13288,

13 Marseille, France

14 <sup>4</sup> Sorbonne Université, CNRS, Institut de la Mer de Villefranche, IMEV, 06230 Villefranche-sur-

15 Mer, France

16 <sup>5</sup> Scripps Institution of Oceanography, University of California San Diego, USA

17 <sup>6</sup> CNRS, Sorbonne Université, Laboratoire d'Océanographie Microbienne, LOMIC, F-66650

18 Banyuls-sur-Mer, France

19 Correspondence to: Frédéric Gazeau ([f.gazeau@obs-vlfr.fr](mailto:f.gazeau@obs-vlfr.fr))

20 Keywords: Mediterranean Sea; Atmospheric deposition; Plankton community; Ocean

21 acidification; Ocean warming

## 23 Abstract

24 In Low Nutrient Low Chlorophyll areas, such as the Mediterranean Sea, atmospheric  
25 fluxes represent a considerable external source of nutrients likely supporting primary production  
26 especially during stratification periods. These areas are expected to expand in the future due to  
27 lower nutrient supply from sub-surface waters caused by ~~climate-driven enhanced stratification~~,  
28 likely further increasing the role of atmospheric deposition as a source of new nutrients to  
29 surface waters. Yet, whether plankton communities will react differently to dust deposition in a  
30 warmer and acidified environment remains an open question. The ~~potential~~ impact of dust  
31 deposition both in present and future climate conditions was ~~investigated~~ through three  
32 perturbation experiments in the open Mediterranean Sea. Climate reactors (300 L) were filled  
33 with surface water collected in the Tyrrhenian Sea, Ionian Sea and in the Algerian basin during a  
34 cruise conducted in May/June 2017 in the frame of the PEACETIME project. The experimental  
35 protocol comprised two unmodified control tanks, two tanks enriched with a Saharan dust analog  
36 and two tanks enriched with the dust analog and maintained under warmer (+3 °C) and acidified  
37 (-0.3 pH unit) conditions. Samples for the analysis of an extensive number of biogeochemical  
38 parameters and processes were taken over the duration of the experiments (3-4 d). Here, we  
39 present the general setup of the experiments and the impacts of dust seeding ~~with and without~~  
40 ~~addressing the effects of environmental changes~~ on nutrients and biological stocks. Dust addition  
41 led to a rapid and maximum input of nitrate whereas phosphate release from the dust analog was  
42 much smaller. Our results showed that the impacts of Saharan dust deposition in three different  
43 basins of the open Northwestern Mediterranean Sea are at least as strong as those observed  
44 previously in coastal waters. However, interestingly, the effects of dust deposition on biological  
45 stocks were highly different between the three investigated stations and could not be attributed to  
46 differences in their degree of oligotrophy but rather to the initial metabolic state of the  
47 community. ~~O~~cean acidification and warming did not drastically modify the composition of the

Deleted: enhanced stratification

Deleted: assessed

Deleted: and/or future climate change scenario

Formatted: English (US)

Deleted: Finally,

Formatted: English (US)

Deleted: o

53 autotrophic assemblage with all groups positively impacted by warming and acidification.

Formatted: English (US)

54 ~~Although autotrophic biomass was more positively impacted than heterotrophic biomass under~~

Formatted: English (US)

55 ~~future environmental conditions, a stronger impact of warming and acidification on~~

Formatted: English (US)

56 ~~mineralization processes suggests a decreased capacity of Mediterranean surface plankton~~

57 ~~communities to sequester atmospheric CO<sub>2</sub> following the deposition of atmospheric particles.~~

Formatted: English (US)

Deleted: , suggesting an exacerbation of effects from atmospheric dust deposition in the future.

## 60 1. Introduction

61 Atmospheric deposition is well recognized as a significant source of micro- and macro-  
62 nutrients for surface waters of the global ocean (Duce et al., 1991; Jickells et al., 2005; Moore et  
63 al., 2013). The potential modulation of the biological carbon pump efficiency and the associated  
64 export of carbon by atmospheric deposition events are still poorly understood and quantified  
65 (Law et al., 2013). This is especially true for Low Nutrient Low Chlorophyll (LNLC) areas  
66 where atmospheric fluxes can play a considerable role in nutrient cycling and that represent 60%  
67 of the global ocean surface area (Longhurst et al., 1995) as well as 50% of global carbon export  
68 (Emerson et al., 1997). These regions are characterized by a low availability of macronutrients  
69 (N, P) and/or metal micronutrients (e.g. Fe) that can severely limit or co-limit phytoplankton  
70 growth during large periods of year.

71 The Mediterranean Sea is a **typical** example of these LNLC regions and exhibits **surface**  
72 chlorophyll *a* concentrations **below** 0.2  $\mu\text{g L}^{-1}$  all year round over most of its area, except in the  
73 Ligurian Sea where relatively large blooms can be observed in late winter-early spring (e.g.  
74 Mayot et al., 2016). Recent assessments showed that the atmospheric input of nutrients in the  
75 Mediterranean Sea is of the same order of magnitude as riverine inputs (Powley et al., 2017),  
76 making the atmosphere a considerable external source of nutrients (Richon et al., 2018).  
77 **Atmospheric deposition originates both from natural (mainly Saharan dust) and anthropogenic**  
78 **sources** (e.g. Bergametti et al., 1989; Desboeufs et al., 2018). **Dust deposition, mostly in the form**  
79 **of pulsed inputs, is mainly associated with wet deposition** (Loÿe-Pilot and Martin, 1996). Ternon  
80 et al. (2010) reported an average annual dust flux over four years of 11.4  $\text{g m}^{-2} \text{yr}^{-1}$  (average  
81 during the period 2003–2007) at the DYFAMED station in the Northwestern Mediterranean Sea.  
82 In this region, the most important events reported in the 2010 decade amounted to  $\sim 22 \text{ g m}^{-2}$   
83 (Bonnet and Guieu, 2006; Guieu et al., 2010b).

Deleted:

Deleted: perfect

Formatted: English (US)

Deleted: of less than

Formatted: English (US)

Deleted:

Moved (insertion) [1]

Formatted: English (US)

Deleted: Atmospheric depositions are mostly in the form of pulsed inputs of aerosols from both natural (Saharan dust) and anthropogenic origins (e.g. Bergametti et al., 1989; Desboeufs et al., 2018). Dust deposition is mainly associated with wet deposition and occurs in the form of extreme even

Moved up [1]: (e.g. Bergametti et al., 1989; Desboeufs et al., 2018).

Deleted: on

96 Atmospheric deposition provides new nutrients to the surface waters (Guieu et al., 2010b;  
97 Kouvarakis et al., 2001; Markaki et al., 2003; Ridame and Guieu, 2002), Fe (Bonnet and Guieu,  
98 2006) and other trace metals (Desboeufs et al., 2018; Guieu et al., 2010b; Theodosi et al., 2010),  
99 that represent significant inputs likely supporting the primary production especially during the  
100 stratification period (Bonnet et al., 2005; Ridame and Guieu, 2002), although no clear correlation  
101 between dust and ocean color could be evidenced from long series of satellite observation in that  
102 part of the basin (Guieu and Ridame, 2020).

103 Experimental approaches have shown that wet dust deposition events in the Northwestern  
104 Mediterranean Sea (the dominant deposition mode in that basin) present a higher impact as a  
105 source of bioavailable fertilizing nutrients compared to dry deposition. Indeed, wet deposition  
106 provides both new N and P while dry deposition supplies only P and does not allow to stimulate  
107 the autotrophic community, (except diazotrophs; Ridame et al., 2013), resulting in no increase in  
108 chlorophyll *a* concentrations and primary production (Guieu et al., 2014a). This so-called  
109 fertilizing effect has been experimentally shown using both micro- and mesocosms where the  
110 wet deposition of Saharan dust analog strongly stimulated primary production and phytoplankton  
111 biomass (Guieu et al., 2014a; Ridame et al., 2014) while also modifying phytoplankton diversity  
112 (Giovagnetti et al., 2013; Lekunberri et al., 2010; Romero et al., 2011). In addition, besides  
113 phytoplankton, dust deposition also modified also the bacterial community assemblage and led to  
114 even stronger enhancements of production and/or respiration rates (Pulido-Villena et al., 2014).  
115 The carbon budget established from four artificial seeding experiments during the DUNE project  
116 (Guieu et al., 2014a) showed that by stimulating predominantly heterotrophic bacteria,  
117 atmospheric dust deposition can enhance the heterotrophic biological behavior of these  
118 oligotrophic waters. This has the potential to reduce the fraction of organic carbon that can be  
119 exported to deep waters during the winter mixing period (Pulido-Villena et al., 2008) and  
120 ultimately limit net atmospheric CO<sub>2</sub> drawdown.

Deleted:

Formatted: Indent: First line: 1.27 cm

Formatted: French

Field Code Changed

Deleted: →

Formatted: English (US)

Formatted: Font: Italic

Formatted: English (US)

Formatted: English (US)

Deleted: Experimental approaches have shown that wet dust deposition events in the Northwestern Mediterranean Sea (the dominant deposition mode in that basin) present a highest positive impact, by supplying bioavailable new nutrients, compared to dry deposition on all tested parameters and processes (Guieu et al., 2014a), except for N<sub>2</sub> fixation (Ridame et al., 2014).

Formatted: English (US)

Deleted: cosms or

Deleted: but also modified

Deleted: the

Deleted: However

Formatted: English (US)

Deleted: s

135 Another effect induced by Saharan dust deposition is the export of particulate organic  
 136 carbon (POC), as lithogenic particles can aggregate and ballast dissolved organic matter (Bressac  
 137 et al., 2014; Desboeufs et al., 2014; Louis et al., 2017a; Ternon et al., 2010). This so-called  
 138 lithogenic carbon pump can represent a major part of the carbon export following a dust  
 139 deposition event (up to 50% during the DUNE experiment; Bressac et al., 2014). Recently, Louis  
 140 et al. (2017a) showed that Saharan dust deposition triggers the abiotic formation of transparent  
 141 exopolymeric particles (TEP), leading to the formation of organic-mineral aggregates, a  
 142 formation process that is highly dependent on the quality and quantity of TEP-precursors initially  
 143 present in seawater.

Formatted: French

144 In response to ocean warming and increased stratification, nutrient cycling in the open  
 145 ocean is being and will continue to be perturbed in the next decades, resulting very likely in  
 146 regionally variable impacts (IPCC, 2019). Overall, LNLC areas are expected to expand in the  
 147 future (Irwin and Oliver, 2009; Polovina et al., 2008) due to a thermal stratification related  
 148 reduction of nutrients supply from sub-surface waters (Behrenfeld et al., 2006). As such, the role  
 149 of atmospheric deposition might increase as an alternative source of new nutrients to surface  
 150 waters. Ongoing warming and acidification of the global ocean (IPCC, 2019) are also evidenced  
 151 in the Mediterranean Sea (e.g. Kapsenberg et al., 2017; The Mermex group, 2011). Whether or  
 152 not plankton communities will respond differently to dust deposition in future conditions is still  
 153 largely unknown. Although dependent on resource availability, it is well known that  
 154 remineralisation by bacteria is subject to positive temperature control (López-Urrutia and Morán,  
 155 2007). As under severe nutrient limitation, warming has no effect on primary productivity  
 156 (Marañón et al., 2018), it will most likely further push the balance towards net heterotrophy in  
 157 oligotrophic areas.

Deleted: open ocean

Deleted: cycles

Deleted: are

Deleted: with a high confidence of having regionally variable impacts on primary producers

Deleted: very likely

Deleted: ing very likely

Deleted: lower

Deleted: ,

Deleted: likely further

Deleted: increasing the role of

Deleted: a

Deleted: significant

Deleted: The o

Deleted: , both

Deleted: raise the question on whether plankton communities will react differently to dust deposition in a warmer and acidified environment

Formatted: English (US)

Deleted: U

Formatted: English (US), Not Highlight

Deleted: there is no evidence that

Deleted: will lead to an enhancement of

Formatted: English (US), Not Highlight

Deleted:

Formatted: Not Highlight

Deleted: ing

158 With respect to ocean acidification, an *in situ* mesocosm experiment conducted during  
 159 the summer stratified period in the Northwestern Mediterranean Sea showed that the plankton

183 community was rather insensitive to this perturbation under strong nutrient limitation  
184 (Maugendre et al., 2017, and references therein). This is coherent with results from Maugendre et  
185 al. (2015), based on a batch experiment, showing that, under nutrient-depleted conditions in late  
186 winter, ocean acidification has a very limited impact on the plankton community and that small  
187 species (e.g. Cyanobacteria) might benefit from warming with a potential decrease of the export  
188 and energy transfer to higher trophic levels. In contrast, in more eutrophic coastal conditions,  
189 Sala et al. (2016) showed that ocean acidification exerted a positive effect on phytoplankton,  
190 especially on pico- and nano-phytoplankton. Similarly, Neale et al. (2014) showed in a coastal  
191 ecosystem of the Alboran Sea that ocean acidification could lead, although moderately, to high  
192 chlorophyll levels under low light conditions with an opposite effect under high irradiance.

193 To date and to the best of our knowledge, there ~~have~~ been no attempts to evaluate the  
194 behavior of plankton communities after the deposition of atmospheric particles in the context of  
195 future levels of temperature and pH. Yet, following the recommendation from Maugendre et al.  
196 (2017), any perturbation experiment for future climate conditions in the Mediterranean Sea  
197 should consider atmospheric deposition as a source of new nutrients and consider both  
198 temperature and pH as external forcings. Such experiments were conducted in the frame of the  
199 PEACETIME project (ProcEss studies at the Air-sEa Interface after dust deposition in the  
200 MEditerranean sea; <http://peacetime-project.org/>) during the cruise on board the R/V “Pourquoi  
201 Pas?” in May/June 2017. The project aimed at extensively studying and parameterizing the chain  
202 of processes occurring in the Mediterranean Sea after atmospheric deposition, and to put them in  
203 perspective of on-going environmental changes (Guieu et al., 2020). During that cruise, three  
204 perturbation experiments were conducted in climate reactors (300 L tanks) filled with surface  
205 water collected in the Tyrrhenian Sea (TYR), Ionian Sea (ION) and in the Algerian basin (FAST;  
206 Fig. 1). Six tanks were used to follow simultaneously and with a high temporal resolution, the  
207 evolution of biological activity and stocks, nutrients stocks, dissolved organic matter as well as

Formatted: English (US)

Deleted: s

Deleted: , especially of Saharan dust,

210 particles dynamics and export, following a dust deposition event simulated at their surface, both  
211 under present environmental conditions and following a realistic climate change scenario for  
212 2100 (ca. +3 °C and -0.3 pH units; IPCC, 2013). In this manuscript, we will present the general  
213 setup of the experiments ~~and the evolution of nutrient and biological stocks (heterotrophic and~~  
214 ~~autotrophic prokaryotes, photosynthetic eukaryotes as well as micro- and meso-zooplankton).~~  
215 ~~Several other manuscripts, related to these experiments and currently submitted to or published~~  
216 ~~in this special issue, focus on plankton metabolism (primary production, heterotrophic~~  
217 ~~prokaryote production) and carbon export (Gazeau et al., 2021), on the microbial food web~~  
218 ~~(Dinasquet et al., 2021), on nitrogen fixation (Céline Ridame, unpublished results) and on the~~  
219 ~~release of insoluble elements (Fe, Al, REE, Th, Pa) from dust (Roy-Barman et al., 2020).~~

**Deleted:** , the impacts of dust seeding and/or future climate change scenario on

**Deleted:** s

**Formatted:** English (US)

**Deleted:** Among several

**Deleted:** currently

**Formatted:** English (US), Not Highlight

**Formatted:** English (US), Not Highlight

**Formatted:** English (US), Not Highlight

**Formatted:** Not Highlight

**Deleted:** that are introduced here, a companion paper will be ...

**Deleted:** ing

**Deleted:** as well as on carbon budget

**Formatted:** English (US)

**Deleted:** (Ridame et al., in preparation)

**Deleted:** !



## 231 2. Material and Methods

### 232 2.1. General setup

233 Six experimental tanks (300 L; Fig. 2), in which the irradiance spectrum and intensity can  
234 be finely controlled and in which future ocean acidification and warming conditions can be fully  
235 reproduced, were installed in a temperature-controlled container. The tanks are made of high-  
236 density polyethylene (HDPE) and ~~are~~ trace-metal free in order to avoid contaminations, with a  
237 height of 1.09 m, a diameter of 0.68 m, a surface area of 0.36 m<sup>2</sup> and a volume of 0.28 m<sup>3</sup>. All  
238 tanks were cleaned before the experimental work following the protocol described by Bressac  
239 and Guieu (2013). A weak turbulence was generated by a rotating PVC blade (9 rpm) in order to  
240 mimic natural conditions. Each tank was equipped with a lid containing six rows of LEDs  
241 (Alpheus©). Each of these rows were composed of blue, green, cyan and white units in order to  
242 mimic the natural sun spectrum. At the conical base of each tank, a polyethylene (PE) bottle  
243 collecting the exported material from above was screwed onto a polyvinyl chloride (PVC) valve  
244 that remained open during the duration of the whole experiment. Photosynthetically active  
245 radiation (PAR; 400-700 nm) and temperature were continuously monitored in each tank using  
246 respectively QSL-2100 Scalar PAR Irradiance Sensors (Biospherical Instruments©) and pt1000  
247 temperature sensors (Metrohm©) connected to a D230 datalogger (Consort©).

248 The experimental protocol comprised two unmodified control tanks (C1 and C2), two  
249 tanks enriched with Saharan dust (D1 and D2) and two tanks enriched with Saharan dust and  
250 maintained under warmer (+3 °C) and acidified (-0.3 pH unit) conditions (G1 and G2). The  
251 atmosphere above tanks C1, C2, D1 and D2 was flushed with ambient air (ca. 400 ppm, 6 L min<sup>-1</sup>)  
252 and tanks G1 and G2 were flushed with air enriched with CO<sub>2</sub> (ca. 1000 ppm, 6 L min<sup>-1</sup>) in  
253 order to prevent CO<sub>2</sub> degassing from the acidified tanks. CO<sub>2</sub> partial pressure (*p*CO<sub>2</sub>) in both

Deleted: were

255 ambient air and CO<sub>2</sub>-enriched air was monitored using two gas analysers (LI-820, LICOR©).  
256 The CO<sub>2</sub> concentration in the CO<sub>2</sub>-enriched air was manually controlled through small injections  
257 of pure CO<sub>2</sub> (Air Liquide©) using a mass flow controller.

258 Three experiments were performed at the long duration stations TYR, ION and FAST.  
259 The tanks were filled by means of a large peristaltic pump (Verder© VF40 with EPDM hose,  
260 flow of 1200 L h<sup>-1</sup>) collecting seawater below the base of the boat (depth of ~ 5 m), used to  
261 supply continuously surface seawater to a series of instruments during the entire campaign. In  
262 order to homogeneously fill the tanks, the flow was divided into six HDPE pipes distributing the  
263 water simultaneously into the different tanks. Overall, the filling of the six tanks took ~2 h  
264 (including rinsing and initial sampling, see thereafter). At the three stations, tanks were always  
265 filled at the end of the day before the start of the experiments: TYR (17/05/2017), ION  
266 (25/05/2017) and FAST (02/06/2017). While filling the tanks, this surface seawater was sampled  
267 for the measurements of selected parameters (sampling time = t-12h **before dust seeding**, see  
268 Table 1). After filling the tanks, seawater was slowly warmed using 500 W heaters, controlled by  
269 temperature-regulation units (COREMA©), in G1 and G2 overnight to reach an offset of +3 °C.  
270 <sup>13</sup>C-bicarbonate was added to all tanks at 4:00 am (local time; Gazeau et al., 2021) and G1 and  
271 G2 were acidified by addition of CO<sub>2</sub>-saturated filtered (0.2 µm) seawater (~1.5 L in 300 L;  
272 collected when filling the tanks at each station) at 4:30 am to reach a pH offset of -0.3. Sampling  
273 for **most** parameters took place prior to dust seeding (sampling time = t<sub>0</sub>, see Table 1). Dust  
274 seeding was performed **right after t<sub>0</sub>** between 7:00 and 9:00 (local time) in tanks D1, D2, G1 and  
275 G2. The same dust analog was used and the same dust flux was simulated as for the DUNE 2009  
276 experiments described in Desboeufs et al. (2014). Briefly, the fine fraction (< 20 µm) of Saharan  
277 soils collected in southern Tunisia, which is a major source of dust deposition over the  
278 northwestern Mediterranean basin, was used in the seeding experiments. The particle size  
279 distribution showed that 99% of particles had a size smaller than 0.1 µm, and that particles were

**Deleted:** (local time; Gazeau et al., in preparation, this issue)

**Deleted:** many

282 mostly made of quartz (40%), calcite (30%) and clay (25%; Desboeufs et al., 2014). This  
283 collected dust underwent an artificial chemical aging process by addition of nitric and sulfuric  
284 acid (HNO<sub>3</sub> and H<sub>2</sub>SO<sub>4</sub>, respectively) to mimic cloud processes during atmospheric transport of  
285 aerosol with anthropogenic acid gases (Guieu et al., 2010a, and references therein). To mimic a  
286 realistic wet flux event of 10 g m<sup>-2</sup>, 3.6 g of this analog dust were quickly diluted into 2 L of  
287 ultrahigh-purity water (UHP water; 18.2 MΩ cm<sup>-1</sup> resistivity), and sprayed at the surface of the  
288 tanks using an all-plastic garden sprayer (duration = 30 min). The N and P total contents in the  
289 dust were 1.36 ± 0.09% of N and 0.055 ± 0.003% of P (see Desboeufs et al., 2014, for a full  
290 description of dust chemical composition). The experimental protocol included the analysis of an  
291 extensive number of biogeochemical parameters and processes, not all shown and discussed in  
292 this paper, [and](#) are listed in Table 1. The experiment at stations TYR and ION lasted 72 h (3  
293 days) whereas the last experiment at station FAST was extended to four days. This relatively  
294 short duration of the experiments was constrained by the time available between stations and the  
295 time needed to properly clean the tanks between the experiments, following the protocol  
296 described by Bressac and Guieu (2013). As a larger time window was possible at the end of the  
297 cruise, the experiment at FAST was extended to four days. Seawater sampling was conducted 1  
298 h (t1h), 6 h (t6h), 12 h (t12h), 24 h (t24h), 48 h (t48h) and 72 h (t72h) (+ 96 h = t96h for station  
299 FAST) after dust addition. Acid-washed silicone tubes were used for transferring the water  
300 collected from the tanks to the different vials or containers. For some parameters (e.g. micro- and  
301 macro-nutrients), sampled seawater was directly filtered at the exit of the sampling tubes  
302 connected to each tank on sterile membrane filter capsules (gravity filtration with Sartobran©  
303 300; 0.2 μm).

Deleted: that

Deleted: , dissolved organic carbon

Deleted: online

Deleted: of the tanks

## 308 2.2. Analytical methods

### 309 2.2.1. Carbonate chemistry

310 Seawater samples for pH measurements were stored in 300 mL glass bottles with a glass  
311 stopper, pending analysis on board (within 2 h). Samples were transferred to 30 mL quartz cells  
312 and absorbances at 434, 578 and 730 nm were measured at 25 °C on an Cary60 UV-  
313 Spectrophotometer (Agilent©) before and after addition of 50 µL of purified meta-cresol purple  
314 provided by Robert H. Byrne (University of South Florida, USA) following the method  
315 described by Dickson et al. (2007). pH on the total scale (pH<sub>T</sub>) was computed using the formula  
316 and constants of Liu et al. (2011). The accuracy of pH measurements was estimated to 0.007 pH  
317 units, using a TRIS buffer solution (salinity 35, provided by Andrew Dickson, Scripps  
318 university, USA).

319 Seawater samples for total alkalinity ( $A_T$ ; 500 mL) measurements were filtered on GF/F  
320 membranes and analyzed onboard within one day.  $A_T$  was determined potentiometrically using a  
321 Metrohm© titrator (Titrand 888) and a glass electrode (Metrohm©, ecotrode plus) calibrated  
322 using first NBS buffers (pH 4.0 and pH 7.0, to check that the slope was Nernstian) and then  
323 using a TRIS buffer solution (salinity 35, provided by Andrew Dickson, Scripps university,  
324 USA). Triplicate titrations were performed on 50 mL sub-samples at 25 °C and  $A_T$  was calculated  
325 as described by Dickson et al. (2007). Titrations of standard seawater provided by Andrew  
326 Dickson (Scripps university, USA; batch 151) yielded  $A_T$  values within 5 µmol kg<sup>-1</sup> of the  
327 nominal value (standard deviation = 1.5 µmol kg<sup>-1</sup>, n = 40).

328 All parameters of the carbonate chemistry were determined from pH<sub>T</sub>,  $A_T$ , temperature,  
329 salinity, as well as phosphate and silicate concentrations using the R package seacarb.  
330 Propagation of errors on computed parameters was performed using the new function “error” of

331 this package, considering errors associated with the estimation of  $A_T$ ,  $pH_T$  as well as errors on  
332 dissociation constants (Orr et al., 2018).

### 333 2.2.2. Nutrients

334 Seawater samples for dissolved nutrients were filtered directly at the exit of the sampling  
335 tubes connected to each tank (Sartobran© 300; 0.2  $\mu\text{m}$ ), collected in polyethylene bottles and  
336 immediately analyzed on board. Nitrate + nitrite ( $\text{NO}_x$ ) and silicate ( $\text{Si}(\text{OH})_4$ ) measurements  
337 were conducted using a segmented flow analyzer (AIII HR Seal Analytical©) according to  
338 Aminot and K  rouel (2007) with a limit of quantification of  $0.05 \mu\text{mol L}^{-1}$  for  $\text{NO}_x$  and  $0.08$   
339  $\mu\text{mol L}^{-1}$  for  $\text{Si}(\text{OH})_4$ . In addition, for t-12h samples, the analysis of  $\text{NO}_x$  was also performed by  
340 a spectrometric method in the visible at 540 nm, with a 1 m Liquid Waveguide Capillary Cell  
341 (LWCC). The limit of detection was  $\sim 10 \text{ nmol L}^{-1}$  and the reproducibility was  $\sim 6\%$ . Also from  
342 samples taken at t-12h, the measurement of ammonium concentrations was performed on board  
343 using a Fluorimeter TD-700 (Turner Designs©) according to Holmes et al. (1999). This  
344 fluorimetric method is based on the reaction of ammonia with orthophthaldialdehyde and sulfite  
345 and has a limit of quantification of  $0.01 \mu\text{mol L}^{-1}$ . Dissolved inorganic phosphorus (DIP)  
346 concentrations were quantified using the Liquid Waveguide Capillary Cell (LWCC) method  
347 according to Pulido-Villena et al. (2010). The LWCC was 2.5 m long and the limit of detection  
348 was  $1 \text{ nmol L}^{-1}$ .

### 349 2.2.3. Pigments

350 A volume of 2.5 L of sampled seawater was filtered onto GF/F filters, immediately  
351 frozen in liquid nitrogen and stored at  $-80 \text{ }^\circ\text{C}$  pending analysis at the SAPIGH analytical platform  
352 at the Institut de la Mer de Villefranche (IMEV, France). Filters were extracted at  $-20 \text{ }^\circ\text{C}$  in 3 mL  
353 methanol (100%) containing an internal standard (vitamin E acetate, Sigma©), disrupted by

Deleted: online

Deleted: <0.2  $\mu\text{m}$

356 sonication and clarified one hour later by vacuum filtration through GF/F filters. The extracts  
357 were rapidly analyzed (within 24 h) on a complete Agilent© Technologies 1200 series HPLC  
358 system. The pigments were separated and quantified as described in Ras et al. (2008).

#### 359 **2.2.4. Flow cytometry**

360 For the enumeration of autotrophic prokaryotic and eukaryotic cells, heterotrophic  
361 prokaryotes and heterotrophic nanoflagellates (HNF) by flow cytometry, subsamples (4.5 mL)  
362 were fixed with glutaraldehyde grade I 25% (1% final concentration), and incubated for 30 min  
363 at 4 °C, then quick-frozen in liquid nitrogen and stored at -80 °C until analysis. Samples were  
364 thawed at room temperature. Counts were performed on a FACSCanto II flow cytometer (Becton  
365 Dickinson©) equipped with 3 air-cooled lasers: blue (argon 488 nm), red (633 nm) and violet  
366 (407 nm). The separation of different autotrophic populations was based on their scattering and  
367 fluorescence signals according to Marie et al. (2010). *Synechococcus* spp. was discriminated by  
368 its strong orange fluorescence ( $585 \pm 21$  nm), and pico- and nano-eukaryotes were discriminated  
369 by their scatter signals of red fluorescence ( $> 670$  nm). For the enumeration of heterotrophic  
370 prokaryotes, cells were stained with SYBR Green I (Invitrogen – Molecular Probes) at 0.025%  
371 (vol / vol) final concentration for 15 min at room temperature in the dark. Stained prokaryotic  
372 cells were discriminated and enumerated according to their right-angle light scatter (SSC) and  
373 green fluorescence at 530/30 nm. In a plot of green versus red fluorescence, heterotrophic  
374 prokaryotes were distinguished from autotrophic prokaryotes. For the enumeration of HNF,  
375 staining was performed with SYBR Green I (Invitrogen—Molecular Probes) at 0.05% (v/v) final  
376 concentration for 15-30 min at room temperature in the dark (Christaki et al., 2011). Cells were  
377 discriminated and enumerated according to their SSC and green fluorescence at 530/30 nm.  
378 Fluorescent beads (1.002  $\mu$ m; Polysciences Europe©) were systematically added to each  
379 analyzed sample as internal standard. The cell abundance was determined from the flow rate,

380 which was calculated with TruCount beads (BD biosciences©). Biomasses of each group were  
381 estimated based on conversion equations and/or factors found in the literature (see section 2.3.2).

## 382 2.2.5. Micro-phytoplankton and -heterotrophs

383 At t-12h (i.e. seawater sampled during the filling of the tanks), a volume of 500 mL was  
384 sampled in glass vials and immediately preserved in a 5% acidic Lugol's solution pending  
385 analysis. At the Laboratoire d'Océanographie de Villefranche (LOV, France), 100 mL aliquots  
386 were transferred to sedimentation chambers (Utermohl) and counted under an inverted  
387 microscope at 200 to 400 magnifications.

## 388 2.2.6. Meso zooplankton

389 At the end of each experiment (t+72h for TYR and ION and t+96 h for FAST, after  
390 artificial dust seeding), the sediment traps were removed, closed and stored with formaldehyde  
391 4% (see Gazeau et al., 2021). The valve at the base of the tanks was then reopened to let the  
392 remaining water inside the tanks (TYR 165-180 L; ION = 172.5 L and FAST = 150 L) pass  
393 through a large PVC sieve (100 µm). The organisms retained on that mesh were gently removed  
394 from the sieve using a washing bottle filled with filtered seawater (0.2 µm), and transferred  
395 directly inside a 250 mL bottle. The bottle was filled with the sample (1/3 of the volume), and  
396 was completed with formaldehyde 4%. The zooplankton digital images were obtained using a  
397 ZooSCAN (Hydroptic©; Gorsky et al., 2010) at the PIQv-platform of EMBRC-France. The  
398 identification of species was performed **by automatic classification with a reference dataset in**  
399 **EcoTaxa** (<https://ecotaxa.obs-vlfr.fr/>, last access: 17/04/2020) and then all validated and  
400 corrected **manually**.

Deleted: (see Gazeau et al., in preparation, this issue)

Deleted:

Deleted: by automatic comparison with the library data set  
EcoTaxa ...

Formatted: English (US)

Deleted: by a human operator

Formatted: English (US)

## 406 **2.3. Data analyses**

### 407 **2.3.1. Nutrient inputs from dust**

408 ~~The maximum percentage of dust-born dissolved N and P~~ was calculated considering that  
409 these evapo-condensated dust contain  $1.36 \pm 0.09\%$  of N and  $0.055 \pm 0.003\%$  of P (Desboeufs et  
410 al., 2014). Based on maximal concentrations observed in the D and G tanks after seeding (two  
411 discrete sampling within 6 h ~~following dust seeding, t1h and t6h~~), one can estimate the maximal  
412 % of dissolution of dust in seawater during the three experiments:

$$413 \%_{dissolution} = \frac{CONC_{max} - CONC_{init}}{CONC_{dust}} \cdot 100 \quad (1)$$

414 where  $CONC_{init}$  is the concentration of the corresponding nutrient in each tank before seeding  
415 ( $t_0$ ),  $CONC_{max}$  corresponds to the concentration of the corresponding nutrient in each tank when  
416 nutrient concentration was at a maximum over the first 6 h after seeding as observed based on  
417 our discrete sampling procedure, and  $CONC_{dust}$  ~~is the maximum addition, corresponding to a~~  
418 ~~100% dissolution of its total concentration in the dust analog~~ (as estimated based on dust  
419 chemical composition; Desboeufs et al., 2014; see above).

### 420 **2.3.2. Autotrophic and heterotrophic biomass**

421 As micro-phytoplankton counting was not performed throughout the experiment, as a  
422 first approximation, autotrophic biomass was calculated as the sum of carbon contained in  
423 *Synechococcus*, pico-eukaryotes and nano-eukaryotes (abundances based on flow cytometry) and  
424 is therefore restricted to the fraction  $< 20 \mu\text{m}$ . For *Synechococcus*, conversion to carbon units  
425 ~~was~~ done considering  $250 \text{ fg C cell}^{-1}$  (Kana and Glibert, 1987), while the equation proposed by  
426 Verity et al. (1992;  $0.433 \text{ BV}^{0.863}$  where BV refers to the biovolume) was used for pico- and  
427 nano-eukaryotes assuming a spherical shape and a diameter of 2 and  $6 \mu\text{m}$  for the two groups,

Deleted: Computations

Formatted: Font: Bold

Formatted: Font colour: Black

Formatted: Font: Bold

Deleted: ->

Formatted: English (US)

Deleted: The maximum percentage of dissolution from dust observed with respect to N and P

Formatted: English (US)

Deleted: ->

Formatted: English (US)

Deleted: corresponds to the maximum input of each nutrient, if 100% of its total concentration in the dust analog dissolves ...

Deleted: ->

Formatted: Indent: First line: 1.27 cm

Deleted: were

Formatted: English (US)



438 respectively. Percentages of these different groups were calculated in order to estimate the  
439 composition of the communities at the start and its evolution during the experiments.  
440 Furthermore, heterotrophic biomass was computed as the sum of heterotrophic prokaryotes  
441 biomass and heterotrophic nanoflagellates biomass. For heterotrophic prokaryotes, conversion to  
442 carbon units were done considering  $20 \text{ fg C cell}^{-1}$  (Lee and Fuhrman, 1987) and for heterotrophic  
443 nanoflagellates assuming  $220 \text{ fg C } \mu\text{m}^{-3}$  (Børsheim and Bratbak, 1987), a spherical shape and a  
444 diameter of  $3 \mu\text{m}$ . The ratio of autotrophic and heterotrophic biomass during the experiments was  
445 used to evaluate the trophic status of the investigated communities and its evolution. Finally, a  
446 proxy for micro-phytoplankton biomass ( $B_{\text{micro}}$ ) was estimated following Vidussi et al. (2001), as  
447 the sum of Fucoxanthin and Peridinin.

## 448 3. Results

### 449 3.1. Initial conditions

450 Initial conditions of various measured parameters at the three sampling stations while  
451 filling the tanks (t-12h before seeding) are shown in Table 2. pH<sub>T</sub> and total alkalinity  
452 concentrations followed a west to east increasing gradient (8.03, 8.04 and 8.07; 2443, 2529 and  
453 2627  $\mu\text{mol kg}^{-1}$  at FAST, TYR and ION, respectively). NO<sub>x</sub> concentrations were maximal at  
454 station FAST with a NO<sub>x</sub>:DIP molar ratio of  $\sim 4.6$ . Very low NO<sub>x</sub> concentrations were observed  
455 at stations TYR and ION (14 and 18  $\text{nmol L}^{-1}$ , respectively). DIP concentrations were the highest  
456 at station TYR (17  $\text{nmol L}^{-1}$ ) and the lowest at the most eastern station (ION, 7  $\text{nmol L}^{-1}$ ).  
457 Consequently, the lowest NO<sub>x</sub>:DIP ratio was measured at TYR (0.8), compared to ION and  
458 FAST (2.8 and 4.6, respectively). Ammonium concentrations were maximal at TYR (0.045  $\mu\text{mol}$   
459  $\text{L}^{-1}$ ), intermediate at ION (0.022  $\mu\text{mol L}^{-1}$ ), and minimal at FAST (below detection limit).  
460 Silicate concentrations were similar at stations TYR and ION ( $\sim 1 \mu\text{mol L}^{-1}$ ) and higher than at  
461 station FAST (0.64  $\mu\text{mol L}^{-1}$ ).

462 Very low and similar concentrations of chlorophyll *a* were measured at the three stations  
463 (0.063 - 0.072  $\mu\text{g L}^{-1}$ ). The proportion of the different major pigments (Fig. 3) showed that  
464 phytoplankton communities at stations TYR and ION were very similar with a dominance of  
465 Prymnesiophytes (i.e. 19'-hexanoyloxyfucoxanthin; Ras et al., 2008) followed by Cyanobacteria  
466 (i.e. Zeaxanthin; Ras et al., 2008). In contrast, at station FAST, the plankton community was  
467 clearly dominated by photosynthetic prokaryotes (i.e. Zeaxanthin and Divinyl-chlorophyll *a*;  
468 Cyanobacteria and Prochlorophytes, respectively; Ras et al., 2008). At all three stations, the  
469 proportion of pigments representative of larger species (i.e. Fucoxanthin and Peridinin; diatoms  
470 and dinoflagellates respectively; Ras et al., 2008) were very small ( $< 5\%$  for each pigment).

Formatted: English (US)

Deleted: observed when pumping seawater for the experiments (before <sup>13</sup>C-bicarbonate addition and dust seeding: t-12h) ...

Deleted: ic

Formatted: English (US)

475 Cellular abundances of all studied microorganisms (phytoplankton, micro-grazers,  
476 heterotrophic bacteria) were the highest at FAST (Table 2). Picoeukaryotes, *Synechococcus* and  
477 heterotrophic prokaryotes abundances followed an east to west increasing trend (ION < TYR <  
478 FAST). In contrast, nano-eukaryotes abundance was similar at FAST and ION, and minimal at  
479 TYR. The abundance of heterotrophic nanoflagellates (HNF) were similar at TYR and FAST  
480 (~110-125 cells mL<sup>-1</sup>), twice as high as the one observed at station ION. This east to west  
481 increasing trend was also observed for micro-phytoplankton and micro-heterotrophs abundances  
482 (microscopic analyses; Table 2). The ratio between autotrophic biomass and heterotrophic  
483 biomass was clearly in favor of the heterotrophic compartment at stations TYR and FAST (~0.6  
484 at the two stations) but the opposite was found at station ION (ca. 1.3).

### 485 **3.2. Conditions of irradiance, temperature and pH during** 486 **the experiments**

487 Irradiance levels, during the experiments in the control tanks (C1, C2), were maximal at  
488 station ION and minimal at station FAST (daily average maximum levels in controls: ~ 1050, ~  
489 1130 and ~ 1020  $\mu\text{mol photons m}^{-2} \text{s}^{-1}$  at TYR, ION and FAST, respectively; Fig. 4). Decreases  
490 of water transparency after dust addition was observed at all three stations with a maximum dust  
491 impact at station ION and the lowest impact at station FAST where irradiance levels decreased  
492 by only 60  $\mu\text{mol photons m}^{-2} \text{s}^{-1}$  after dust addition (average between tanks D and G). At station  
493 TYR, a more pronounced decrease was observed in acidified and warmed tanks (G1 and G2)  
494 with a decrease of daily average maximum irradiance of ~ 60 and ~ 160  $\mu\text{mol photons m}^{-2} \text{s}^{-1}$  as  
495 compared to dust-amended tanks D and controls, respectively. Temperature control (Fig. 4) was  
496 not optimal showing deviations between replicates of treatment G of up to 1.5 °C (station ION).  
497 Temperature in controls and D tanks displayed a daily cycle with an increase during the day and

Deleted: Experimental c

Formatted: English (US)

Formatted: English (US)

Formatted: English (US)

Formatted: English (US)

Formatted: English (US)

Deleted: s

500 a decrease at night. Overall, the differences between the warmed treatment (G) and the other  
501 tanks were +3, +3.2 and +3.6 °C at TYR, ION and FAST, respectively.

502 Addition of CO<sub>2</sub>-saturated filtered seawater led to a decrease of pH<sub>T</sub> from 8.05 ± 0.004  
503 (average ± SD between C1, C2, D1 and D2 at t0) to 7.74 (average between G1 and G2) at station  
504 TYR, from 8.07 ± 0.002 to 7.78 at station ION and 8.05 ± 0.001 to 7.72 at station FAST (Fig. 5).  
505 pH<sub>T</sub> levels remained more or less constant in ambient pH levels tanks during all three  
506 experiments with no clear impact of dust addition in tanks D1 and D2. In lowered pH tanks, pH  
507 levels gradually increased during the experiments with a systematic larger increase in one of the  
508 duplicates (G1). Yet pH<sub>T</sub> increases remained moderate thanks to the flushing of CO<sub>2</sub>-enriched air  
509 above the tanks (pCO<sub>2</sub> of 1017 ± 11, 983 ± 96, 1023 ± 25 ppm at TYR, ION and FAST,  
510 respectively; data not shown). Partial pressure of CO<sub>2</sub> in ambient air was similar at the three  
511 stations, i.e. 410 ppm (data not shown). At all three stations, ~~the addition of <sup>13</sup>C-bicarbonate to~~  
512 ~~all tanks before t0~~ led to an increase of total alkalinity between 6 and 11 μmol kg<sup>-1</sup> ~~at t0~~. ~~Dust~~  
513 addition, ~~performed right after t0 in tanks D and G~~, led to a ~~4x~~ decrease in ~~these tanks~~ between 8  
514 and 16 μmol kg<sup>-1</sup> ~~at t24h~~ with no apparent effects of warming and acidification. Overall, no large  
515 changes in this parameter were observed during the experiments (Fig. 5).

### 516 3.3. Changes in nutrient concentrations

517 Dust addition in tanks D and G led to a rapid and maximum input of NO<sub>x</sub> (as observed  
518 during the first 6 h; Fig. 6; Table 3) of ~ 11 μmol L<sup>-1</sup> at all three stations with no differences  
519 between both treatments. The corresponding dissolution percentage of N contained in the dust  
520 analog was between 94 and 99%. In contrast, maximum DIP release (within 6 h after dust  
521 addition) from the dust analog was much smaller and comprised between 20 and 37 nmol L<sup>-1</sup>,  
522 with slightly higher release at FAST (31-37 nmol L<sup>-1</sup>) as compared to the other stations.  
523 Dissolution percentages for DIP were estimated between 9.2 and 17.3% of total phosphorus

Formatted: English (US)

Formatted: English (US)

Deleted: <sup>13</sup>C-addition

Formatted: Not Superscript/ Subscript

Formatted: English (US), Not Superscript/ Subscript

Formatted: Not Superscript/ Subscript

Deleted: and d

Formatted: English (US)

Deleted:

Formatted: Font: Italic, English (US)

Formatted: English (US), Subscript

Formatted: English (US)

Deleted: tanks D and G

Formatted: English (US)

Formatted: English (US)

528 contained in dust. As a consequence of these contrasted dissolution of N and P, NO<sub>x</sub>:DIP ratios  
529 increased from initial values below 5 to above 300, within 6 h after dust seeding, in the dust  
530 amended (D and G) tanks (Fig. 6).

531 After these rapid increases due to N and P releases in dust amended tanks, both variables  
532 decreased with time. While nutrient variability was small in control tanks over the duration of the  
533 experiments (NO<sub>x</sub> and DIP variations below 20 and 3 nmol L<sup>-1</sup>, respectively), large decrease of  
534 both elements was measured in dust amended tanks (D and G; Table 4). For NO<sub>x</sub>, similar linear  
535 decreases were observed throughout the experiments at stations TYR and ION with no visible  
536 differences between tanks D and G. In contrast, at station FAST, a more pronounced decrease in  
537 NO<sub>x</sub> was observed in dust-amended (D and G) tanks as compared to the other stations, with  
538 detectable larger decreases in warmed and acidified tanks relative to the D treatment.  
539 Nevertheless, at all stations, NO<sub>x</sub> concentrations in D and G treatments remained far above  
540 ambient levels throughout the experiments (> 9 μmol L<sup>-1</sup>). Abrupt decreases in DIP were  
541 observed during the three experiments after the initial increase. At station TYR, after 24 h, all  
542 DIP released from dust decreased to initial levels in tanks G while it took two more days to reach  
543 initial levels in tanks D. In contrast, at station ION, no clear difference in DIP dynamics was  
544 observed between treatments D and G, with concentrations that decreased rapidly during the first  
545 24 h but that remained above initial levels until the end of the experiment. At station FAST,  
546 similarly to station TYR, DIP decreased rapidly from t12h in treatment G, reaching levels close  
547 to initial conditions at the end of the experiment. DIP decrease was much lower in treatment D  
548 (Table 4) with concentrations maintained far above ambient levels throughout the experiment.  
549 As a consequence of these differences between NO<sub>x</sub> and DIP dynamics as well as differences  
550 among stations, NO<sub>x</sub>:DIP ratio increased during the experiments with clear differences between  
551 stations (Fig. 6) and remained much higher than that in the controls over the duration of the three  
552 experiments.

553 Silicate dynamics showed at all stations higher concentrations in dust amended (D and G)  
554 tanks relative to the controls. At TYR, while concentrations remained stable in control tanks,  
555 they increased linearly with time in the other tanks (D and G) with no apparent effect of the  
556 imposed increase in temperature and decrease in pH (i.e. tanks G). Difference of  $\text{Si(OH)}_4$   
557 concentration between dust amended treatments (D and G) and controls was  $\sim 0.1 \mu\text{mol L}^{-1}$  at the  
558 end of the experiment. At station ION, after an initial decrease of concentrations between t-12h  
559 and t0, concentrations increased in all tanks until the end of the experiment with higher  
560 concentration in dust amended tanks (D and G) than in controls (no difference between D and G  
561 treatments). In contrast, at FAST, concentrations increased between t-12h and t0, and continued  
562 to increase in all tanks (with higher values in dust amended tanks) until t48h and then decreased  
563 until the end of the experiment. At the end of the experiment (t96h),  $\text{Si(OH)}_4$  concentration was  
564 higher in the G treatment than in the D treatment which was similar to the controls.

### 565 3.4. Changes in biological stocks

566 Regarding biological stocks, temporal dynamics showed very different patterns amongst  
567 the three studied stations. At TYR, total chlorophyll *a* concentrations did not change in dust  
568 amended tanks maintained under ambient levels of temperature and pH (Fig. 7) and even led to  
569 slightly decreased values 24 h after dust addition (e.g. -35 to -38% in D1 and D2, respectively as  
570 compared to controls; Table 5). No clear effect of dust addition (tanks D vs. C) were detectable  
571 for all groups based on pigment analyses (Fig. 7). Results obtained based on flow cytometry  
572 counting (Fig. 8) were coherent with these observations and showed stronger decreases in cell  
573 abundances for  $< 20 \mu\text{m}$  autotrophic groups in tanks D1 and D2 (-77 to -80%). In contrast, at this  
574 station, the abundance of heterotrophic prokaryotes (HP) increased rapidly after dust addition  
575 both under ambient (+53-68%) and future (+68%) environmental conditions, with no clear  
576 difference among those treatments. In warmed and acidified tanks, strong discrepancies between

Formatted: English (US)

Deleted: concentrations remained stable,

Deleted: temporal dynamics showed very different patterns with respect to the sampling station

580 the duplicates were observed for pigments and autotrophic cell abundances. Indeed, tank G1  
581 showed moderately higher levels for all variables as compared to tanks C ~~with~~ the exception of  
582 pico-eukaryotes, while in G2 all variables responded strongly to dust addition with maximum  
583 relative changes of > 300% (~~with~~ the exception of nano-eukaryotes: +119%). While HNF  
584 abundances responded positively to the treatments in D1, D2 and G2 (+100-352%), abundances  
585 increased sharply in tank G1 towards the end of the experiment (+1095%).

586 ~~At ION, a clear distinction between treatments could be observed for almost all pigments~~  
587 and cell abundances (Fig. 7, Fig. 8). ~~With~~ the exception of nano-eukaryotes and HNF, all  
588 variables (pigments and cell abundances) increased as a response to both dust addition and  
589 warmed/acidified conditions (i.e. C < D < G). As an example (Table 5), the maximum relative  
590 changes as compared to controls observed for total chlorophyll *a* were 109-183% and 399-426%  
591 in tanks D and G, respectively. The highest stimulation to dust addition was observed for  
592 *Synechococcus* with a +317-390% increase and +805-1425% increase in D and G tanks  
593 respectively (Table 5). Abundances of nano-eukaryotes and HNF suggested no impact of dust  
594 addition under ambient conditions but a positive impact in treatment G. In contrast to what was  
595 observed at TYR for HP abundances, an effect of temperature and pH was observed at station  
596 ION with a higher impact of dust addition under future environmental conditions.

597 ~~At station FAST, all above mentioned variables related to biological stocks increased~~  
598 strongly after dust addition (Fig. 7, Fig. 8 and Table 5). For instance, total chlorophyll *a*  
599 increased following an exponential trend until the end of the experiment reaching maximal  
600 values at t96h with slightly lower values observed under ambient environmental conditions  
601 (+237-318% in D tanks vs. ~+400% in G tanks). Prymnesiophytes (i.e. 19'-  
602 hexanoyloxyfucoxanthin) and diatoms (i.e. Fucoxanthin) appeared as the groups benefiting the  
603 most from dust addition with no large impacts of warming/acidification. In contrast,  
604 Pelagophytes (i.e. 19'-butanoyloxyfucoxanthin) and green algae (i.e. Total Chlorophyll *b*)

Formatted: English (US)

Deleted: at

Deleted: at

Formatted: English (US)

Deleted:

Formatted: English (US)

Deleted: At

Deleted:

610 responded much more in treatment G than in treatment D. Finally, although Cyanobacteria (i.e.  
611 Zeaxanthin) responded faster to dust addition under future environmental conditions (tanks G),  
612 this effect tended to attenuate towards the end of the experiment. In contrast to estimates based  
613 on HPLC data, increases in cell abundances did not generally take place until the end of the  
614 experiment. While abundances in pico-eukaryotes increased until t96h in treatment D,  
615 abundances sharply declined between t72h and t96h for this group in treatment G. The same  
616 trend was observed for *Synechococcus* during this experiment, although discrepancies between  
617 duplicates in treatment D at sampling time t96h did not allow drawing conclusions on the  
618 behavior of this group at the end of the experiment. Both under ambient and future conditions,  
619 abundances of nano-eukaryotes declined sharply between t72h and t96h. The decline in HP  
620 abundances appeared even earlier during the experiment with moderate maximum relative  
621 differences as compared to controls observed at t48h. HP abundances declined very sharply  
622 between t48h and t96h in treatment G, reaching control levels, while this decline was less sharp  
623 under ambient environmental levels. Finally, HNF dynamics during this experiment was hard to  
624 evaluate with no clear effects of dust addition or pH/temperature conditions and with a large  
625 increase in abundances in only one duplicate of treatment G (t24h) followed by a gradual  
626 decrease.

627 Abundances of meso-zooplankton at the end of the experiments showed relatively similar  
628 values at stations TYR and ION while much higher levels were observed at station FAST (Fig.  
629 9). As a consequence of large variability between duplicates at stations TYR and ION, no clear  
630 effects of treatments were detected. At station FAST, although the sample size was too low to  
631 statistically test for differences, higher total abundances of meso-zooplankton species were  
632 observed in the dust-amended tanks with no differences between ambient and future conditions  
633 of temperature and pH. However, differences in abundance were visible between these two



- 634 treatments for specific groups, with respectively higher abundance of Harosa and lower  
635 abundance of Crustacea (other than copepods) and Mollusca in warmed and acidified tanks.

636 **4. Discussion**

637 **4.1. Initial conditions**

638 Over the transect, the mixed layer occupied the first 20 m. It was shallower at TYR as  
639 compared to ION and FAST (mixed layer depth, MLD of ~ 10 vs ~15 m, respectively) at the  
640 time of the sampling (Van Wambeke et al., 2020a). Such shallow MLD is well representative of  
641 stratified conditions encountered in the western Mediterranean basin in late spring/early summer  
642 (D'Ortenzio et al., 2005). Overall, the three experiments were conducted with surface seawater  
643 collected during oligotrophic conditions typical of the open Mediterranean Sea at this period of  
644 the year (late spring). Although direct measurements of NO<sub>x</sub> and DIP concentrations using  
645 nanomolar techniques (as performed in our study) are scarce in the Mediterranean Sea, the low  
646 levels measured during the cruise are in agreement with DIP values reported for the three studied  
647 basins (Djaoudi et al., 2018) and with NO<sub>x</sub> and DIP concentrations measured in coastal waters of  
648 Corsica in late spring/early summer (Louis et al., 2017b; Pulido-Villena et al., 2014; Ridame et  
649 al., 2014). Furthermore, at all three stations, NO<sub>x</sub>:DIP molar ratios in the tested surface waters  
650 were well below the Redfield ratio (16:1) and are consistent with ratios found in these previously  
651 cited studies. Both low NO<sub>x</sub>:DIP ratio and low nutrient concentrations suggest that communities  
652 found at the three stations experienced N and P co-limitation at the start of the experiments, as  
653 previously shown by Tanaka et al. (2011). A side nutrient enrichment experiment confirmed that,  
654 at the three sites, heterotrophic bacteria were mainly N-P co-limited (Van Wambeke et al.,  
655 2020b). In contrast to N and P, initial concentrations of dissolved Fe in the sampled seawater  
656 ranging from 1.5 nmol L<sup>-1</sup> at TYR to 2.5 nmol L<sup>-1</sup> at ION (Roy-Barman et al., 2020) were  
657 unlikely limiting for biological activity as previously shown in the Mediterranean Sea under  
658 stratified conditions (Bonnet et al., 2005; Ridame et al., 2014).

Formatted [1]

Field Code Changed

Formatted [2]

Deleted: typical stratified

Formatted [3]

Deleted: However, at all three stations, initial concentrations of NO<sub>x</sub> (14, 18 and 59 nmol L<sup>-1</sup> at TYR, ION and FAST, respectively; Table 2) were lower than the ones reported by Manca et al. (2004) in surface waters (5 m) in these areas in spring (0.036 ± 0.10, 0.275 ± 0.358 and 0.183 ± 0.282 μmol L<sup>-1</sup> for the areas corresponding to TYR, ION and FAST, respectively; <http://doga.ogs.trieste.it/medar/climatologies/>, last access: 28/04/2020). Similarly, surface DIP concentrations as measured at the three stations were lower than values extracted from the compilation of Manca et al. (2004) for the same period (0.072 ± 0.072, 0.054 ± 0.035 and 0.115 ± 0.078 μmol L<sup>-1</sup> in the areas corresponding to TYR, ION and FAST, respectively). However, d

Formatted [4]

Deleted: , limiting our ability to compare our results with these published values which, in any case, show large interannual variability. the

Formatted [5]

Deleted: measured during PEACETIME

Formatted [6]

Field Code Changed

Formatted: French

Deleted: Djaoudi et al. (2018) reported low DIP values in the three studied basins. Furthermore, low observed concentrations of NO<sub>x</sub> and DIP at all three stations during our study were also in agreement with reported concentrations in the coastal waters of Corsica during experiments using *in situ* mesocosms in June, whether during the DUNE project (DIP ~5 nmol L<sup>-1</sup>; Pulido-Villena et al., 2014; NO<sub>x</sub> < 30 nmol L<sup>-1</sup>).

Formatted [8]

Deleted: Some enrichment experiments in DIP, NO<sub>3</sub>+I

Formatted [10]

Deleted: I

Formatted [11]

Deleted: ...anged

Formatted: English (US)

Deleted: (

Formatted: English (US)

Deleted: )...to 2.5 nmol L<sup>-1</sup> ... HYPERLINK

Formatted: English (US)

Deleted: (ION; Roy-Barman et al., 2020)et al., in

Formatted: English (US)

Deleted: . Such concentrations

Formatted [15]

758 Low total chlorophyll *a* concentrations in the tested waters were representative of surface  
759 concentrations reported for the Western and Central Mediterranean Sea in late spring/early  
760 summer, both from remote sensing images (Bosc et al., 2004), and from *in situ* measurements  
761 provided in a database from Manca et al. (2004), While large species (i.e. diatoms,  
762 dinoflagellates) represented only ~10% of the total chlorophyll *a* biomass of the tested waters,  
763 the composition of the smaller size phytoplankton communities differed substantially. Indeed,  
764 communities were clearly dominated by nano-eukaryotes at stations TYR and ION, and a larger  
765 contribution from pico-eukaryotes and Cyanobacteria was observed at station FAST. Due to their  
766 low competitiveness under nutrient limitation, the small contribution of large phytoplankton cells  
767 at the start of the experiment is a fingerprint of LNLC areas in general, and of surface  
768 Mediterranean waters in late spring and summer (Siokou-Frangou et al., 2010).

769 As biomass of both heterotrophic nanoflagellates and prokaryotes followed a west to east  
770 gradient (FAST > TYR > ION), the ratio of autotrophic vs heterotrophic biomass appeared  
771 clearly in favor of the heterotrophic compartment at stations TYR and FAST (ratio of 0.6) while  
772 a value above 1 was estimated at ION (ratio of 1.3). This is coherent with the highest net  
773 community production (NCP) rates being reported at this station by Gazeau et al. (2021),  
774 showing that the initial community at the start of this experiment was very close to metabolic  
775 balance (mean ± SE: -0.06 ± 0.09 μmol O<sub>2</sub> L<sup>-1</sup> d<sup>-1</sup>). The highest community respiration rates and  
776 consequently lowest NCP rates were measured at station TYR (-1.9 μmol O<sub>2</sub> L<sup>-1</sup> d<sup>-1</sup>) further  
777 suggesting that the autotrophic plankton community was not very active and relying on  
778 regenerated nutrients, as shown by the highest level of NH<sub>4</sub><sup>+</sup> measured at the start of this  
779 experiment. In contrast, although slightly heterotrophic (Gazeau et al., 2021) and limited by the  
780 low amount of nutrients, the community of the tested waters at FAST was the most active as  
781 shown by the highest levels of <sup>14</sup>C production and heterotrophic prokaryote production (Gazeau  
782 et al., 2021), as well as N<sub>2</sub> fixation (Céline Ridame, unpublished results). Altogether, the

- Deleted: T
- Formatted [16]
- Deleted: of ~ 0.06 - 0.07 μg L<sup>-1</sup> (Table 2)
- Formatted [18]
- Deleted: typical of
- Formatted [17]
- Formatted [19]
- Deleted: chlorophyll *a* levels found
- Deleted: in these areas of the surface Mediterranean [21]
- Formatted [20]
- Formatted [22]
- Deleted: as seen by
- Formatted [23]
- Deleted: satellite (Bosc et al., 2004)... or from a data [24]
- Formatted [25]
- Deleted: (Manca et al., 2004)... During the DUNE a [26]
- Formatted [27]
- Deleted: ,
- Formatted [28]
- Deleted: ...based on HPLC pigment analyses, ...iffc [29]
- Formatted [30]
- Deleted: . Indeed, while the communities were domit [31]
- Formatted [32]
- Deleted: eukaryotic
- Formatted [33]
- Deleted: species
- Formatted [34]
- Deleted: , both HPLC and flow cytometry data sugg [35]
- Formatted [36]
- Deleted: and
- Deleted: ...t station FAST. Micro-autotrophs (e.g. la [38]
- Formatted [37]
- Formatted [39]
- Deleted: at this period of the year
- Formatted [40]
- Deleted: Autotrophic biomasses, as estimated based [41]
- Formatted [42]
- Deleted: the metabolic balance
- Formatted [43]
- Deleted: (in preparation, this issue)
- Formatted [44]
- Deleted: (Ridame et al., in preparation, this issue) als [45]
- Formatted [46]
- Deleted: (Table 2) ...as the most active as shown by [47]
- Formatted [48]
- Deleted:
- Formatted [49]
- Deleted: (Ridame et al., in preparation, this issue)

914 heterotrophic signature of the three investigated stations, although closer to metabolic balance ~~at~~  
915 ION, reflected typical biogeochemical conditions in the Mediterranean Sea during late spring to  
916 early summer (Regaudie-de-Gioux et al., 2009).

## 917 **4.2. Critical assessment of the experimental system and** 918 **methodology**

919 The experimental tanks used in this study have been ~~successfully~~ validated in ~~previous~~  
920 studies designed to investigate the inputs of macro- and micro-nutrients (e.g. NO<sub>x</sub>, DIP, DFe)  
921 and the export of organic matter, under close-to-abiotic conditions (seawater filtration onto 0.2  
922 μm) following simulated wet dust events using the same analog as used in our study (Bressac  
923 and Guieu, 2013; Louis et al., 2017a, 2018). Louis et al. (2017a, 2018) further investigated these  
924 impacts under lowered pH conditions, ~~although~~ no control of atmospheric pCO<sub>2</sub> was performed,  
925 ~~resulting in a rapid increase of~~ pH levels in the acidified filtered seawater due to CO<sub>2</sub> ~~outgassing~~  
926 (from ~7.4 to ~7.7 in six days). ~~Since those above-mentioned studies, in order to avoid this, we~~  
927 improved our experimental system to allow mimicking future conditions by controlling  
928 atmospheric pCO<sub>2</sub> in addition to light and temperature (i.e. climate reactors). ~~This allowed to~~  
929 ~~significantly reduce~~ CO<sub>2</sub> ~~outgassing~~ and maintain pH levels close to experimental targets. ~~Still,~~  
930 as ~~illustrated~~ in Fig. 5, the regulation ~~of atmospheric CO<sub>2</sub>~~ was consistently more efficient in tank  
931 G2 compared to G1, ~~resulting in a~~ small discrepancy ~~in terms of~~ pH (highest difference of 0.04  
932 pH units between the two G tanks at FAST), ~~possibly due to a~~ potential leak or a longer flushing  
933 time above tank G1. Nevertheless, ~~as no systematic differences in terms of biological response~~  
934 ~~were observed between these two tanks, we believe that these small differences in terms of~~  
935 ~~regulated pH had no consequences on the obtained results,~~

936 The lids above tanks, equipped with LEDs in order to reproduce sunlight intensity and  
937 spectrum, were used for the first time during these experiments. ~~While~~ simulated intensities were

Deleted: for

Formatted: English (US)

Deleted: natural

Formatted: English (US)

Deleted: Experimental

Formatted: English (US)

Deleted: already

Formatted: English (US)

Deleted: several

Formatted

... [50]

Field Code Changed

Deleted: . During these experiments,

Formatted: English (US)

Deleted: and

Deleted: rapidly increased ...ue to CO<sub>2</sub> degassing ... [51]

Formatted: English (US)

Formatted

... [52]

Deleted: Prior to the cruise, ...e improved our experimental system to allow mimicking future conditions by controlling atmospheric pCO<sub>2</sub> in addition to light and temperature (i.e. climate reactors). During our experiments, thanks to the control of atmospheric pCO<sub>2</sub> (~ 1000 ppm), ... [53]

Formatted: English (US)

Deleted: we ...ignificantly reduced ... [54]

Formatted: English (US)

Deleted: de...assing and maintained...pH levels close to experimental targets. However ... [55]

Formatted: English (US)

Deleted: can be seen

Formatted

... [56]

Deleted: as ...ompared to G1. ... [57]

Formatted: English (US)

Deleted: We attribute this

Formatted

... [58]

Deleted: to

Formatted

... [59]

Deleted: **we do not anticipate this as an issue.**

Deleted: The maximal intensity reached under control conditions (C1, C2) was between 900 and 1000 μmol photons m<sup>-2</sup> d<sup>-1</sup>. Although slightly lower than estimates for the Northwestern Mediterranean Sea at 5 m depth in June (~1100 μmol photons m<sup>-2</sup> d<sup>-1</sup>; Bernard Gentili, personal communication, 2017)

Formatted: English (US)

Deleted: ,

1001 close to estimates for the Northwestern Mediterranean Sea at 5 m depth in June (~1100  $\mu\text{mol}$

1002 photons  $\text{m}^{-2} \text{s}^{-1}$ ; Bernard Gentili, personal communication, 2017) and fairly consistent between

1003 duplicates under control and dust-amended conditions. Larger differences were observed between

1004 the two warmed and acidified tanks. The reasons of these discrepancies could result from small

1005 differences in terms of light intensity regulation between lids, of PAR sensors calibration and/or

1006 of different turbidity related to the amount of particles remaining in the tanks. As for pH

1007 discussed above, replication in terms of biological response appeared satisfactory for this

1008 treatment (except at station TYR; see below), and we believe these technical issues had no

1009 significant impacts on our results.

1010 Continuous measurements in the tanks showed that temperature was not spatially

1011 homogeneous, leading to significant differences among replicates. This was especially the case

1012 for warmed tanks (treatment G) for which a maximal average difference over the experimental

1013 period of 0.7 °C was observed during the FAST experiment. As for the other controlled

1014 parameters discussed above, these discrepancies did not systematically lead to observable

1015 differences in the investigated stocks and processes between duplicates (except at TYR, see

1016 below).

1017 The relatively low number of experimental units that could be installed inside an

1018 embarkable clean container, restrained our possibility to consider more than two replicates per

1019 treatment. Fortunately, as already said, differences between duplicates were, for the vast majority

1020 of studied variables and processes, lower than differences between treatments and appear

1021 acceptable considering the difficulty to incubate plankton communities for which slight

1022 differences in their initial composition can translate into very important differences in dynamics

1023 (Eggers et al., 2014). Nevertheless, we have to note that important discrepancies were detected

1024 regarding autotrophic stocks and processes (Gazeau et al., 2021) for tanks of the warmed and

1025 acidified treatment at station TYR. The reasons behind these differences are not fully understood

- Formatted ... [60]
- Deleted: conditions (C1, C2) ...nd under ...ust-amended conditions (D1, D2) ... [61]
- Deleted: . In contrast,
- Formatted: English (US)
- Formatted ... [62]
- Deleted: (G1 and G2; maximal differences of 100-200  $\mu\text{mol photons m}^{-2} \text{d}^{-1}$  depending on the experiment) that generally increased during each experiment...The reasons of these discrepancies are not clear and ... [63]
- Formatted: English (US)
- Deleted: of
- Formatted: English (US)
- Deleted: light intensity generated by the lids... of PAR sensors sensitivity ... [64]
- Formatted ... [65]
- Deleted: Unfortunately, a
- Formatted: English (US)
- Deleted: lthough r
- Formatted ... [66]
- Deleted: ), we can not fully exclude
- Formatted ... [67]
- Deleted: a potential
- Formatted ... [68]
- Deleted: of these technical issues ...n our results for this warmer and acidified treatment ... [69]
- Deleted: A similar conclusion can be drawn regarding temperature regulation in the container where
- Formatted: Indent: First line: 1.27 cm
- Formatted ... [70]
- Deleted:
- Formatted ... [71]
- Deleted: After this study, experimental tanks were installed in a new container in order to solve these problems.
- Formatted: English (US)
- Deleted: The experimental strategy chosen during thi ... [72]
- Formatted: English (US)
- Deleted: considering three
- Formatted: English (US)
- Deleted: different treatments: control, simulation of c ... [73]
- Formatted: English (US)
- Deleted: ery
- Formatted: English (US)
- Deleted: the different behavior of the autotrophic ... [74]
- Formatted: English (US)

1144 but we strongly suspect that heterotrophic nano-flagellates, feeding mainly on prokaryotic  
 1145 picoplankton (Sherr and Sherr, 1994), exerted a strong top-down control on this group in tank G1  
 1146 in which HNF abundance sharply increased during the experiment. ~~All in all, while the~~  
 1147 ~~methodology used in this study allowed to successfully evaluate the impacts of dust addition~~  
 1148 ~~under both present and future environmental conditions at two out of three tested waters, these~~  
 1149 discrepancies at station TYR prevent us from drawing any ~~strong conclusion on the effect of dust~~  
 1150 ~~addition on the dynamics of the community under future environmental conditions at that station.~~

### 1151 **4.3. Impact of dust addition under present environmental** 1152 **conditions**

1153 During the three experiments, the observed increases in NO<sub>x</sub> and DIP few hours after  
 1154 dust addition ~~under present environmental conditions~~ were rather similar to the enrichment levels  
 1155 obtained during the DUNE experiments at the surface of the mesocosms (~ 50 m<sup>3</sup>) after the  
 1156 simulation of a wet dust deposition using the same dust analog and the same simulated flux  
 1157 (Pulido-Villena et al., 2014; Ridame et al., 2014). ~~The intensity of this simulated wet deposition~~  
 1158 ~~event (i.e. 10 g m<sup>-2</sup>) represents a high but realistic scenario, as several studies reported even~~  
 1159 ~~higher short wet deposition events in this area of the Mediterranean Sea (Bonnet and Guieu,~~  
 1160 2006; Loÿe-Pilot and Martin, 1996; Temon et al., 2010). ~~Furthermore, based on previous studies~~  
 1161 ~~reporting the mixing between dust and polluted air masses during the atmospheric transport of~~  
 1162 ~~dust particles (e.g. Falkovich et al., 2001; Putaud et al., 2004), we chose to use an evapo-~~  
 1163 ~~condensed dust analog that mimics the processes taking place in the atmosphere prior to~~  
 1164 ~~deposition, essentially the adsorption of inorganic and organic soluble species (e.g. sulfate and~~  
 1165 nitrate; see Guieu et al., 2010a, for further details). ~~The imposed evapo-condensation processes~~  
 1166 ~~are responsible for the large nitrate releasing capacity of the dust particles used in our study. As a~~  
 1167 ~~consequence, the addition of new nutrients from dust in our study and during the P and R DUNE~~

- Deleted:** (+1100% in G1 vs. +300% in G2)
- Deleted:** Interestingly, while autotrophic prokaryotes were clearly impacted, no differences between the two tanks G1 and G2 were observed for heterotrophic prokaryotes although nanoflagellates are known to feed to this group as well (Sherr and Sherr, 1994). Heterotrophic nano-flagellates were likely not the only group of grazers which abundance increased during this experiment in tank G1 as the biomass of diatoms (i.e. Fucoxanthin) did not increase in this tank. Nevertheless, as no analyses of micro-grazer abundances were performed during the experiments, this hypothesis can not be verified. All in all
- Formatted:** English (US)
- Formatted:** English (US)
- Deleted:** our
- Deleted:** for this treatment
- Deleted:** remain an issue and
- Formatted:** English (US)
- Deleted:** combined effect of temperature and pH
- Formatted:** English (US)
- Deleted:**
- Deleted:** for
- Formatted:** English (US)
- Formatted:** English (US)
- Formatted:** English (US)
- Formatted:** English (US)
- Formatted:** English (US)
- Formatted:** English (US)
- Formatted:** English (US), Not Superscript/ Subscript
- Formatted:** English (US)
- Formatted:** English (US)
- Formatted:** English (US)
- Deleted:** P and R

1187 experiments were much higher, especially for NO<sub>x</sub>, than those observed by Pitta et al. (2017, and  
1188 references therein) and Ridame et al. (2014), following the simulation of a dry Saharan dust  
1189 deposition event. This confirms that wet dust deposition is a more efficient source of  
1190 bioavailable nutrients compared to dry dust deposition.

1191 Although NO<sub>x</sub> and DIP increases after dust addition were rather similar during our three  
1192 experiments, the subsequent dynamics of these elements and the impacts on plankton community  
1193 composition and functioning were drastically different. While NO<sub>x</sub> levels decreased moderately  
1194 over the course of our experiments due to biological uptake, more abrupt decreases were  
1195 observed for DIP released by dust, reaching values close to the ones observed in the controls,  
1196 except at station FAST, where concentrations were still above ambient levels at the end of the  
1197 experiment.

1198 Regarding biological stocks, most experiments reporting on the effect of dust addition in  
1199 the Mediterranean Sea showed significant increases in chlorophyll *a* concentrations (mean ~90%  
1200 increase; Guieu and Ridame, 2020). Interestingly, no stimulation of autotrophic biomass and  
1201 primary production rates (Gazeau et al., 2021) was observed in dust-amended tanks under  
1202 present conditions at station TYR. To the best of our knowledge, this is the first experimental  
1203 evidence of a complete absence of response from an autotrophic community following dust wet  
1204 deposition. The absence of response from autotrophic stocks could be due to a tight top-down  
1205 control from grazers hiding potential responses from the autotrophic community (Lekunberri et  
1206 al., 2010; Marañón et al., 2010) and/or a competition for nutritive resources with heterotrophic  
1207 prokaryotes (Marañón et al., 2010). Regarding the first hypothesis, Feliú et al. (2020) have  
1208 shown that the mesozooplankton assemblage at TYR was clearly impacted by a dust event that  
1209 took place nine days before sampling at that station as evidenced from particulate inventory of  
1210 lithogenic proxies (Al, Fe) in the water column (Bressac et al., in preparation). This dust  
1211 deposition likely stimulated phytoplankton growth and consequently increased the abundance of

- Deleted: s
- Formatted: English (US)
- Formatted: English (US)
- Formatted: English (US), Not Superscript/ Subscript
- Deleted: and Ridame et al.,
- Deleted: 2014
- Formatted: Indent: First line: 1.27 cm
- Formatted: English (US)
- Formatted: English (US)
- Deleted: moderately
- Deleted: (50-1420 nmol L<sup>-1</sup>, depending on the experiment)
- Formatted: English (US)
- Deleted: . The opposite feature was
- Formatted: English (US)
- Deleted: the
- Deleted: t
- Deleted: hat rapidly decreased during our experiments
- Deleted: in the D treatment
- Deleted: final
- Deleted: did not reach initial levels
- Formatted: English (US)
- Deleted: These enrichment levels, especially for NO<sub>x</sub>, were much higher than those observed by Pitta et al. (2017, and references therein) during land-based mesocosm experiments in the Eastern Mediterranean Sea, in which a dry Saharan deposition was simulated. In contrast to this experiment, the objective of our study was to assess the impact of wet dust deposition, the main dust deposition pathway in the Western Mediterranean Sea (Lojze-Pilot and Martin, 1996). Furthermore, following observations of mixing between dust and polluted air masses during their transport (e.g. Falkovich et al., 2001; Putaud et al., 2004), we chose to use an evapo-condensed dust analog that mimics the processes taking place in the atmosphere prior to deposition, essentially the adsorption of inorganic and organic soluble species (e.g. sulfate and nitrate; see Guieu et al., 2010a, for further details). The imposed evapo-condensation processes are responsible for the large nitrate releasing capacity of the dust particles used in our study. Regarding the intensity of simulated wet deposition event, the 10 g m<sup>-2</sup> deposition event considered here represents a high but realistic scenario, as several studies reported even higher short deposition events in this area (... [75])
- Formatted: English (US)
- Formatted: English (US)
- Formatted: English (US)
- Field Code Changed
- Formatted: English (US)
- Deleted: {Citation}
- Formatted: English (US)
- Deleted: 00/00/0000 00:00:00

1274 herbivorous grazers (copepods) and attracted carnivorous species. With respect to the second  
1275 hypothesis, it is well known that not only phytoplankton but also heterotrophic bacteria are  
1276 limited by inorganic nutrients, mainly DIP, in oligotrophic systems (Obenosterer et al., 2003;  
1277 Van Wambeke et al., 2001). Indeed, many recent studies have shown significant increase in  
1278 heterotrophic bacterial abundance, respiration and/or production following dust deposition (and  
1279 nutrient enrichment) in these areas (Lekunberri et al., 2010; Pitta et al., 2017; Pulido-Villena et  
1280 al., 2008; Romero et al., 2011). Most of the time, heterotrophic processes appear to be more  
1281 stimulated by dust pulses compared to autotrophic processes with increasing degree of  
1282 oligotrophy, the dominant response being modulated by the competition for nutrients between  
1283 phytoplankton and bacteria (Marañón et al., 2010). This is clearly what was observed at this  
1284 station, with heterotrophic prokaryotes reacting quickly and strongly to nutrient addition both in  
1285 terms of abundances and production rates (Gazeau et al., 2021). These two aforementioned  
1286 hypotheses are not mutually exclusive, and the quick response of heterotrophic prokaryotes to  
1287 dust addition is coherent with the strongest net heterotrophy of the tested waters at this station  
1288 (see 4.1). The strong stimulation of heterotrophic prokaryotes and the absence of detectable  
1289 effects on the autotrophic compartment drove the community towards an even stronger net  
1290 heterotrophic state, as illustrated by the decrease in the autotrophic to heterotrophic biomass ratio  
1291 following dust addition (data not shown). This was further shown by increases in community  
1292 respiration and decreases in net community production rates in dust-amended as compared to  
1293 control tanks (Gazeau et al., 2021) and suggest that dust addition to surface waters strongly  
1294 dominated by heterotrophs leads to a reduction of the capacity of these waters to export organic  
1295 matter and sequester atmospheric CO<sub>2</sub>.  
1296 In contrast to what was observed at TYR, fertilization of primary producers was observed at  
1297 stations ION and FAST under present conditions, with overall relative changes much higher than  
1298 from previous studies compiled by Guieu and Ridame (2020). The largest increase in chlorophyll

Formatted: French

Field Code Changed

Formatted: French

Formatted: English (US)

Formatted: English (US)

Formatted: English (US)

Formatted: English (US)

Formatted: English (US)

Formatted: Subscript

Formatted: Font colour: Auto

Deleted: Such

Formatted: English (US)

Deleted: indeed

Formatted: English (US)

Deleted: (maximum change in total chlorophyll *a* relative to the controls was ~280% at FAST and ~150% at ION)



1303 *a* concentrations at station FAST is coherent ~~with the largest NO<sub>x</sub> decrease observed in our~~  
1304 ~~study, which occurred at this station,~~ Interestingly, following dust addition at this station,  
1305 autotrophic production did not lead to DIP exhaustion throughout the experiment as DIP  
1306 concentrations were still above ambient conditions at the end of the experiment. Maximal  
1307 primary production rates (<sup>14</sup>C-incorporation) at this station at the end of the experiment suggest a  
1308 strong DIP recycling and the dominance of regenerated production towards the end of the  
1309 experiment (Gazeau et al., 2021). ~~Although, in some cases, *Synechococcus* appeared stimulated~~  
1310 ~~by dust addition~~ (Herut et al., 2005; Lagaria et al., 2017; Paytan et al., 2009). Guieu et al.  
1311 (2014b) showed ~~that,~~ based on the analysis of ~~several~~ aerosols addition studies, ~~this group~~ had  
1312 ~~generally~~ weak responses to aerosol addition in contrast to nano- and micro-phytoplankton,  
1313 suggesting that aerosol deposition may lead to an increase in larger size class phytoplankton.  
1314 Yet, at stations ION and FAST, ~~the increase in *Synechococcus* abundance in dust-amended tanks~~  
1315 ~~was the highest relative to those of pico- and nano-eukaryotes.~~ This was especially true at station  
1316 ION where no clear response to nutrient enrichment was observed for nano-eukaryotes  
1317 throughout the experiment. However, it must be stressed that our experiments were performed  
1318 over a relatively short period (3 to 4 days), and the sharp increase in Fucoxanthin paralleled by a  
1319 decrease in silicates, at the end of the experiment at station FAST where DIP limitation was not  
1320 yet apparent, suggests a delayed response of diatoms as compared to smaller groups (i.e.  
1321 autotrophic prokaryotes, pico- and nano-eukaryotes). Although this was not observed based on  
1322 pigment analyses, the sharp decline in nano-eukaryote abundances ~~in dust-amended tanks~~ at the  
1323 end of the FAST experiment, further suggests that this group, reacting quickly to nutrient  
1324 enrichment was progressively grazed and/or outcompeted by larger phytoplankton species.  
1325 ~~In contrast to what was observed at TYR,~~ at station FAST, the competition for nutrients  
1326 between autotrophs and heterotrophs was clearly in favor of autotrophs, ~~with a clear increase in~~  
1327 ~~the ratio between autotrophic and heterotrophic biomass reaching values of up to 4 (data not~~

- Deleted: with
- Formatted: Subscript
- Deleted: the largest observed NO<sub>x</sub> decrease following dust addition at this station
- Formatted: English (US)
- Formatted: English (US)
- Deleted:
- Deleted: (Gazeau et al., in preparation, this issue)
- Formatted: English (US)
- Formatted: English (US)
- Deleted: *Synechococcus*
- Deleted: were
- Formatted: English (US)
- Deleted: well stimulated
- Deleted: in some
- Deleted: dust
- Deleted: addition
- Deleted: experiment
- Formatted: English (US)
- Formatted: French
- Field Code Changed
- Formatted: English (US)
- Deleted: eight
- Formatted: English (US)
- Deleted: that *Synechococcus*
- Formatted: English (US)
- Deleted: in most of the cases a
- Formatted: English (US)
- Deleted: , similar to what was observed
- Deleted: both
- Formatted: English (US)
- Formatted: English (US)
- Formatted: English (US)
- Deleted: where *Synechococcus* abundance was clearly enhanced by dust deposition. The increase in *Synecho* (... [76])
- Formatted (... [77])
- Deleted: following dust addition
- Formatted (... [78])
- Deleted: In contrast to what was observed at stations (... [79])
- Formatted (... [80])
- Deleted: A
- Formatted (... [81])
- Formatted (... [82])

1412 ~~shown~~). While, as discussed above, all groups of primary producers benefited from nutrient  
 1413 enrichment at this station, the increases in heterotrophic prokaryote abundances were rather  
 1414 limited following dust deposition, leading to an increase of net community production rates  
 1415 throughout this experiment to reach positive levels while control tanks remained below  
 1416 metabolic balance (Gazeau et al., 2021). At station ION, the situation was somewhat  
 1417 intermediate with a ~~similar~~ enhancement of both autotrophic and heterotrophic stocks ~~and no~~  
 1418 ~~clear changes in the ratio between autotrophic and heterotrophic biomass (data not shown)~~,  
 1419 although the system ~~appeared~~ in favor of net autotrophy at the end of the experiment ~~in dust -~~  
 1420 ~~amended tanks under present environmental conditions~~ (Gazeau et al., 2021).

1421 Transfer of newly produced organic matter to higher trophic levels in the different  
 1422 treatments was evaluated through the quantification of meso-zooplankton abundance at the end  
 1423 of each experiment. Although we are fully aware that such an approach is certainly criticizable  
 1424 considering the low incubation times (3 to 4 days), it may still be representative of lowered  
 1425 mortality or faster growth. Altogether it does not appear as a surprise that an increase in meso-  
 1426 zooplankton abundances was only detected at station FAST where the strongest enhancement of  
 1427 primary production was observed. Such an increase in meso-zooplankton abundance in the dust-  
 1428 amended as compared to control treatment was observed during land-based mesocosm  
 1429 experiments in the Eastern Mediterranean Sea (Pitta et al., 2017).

1430 Finally, although no clear effects of dust deposition under present conditions were  
 1431 detectable on autotrophic prokaryotes at station TYR, the strongest increase in N<sub>2</sub> fixation rates  
 1432 was recorded at this station (~~Céline Ridame, unpublished results~~). However, the potential impact  
 1433 of this process on NO<sub>x</sub> concentration is highly negligible compared to the very large stock of  
 1434 NO<sub>x</sub> present in the dust-amended tanks, as less than 1 nmol L<sup>-1</sup> d<sup>-1</sup> of NO<sub>x</sub> can be produced by  
 1435 this process (~~Céline Ridame, unpublished results~~).

- Deleted:**
- Formatted:** English (US)
- Deleted:** (Gazeau et al., in preparation, this issue)
- Deleted:** parallel
- Formatted:** English (US)
- Formatted:** English (US)
- Deleted:**
- Deleted:** and processes
- Deleted:** was
- Formatted:** English (US)
- Deleted:** slightly
- Deleted:**
- Formatted:** English (US)
- Deleted:** (Gazeau et al., in preparation, this issue)

- Deleted:** (+434-503%, as compared to +173-256% and +41-49% at ION and FAST, respect
- Formatted:** English (US)
- Formatted:** English (US)
- Deleted:** ively; see Ridame et al., in preparation, this issue, for more details)
- Commented [C1]:** Je pense qu'il faut remplacer par "personal communication, 2021"
- Deleted:**
- Formatted:** English (US)
- Formatted:** English (US)
- Formatted:** English (US)
- Deleted:** (Ridame et al., in preparation, this issue)

1451 **4.4. Impact of dust addition under future environmental**  
1452 **conditions**

1453 Very few past studies have investigated the release and fate of nutrients from atmospheric  
1454 particles under climate conditions as expected for the end of the century, and, to the best of our  
1455 knowledge, our study represents the first attempt to test for the combined effect of ocean  
1456 warming and acidification on these processes. Louis et al. (2018) have already shown from an  
1457 experiment performed under close-to-abiotic conditions (seawater filtration onto 0.2 µm) that  
1458 even an extreme ocean acidification scenario (~ -0.6 pH units) does not impact the bioavailability  
1459 of macro- and micro-nutrients (NO<sub>x</sub>, DIP and DFe) from dust addition for surface phytoplankton  
1460 communities in the oligotrophic Northwestern Mediterranean Sea, using the same dust analog  
1461 and simulated flux as used during our experiments. Similar results were presented by Mélançon  
1462 et al. (2016) regarding the release of DFe from dust in high-nutrient low-chlorophyll (HNLC)  
1463 waters of the Northeastern Pacific, following a mild ocean acidification scenario of -0.2 pH  
1464 units. As no differences were observed for NO<sub>x</sub> and DIP concentrations within few hours  
1465 following dust addition under present and future environmental conditions, our results agree with  
1466 these previous findings and further highlights the absence of direct effect of ocean warming (+3  
1467 °C) on the release of nutrients from atmospheric particles.

1468 In contrast, following these similar nutrient releases, different nutrient consumption  
1469 dynamics were observed between ambient and warmed/acidified tanks. These differences were  
1470 substantially dependent on the considered nutrient and investigated station. Regarding NO<sub>x</sub>, no  
1471 impacts of warming and acidification could be observed at stations TYR and ION due to low net  
1472 decreasing rates compared to the large increase following dust addition. In contrast, at the most  
1473 productive station FAST, as a consequence of strongly enhanced biological stocks (see

- Formatted: English (US)
- Deleted: warming and acidification
- Formatted: English (US)

- Formatted: French
- Field Code Changed
- Formatted: French
- Formatted: French
- Deleted: abiotic dust
- Formatted: French
- Formatted: French
- Formatted: French
- Formatted: French
- Formatted: French
- Formatted: English (US)
- Formatted: Subscript
- Deleted: 0
- Formatted: English (US)
- Deleted: highlighted
- Formatted: English (US)
- Formatted: English (US)
- Deleted: The differences
- Formatted: English (US)
- Deleted: in
- Formatted: English (US)
- Deleted: between
- Formatted: English (US)
- Formatted: English (US)
- Deleted:
- Deleted: while
- Formatted: English (US)
- Deleted:
- Deleted: increase following additiono large variability between the duplicates (Table 4),
- Formatted: English (US)
- Deleted: a
- Formatted: English (US)

1487 thereafter) and metabolic rates (Gazeau et al., 2021), larger NO<sub>x</sub> consumption rates were shown  
1488 under future environmental conditions.

1489 The differences in DIP dynamics between the two dust-amended treatments were more  
1490 complex to interpret depending on the investigated station. A clear feature of our experiments is  
1491 that, in contrast to present day pH and temperature conditions, all the stock of DIP released from  
1492 dust was consumed at the end of the three experiments under future conditions, suggesting a  
1493 much faster consumption by autotrophs and heterotrophic prokaryotes. That being said, the rate  
1494 of decrease under future environmental conditions differed depending on the station. While DIP  
1495 dynamics were quite similar between tanks maintained under present and future environmental  
1496 conditions at ION, warming and acidification induced a faster decrease of DIP at TYR and  
1497 FAST, with a full consumption of the released DIP within 24 h. An interesting outcome at station  
1498 TYR was that, despite the important discrepancies observed for autotrophic stocks and metabolic  
1499 rates between the duplicates G1 and G2 (see section 4.2), a very similar dynamics was observed  
1500 for DIP concentrations in these tanks. As heterotrophic prokaryote biomass and production rates  
1501 (Gazeau et al., 2021) did not differ between these duplicate tanks, this further highlights the clear  
1502 dominance of heterotrophic processes at this station, a dominance which was exacerbated by dust  
1503 addition under future environmental conditions, leading to an even stronger heterotrophic state at  
1504 the end of this experiment (Gazeau et al., 2021).

1505 At station ION, large impacts of warming and acidification have been observed,  
1506 especially for primary producers, as shown by almost doubled chlorophyll *a* concentrations as  
1507 compared to dust amended tanks (D). At this station, all autotrophic groups benefited from ocean  
1508 acidification and warming. *Synechococcus* and to a lesser extent pico-eukaryotes appeared as the  
1509 most impacted ones. Yet these differences of sensitivity among autotrophs did not lead to  
1510 detectable changes in the composition of the autotrophic assemblage as compared to ambient  
1511 conditions, with still a large dominance of nano-eukaryote carbon biomass at the end of this

Deleted: (Gazeau et al., in preparation, this issue)

Deleted: climate

Formatted: English (US)

Formatted: English (US)

Deleted:

Formatted: Indent: First line: 1.27 cm

Formatted: English (US)

Formatted: English (US)

Deleted: decreasing rates of

Formatted: English (US)

Deleted: DIP concentrations for that

Formatted: English (US)

Formatted: English (US)

Deleted: treatment

Deleted: (Table 4)

Deleted: quite

Deleted: treatments

Formatted: English (US)

Deleted: a clear effect of

Formatted: English (US)

Formatted: English (US)

Deleted: was shown

Deleted: station

Formatted: English (US)

Deleted: where the vast majority of released DIP was consumed within 24 h ( $\Delta$ DIP = -1.3 and -1.1 to -1.5 nmol L<sup>-1</sup> h<sup>-1</sup> at TYR and FAST, respectively)

Deleted:

Deleted: (Gazeau et al., in preparation, this issue)

Deleted: and

Formatted: English (US)

Deleted: climate

Formatted: English (US)

Formatted: English (US)

Formatted: English (US)

Deleted: .

Deleted: DIP consumption rates were similar following dust addition under present and future conditions. This results appears surprising as

1535 experiment (62% in treatment G vs. 64% in treatment D). Interestingly, although the ratio  
1536 between autotrophic and heterotrophic biomass appeared impacted positively under future  
1537 environmental conditions, reaching values of up to 2 at the end of this experiment (data not  
1538 shown), warming and acidification led to a decrease in net community production (Gazeau et al.,  
1539 2021) suggesting that in the coming decades the capacity of surface seawater to sequester  
1540 anthropogenic CO<sub>2</sub> will be lowered.

1541 Similarly, at FAST, all phytoplankton groups were impacted positively by warming and  
1542 acidification with the strongest changes detected for *Synechococcus* as compared to present  
1543 environmental conditions. However, in contrast to station ION, all groups reached maximal  
1544 abundances (and carbon biomass) after 3 days of incubations, thereafter drastically decreasing  
1545 most likely as a consequence of DIP limitation (see above). It must be stressed that this pattern  
1546 could not be observed through pigment dynamics as no sampling was performed for these  
1547 analyses after 3 days of incubation. Also, in contrast to station ION, the abundance of  
1548 heterotrophic prokaryotes in the warmer and acidified treatment reached a maximum after 2 days  
1549 of incubations and then strongly decreased to reach levels observed in the control treatment. This  
1550 suggests that the heterotrophic compartment was the first to suffer from DIP limitation and  
1551 further highlights the dominance of the autotrophic compartment in terms of nutrient

1552 consumption at this station. As observed at station ION, although the ratio between autotrophic  
1553 and heterotrophic biomass increased under future environmental conditions, Gazeau et al. (2021)  
1554 reported on a decrease in net community production rates in this treatment as compared to  
1555 ambient environmental conditions, suggesting that, in the future, nutrient release from dust will  
1556 lead to a lesser sequestration capacity of surface waters for atmospheric CO<sub>2</sub>.

1557 These positive effects of warming and acidification on the abundance of phytoplankton cells,  
1558 especially for small species, as observed at ION and FAST are in line with previously published  
1559 studies. Indeed, although very contrasted results have been shown on the effect of ocean

**Formatted:** English (US)

**Deleted:** that in the coming decades the

**Formatted:** Not Superscript/ Subscript

**Deleted:** will be lowered

**Deleted:** Very contrasted results have been shown on the effect of ocean acidification on small autotrophic species (e.g. Dutkiewicz et al., 2015) while there are increasing evidences that small phytoplankton species will be favored in a warmer ocean (e.g. Chen et al., 2014; Daufresne et al., 2009; Morán et al., 2010). As mentioned earlier, our experimental protocol was not conceived to discriminate temperature from pH effects, however results concur with those of Maugeud et al. (2015) which further suggested temperature over elevated CO<sub>2</sub> as the main driver of increased picophytoplankton abundance. As heterotrophic prokaryotes were also positively impacted by future environmental conditions, the similarity of DIP dynamics between ambient and future conditions suggests a tight coupling between the autotrophic and heterotrophic compartments at this station. This is further evidenced by the absence of differences detected over the relatively short time duration of our experiment on meso-zooplankton abundance and carbon export efficiency (Gazeau et al., 2021)(Gazeau et al., in preparation, this issue).

**Formatted:** Subscript

**Deleted:** A

**Formatted:** English (US)

**Deleted:** similar to what was observed at station ION,

**Deleted:** ic

**Deleted:** positively

**Formatted:** English (US)

**Deleted:** ambient

**Formatted:** English (US)

**Deleted:** The differential dynamics of these two compartments under warmer and acidified conditions most likely led to an excess production of organic matter that translated, for instance, in higher dissolved organic carbon concentrations in this treatment

**Formatted:** English (US)

**Formatted:** English (US)

**Deleted:** (Gazeau et al., 2021)(Gazeau et al., in preparation, this issue)

**Formatted:** English (US)

**Deleted:** in the future

**Deleted:**

**Deleted:** release from

**Deleted:** involve/

**Deleted:** lead to

**Formatted:** Subscript

**Deleted:** .

**Deleted:** in line

1600 acidification on small autotrophic species (e.g. Dutkiewicz et al., 2015), there is increasing  
 1601 evidence that small phytoplankton species will be favored in a warmer ocean (e.g. Chen et al.,  
 1602 2014; Daufresne et al., 2009; Morán et al., 2010). As mentioned earlier, our experimental  
 1603 protocol was not conceived to discriminate temperature from pH effects, however results concur  
 1604 with those of Maugendre et al. (2015) which further suggested temperature over elevated CO<sub>2</sub> as  
 1605 the main driver of increased picophytoplankton abundance in the Mediterranean Sea.  
 1606 These enhanced fertilizing effects on primary producers at ION and FAST, under future  
 1607 as compared to present environmental conditions, did not seem to reach higher trophic levels as  
 1608 no clear differences in meso-zooplankton abundances were observed between ambient and  
 1609 warmed/acidified tanks at the end of the experiments. We fully acknowledge that the duration of  
 1610 our experiments was certainly too short to carefully assess the proportion of newly formed  
 1611 organic matter consumed by meso-zooplankton, species and its effect on their abundances, yet  
 1612 group-specific variations were observed. Similarly, Gazeau et al. (2021) did not observe an  
 1613 additional impact of future environmental conditions on the export of organic matter after dust  
 1614 addition.  
 1615

- Formatted: English (US)
- Formatted: English (US)
- Field Code Changed
- Formatted: French
- Deleted: (in the Mediterranean Sea?)
- Deleted: This
- Formatted: English (US)
- Formatted: English (US)
- Formatted: English (US)
- Formatted: Indent: First line: 1.27 cm, Line spacing: Double
- Deleted: excess production
- Deleted: ambient
- Formatted: English (US)
- Formatted: English (US)
- Formatted: English (US)
- Deleted: ic
- Deleted: Finally
- Formatted: English (US)
- Formatted: English (US)
- Deleted: it appeared that at least part of this excess organic matter was exported to the bottom of the tanks as a higher carbon export efficiency was observed at this station under warmer and acidified conditions
- Deleted: (Gazeau et al., 2021)(Gazeau et al., in preparation, this issue)
- Formatted: English (US)
- Formatted: English (US)
- Deleted: .
- Formatted: Indent: First line: 1.27 cm

## 1629 5. Conclusion

1630 These experiments conducted during the PEACETIME cruise represent the first attempt  
1631 to investigate the impacts of atmospheric deposition on surface plankton communities both under  
1632 present and future environmental conditions. Despite few experimental issues that are discussed,  
1633 the three experiments provided new insights on these potential impacts in the open  
1634 Mediterranean Sea. Interestingly, the effect of dust deposition was highly different between the  
1635 three investigated stations in the Tyrrhenian Sea, Ionian Sea and in the Algerian basin. As the  
1636 initial conditions in the sampled surface seawater at the three stations were very similar in terms  
1637 of nutrient availability and chlorophyll content, these differences rather seem to be a  
1638 consequence of the initial metabolic states of the community (autotrophy vs. heterotrophy). In all  
1639 three cases, nutrient addition from dust deposition did not strongly modify but rather exacerbated  
1640 this initial state. Relative changes in main parameters presented in this manuscript and processes  
1641 presented in Gazeau et al. (2021) as a consequence of dust addition under present and future  
1642 environmental conditions are shown in Fig. 10, and compared to the compilation of published  
1643 data for the Mediterranean Sea from Guieu and Ridame (2020). At station TYR, under  
1644 conditions of a clear dominance of heterotrophs on the use of resources and potentially a higher  
1645 top-down control from grazers, dust addition drove the community into an even more  
1646 heterotrophic state with no detectable effect on primary producers. At station ION, where the  
1647 community was initially closer to metabolic balance, both heterotrophic and autotrophic  
1648 compartments benefited from dust derived nutrients. At FAST, the most active station in terms  
1649 of autotrophic production, addition of nutrients boosted both compartments but heterotrophic  
1650 prokaryotes became quickly P-limited and overall larger effects were observed for  
1651 phytoplankton. Ocean acidification and warming did not have any detectable impact on the  
1652 release of nutrients from atmospheric particles. Furthermore, these external drivers did not

Deleted: (in preparation, this issue)

Formatted: English (US)

1654 drastically modify the composition of the autotrophic assemblage with all groups benefiting from  
1655 warmer and acidified conditions. However, ~~although for two out of the three stations~~  
1656 ~~investigated,~~ larger increases were observed for autotrophic ~~as compared to~~ heterotrophic stocks  
1657 ~~under future environmental conditions,~~ a stronger impact of warming and acidification on  
1658 ~~mineralization processes~~ (Gazeau et al., 2021) suggests that, in the future, the plankton  
1659 communities of Mediterranean surface waters will have ~~a decreased capacity to sequester~~  
1660 ~~atmospheric CO<sub>2</sub> following the deposition of atmospheric particles,~~

- Formatted: English (US)
- Deleted: very
- Deleted: both
- Deleted: and
- Formatted: English (US)
- Formatted: English (US)
- Formatted: English (US)
- Formatted: English (US)
- Deleted: and processes
- Deleted: ing an exacerbation of effects from atmospheric dust deposition in the future, rather than a change in the
- Formatted: English (US)
- Formatted: English (US)
- Formatted: Subscript
- Deleted: as a source or a sink of CO<sub>2</sub> to or from the atmosphere...
- Formatted: English (US)
- Deleted:
- Formatted: English (US)



1670 **Data availability**

1671 All data and metadata will be made available at the French INSU/CNRS LEFE CYBER database  
1672 (scientific coordinator: Hervé Claustre; data manager, webmaster: Catherine Schmechtig).  
1673 INSU/CNRS LEFE CYBER (2020)

1674 **Author contributions**

1675 FG and CG designed and supervised the study. FG, CG, CR and KD sampled seawater from the  
1676 experimental tanks during the experiments. JMG and GDL participated in the technical  
1677 preparation of the experimental system and all authors participated in sample analyses. FG, CR  
1678 and CG wrote the paper with contributions from all authors.

1679 **Financial support**

1680 This study is a contribution to the PEACETIME project (<http://peacetime-project.org>), a joint  
1681 initiative of the MERMEX and ChArMEx components supported by CNRS-INSU, IFREMER,  
1682 CEA, and Météo-France as part of the programme MISTRALS coordinated by INSU.  
1683 PEACETIME is a contribution to SOLAS and IMBER international programme. The project was  
1684 endorsed as a process study by GEOTRACES. PEACETIME cruise  
1685 (<https://doi.org/10.17600/17000300>). The project leading to this publication has also received  
1686 funding from the European FEDER Fund under project 1166-39417.

1687 **Acknowledgments**

1688 The authors thank the captain and the crew of the RV Pourquoi Pas ? for their professionalism  
1689 and their work at sea. We thank Julia Uitz, Céline Dimier and the SAPIGH HPLC analytical  
1690 service at Institut de la Mer de Villefranche (IMEV) for sampling and analysis of phytoplankton  
1691 pigments, John Dolan for microscopic countings as well as Lynne Macarez and the PIQv-

Formatted: Font: Not Italic

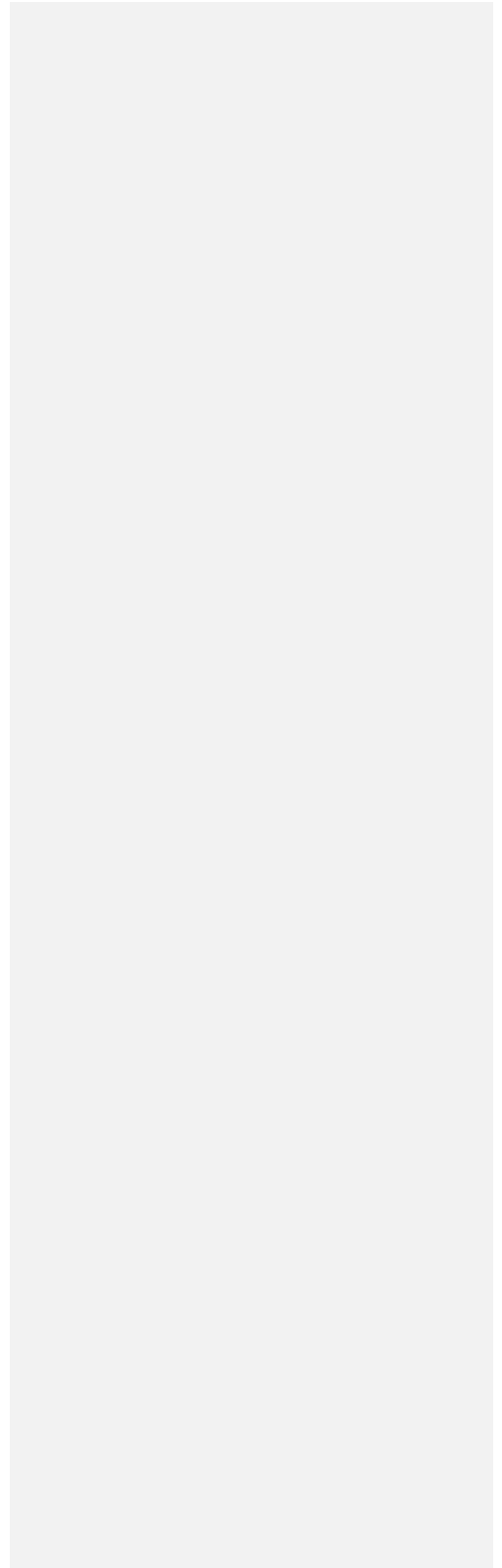
Formatted: Font: Not Italic

Formatted: English (US)

Formatted: Font: Not Italic

Formatted: English (US)

1692 platform of EMBRC-France, a national Research Infrastructure supported by ANR, under the  
1693 reference ANR-10-INSB-02, for mesozooplankton analyses.



1694 **References**

- 1695 Aminot, A. and K erouel, R.: Dosage automatique des nutriments dans les eaux marines :  
1696 m ethodes en flux continu, Editions Ifremer, m ethodes d'analyse en milieu marin., 2007.
- 1697 Behrenfeld, M. J., O'Malley, R. T., Siegel, D. A., McClain, C. R., Sarmiento, J. L., Feldman, G.  
1698 C., Milligan, A. J., Falkowski, P. G., Letelier, R. M. and Boss, E. S.: Climate-driven trends  
1699 in contemporary ocean productivity, *Nature*, 444(7120), 752–755, 2006.
- 1700 Bergametti, Gi., Dutot, A.-L., Buat-M enard, P., Losno, R. and Remoudaki, E.: Seasonal  
1701 variability of the elemental composition of atmospheric aerosol particles over the  
1702 Northwestern Mediterranean, *Tellus B: Chemical and Physical Meteorology*, 41(3), 353–  
1703 361, <https://doi.org/10.3402/tellusb.v41i3.15092>, 1989.
- 1704 Bonnet, S. and Guieu, C.: Atmospheric forcing on the annual iron cycle in the western  
1705 Mediterranean Sea: A 1-year survey, *Journal of Geophysical Research: Oceans*, 111(C9),  
1706 <https://doi.org/10.1029/2005JC003213>, 2006.
- 1707 Bonnet, S., Guieu, C., Chiaverini, J., Ras, J. and Stock, A.: Effect of atmospheric nutrients on the  
1708 autotrophic communities in a low nutrient, low chlorophyll system, *Limnology and*  
1709 *Oceanography*, 50(6), 1810–1819, <https://doi.org/10.4319/lo.2005.50.6.1810>, 2005.
- 1710 B orsheim, K. Y. and Bratbak, G.: Cell volume to cell carbon conversion factors for a  
1711 bacterivorous *Monas* sp. enriched from seawater, *Marine Ecology Progress Series*, 36(2),  
1712 171–175, 1987.
- 1713 Bosc, E., Bricaud, A. and Antoine, D.: Seasonal and interannual variability in algal biomass and  
1714 primary production in the Mediterranean Sea, as derived from 4 years of SeaWiFS  
1715 observations, *Global Biogeochemical Cycles*, 18(1),  
1716 <https://doi.org/10.1029/2003GB002034>, 2004.
- 1717 Bressac, M. and Guieu, C.: Post-depositional processes: What really happens to new atmospheric  
1718 iron in the ocean's surface?, *Global Biogeochemical Cycles*, 27(3), 859–870,  
1719 <https://doi.org/10.1002/gbc.20076>, 2013.

Formatted: French

1720 Bressac, M., Wagener, T., Tovar-Sanchez, A., Ridame, C., Albani, S., Fu, F., Desboeufs, K. and  
1721 Guieu, C.: Residence time of dissolved and particulate trace elements in the surface  
1722 Mediterranean Sea (Peacetime cruise), *Biogeosciences*, in preparation.

1723 Bressac, M., Guieu, C., Doxaran, D., Bourrin, F., Desboeufs, K., Leblond, N. and Ridame, C.:  
1724 Quantification of the lithogenic carbon pump following a simulated dust-deposition event  
1725 in large mesocosms, *Biogeosciences*, 11(4), 1007–1020, [https://doi.org/10.5194/bg-11-](https://doi.org/10.5194/bg-11-1007-2014)  
1726 1007-2014, 2014.

1727 Chen, B., Liu, H., Huang, B. and Wang, J.: Temperature effects on the growth rate of marine  
1728 picoplankton, *Marine Ecology Progress Series*, 505, 37–47,  
1729 <https://doi.org/10.3354/meps10773>, 2014.

1730 Christaki, U., Courties, C., Massana, R., Catala, P., Lebaron, P., Gasol, J. M. and Zubkov, M. V.:  
1731 Optimized routine flow cytometric enumeration of heterotrophic flagellates using SYBR  
1732 Green I, *Limnology and Oceanography: Methods*, 9(8), 329–339,  
1733 <https://doi.org/10.4319/lom.2011.9.329>, 2011.

1734 Daufresne, M., Lengfellner, K. and Sommer, U.: Global warming benefits the small in aquatic  
1735 ecosystems, *PNAS*, 106(31), 12788–12793, <https://doi.org/10.1073/pnas.0902080106>,  
1736 2009.

1737 Desboeufs, K., Leblond, N., Wagener, T., Bon Nguyen, E. and Guieu, C.: Chemical fate and  
1738 settling of mineral dust in surface seawater after atmospheric deposition observed from  
1739 dust seeding experiments in large mesocosms, *Biogeosciences*, 11(19), 5581–5594,  
1740 <https://doi.org/10.5194/bg-11-5581-2014>, 2014.

1741 Desboeufs, K., Bon Nguyen, E., Chevaillier, S., Triquet, S. and Dulac, F.: Fluxes and sources of  
1742 nutrient and trace metal atmospheric deposition in the Northwestern Mediterranean,  
1743 *Atmospheric Chemistry and Physics*, 18(19), 14477–14492, [https://doi.org/10.5194/acp-](https://doi.org/10.5194/acp-18-14477-2018)  
1744 18-14477-2018, 2018.

1745 Dickson, A. G., Sabine, C. L. and Christian, J. R.: Guide to best practices for ocean CO<sub>2</sub>  
1746 measurements, PICES, Sydney., 2007.

1747 Dinasquet, J., Bigeard, E., Gazeau, F., Marañón, E., Ridame, C., Van Wambeke, F.,  
1748 Obernosterer, I. and Baudoux, A.-C.: Impact of dust enrichment on the microbial food web  
1749 under present and future conditions of pH and temperature, Biogeosciences Discussions,  
1750 2021.

1751 Djaoudi, K., Van Wambeke, F., Coppola, L., D'Ortenzio, F., Helias-Nunige, S., Raimbault, P.,  
1752 Taillandier, V., Testor, P., Wagener, T. and Pulido-Villena, E.: Sensitive Determination of  
1753 the Dissolved Phosphate Pool for an Improved Resolution of Its Vertical Variability in the  
1754 Surface Layer: New Views in the P-Depleted Mediterranean Sea, *Front. Mar. Sci.*, 5,  
1755 <https://doi.org/10.3389/fmars.2018.00234>, 2018.

1756 D'Ortenzio, F., Iudicone, D., Montegut, C. de B., Testor, P., Antoine, D., Marullo, S., Santoleri,  
1757 R. and Madec, G.: Seasonal variability of the mixed layer depth in the Mediterranean Sea  
1758 as derived from in situ profiles, *Geophysical Research Letters*, 32(12),  
1759 <https://doi.org/10.1029/2005GL022463>, 2005.

1760 Duce, R. A., Liss, P. S., Merrill, J. T., Atlas, E. L., Buat-Menard, P., Hicks, B. B., Miller, J. M.,  
1761 Prospero, J. M., Arimoto, R., Church, T. M., Ellis, W., Galloway, J. N., Hansen, L.,  
1762 Jickells, T. D., Knap, A. H., Reinhardt, K. H., Schneider, B., Soudine, A., Tokos, J. J.,  
1763 Tsunogai, S., Wollast, R. and Zhou, M.: The atmospheric input of trace species to the  
1764 world ocean, *Global Biogeochemical Cycles*, 5(3), 193–259,  
1765 <https://doi.org/10.1029/91GB01778>, 1991.

1766 Dutkiewicz, S., Morris, J. J., Follows, M. J., Scott, J., Levitan, O., Dyrhman, S. T. and Berman-  
1767 Frank, I.: Impact of ocean acidification on the structure of future phytoplankton  
1768 communities, *Nature Climate change*, 5, 1002–1006, <https://doi.org/10.1038/nclimate2722>,  
1769 2015.

1770 Emerson, S., Quay, P., Karl, D., Winn, C., Tupas, L. and Landry, M.: Experimental  
1771 determination of the organic carbon flux from open-ocean surface waters, *Nature*,  
1772 389(6654), 951–954, <https://doi.org/10.1038/40111>, 1997.

1773 Falkovich, A. H., Ganor, E., Levin, Z., Formenti, P. and Rudich, Y.: Chemical and mineralogical  
1774 analysis of individual mineral dust particles, *Journal of Geophysical Research:*  
1775 *Atmospheres*, 106(D16), 18029–18036, <https://doi.org/10.1029/2000JD900430>, 2001.

1776 Feliú, G., Pagano, M., Hidalgo, P. and Carlotti, F.: Structure and function of epipelagic  
1777 mesozooplankton and their response to dust deposition events during the spring  
1778 PEACETIME cruise in the Mediterranean Sea, *Biogeosciences*, 17, 5417–5441,  
1779 <https://doi.org/10.5194/bg-17-5417-2020>, 2020.

1780 Gazeau, F., Van Wambeke, F., Marañón, E., Pérez-Lorenzo, M., Alliouane, S., Stolpe, C.,  
1781 Blasco, T., Leblond, N., Zäncker, B., Engel, A., Marie, B., Dinasquet, J. and Guieu, C.:  
1782 Impact of dust addition on the metabolism of Mediterranean plankton communities and  
1783 carbon export under present and future conditions of pH and temperature, *Biogeosciences*  
1784 *Discussions*, 2021.

1785 Giovagnetti, V., Brunet, C., Conversano, F., Tramontano, F., Obernosterer, I., Ridame, C. and  
1786 Guieu, C.: Assessing the role of dust deposition on phytoplankton ecophysiology and  
1787 succession in a low-nutrient low-chlorophyll ecosystem: a mesocosm experiment in the  
1788 Mediterranean Sea, *Biogeosciences*, 10(5), 2973–2991, [https://doi.org/10.5194/bg-10-](https://doi.org/10.5194/bg-10-2973-2013)  
1789 [2973-2013](https://doi.org/10.5194/bg-10-2973-2013), 2013.

1790 Gorsky, G., Ohman, M. D., Picheral, M., Gasparini, S., Stemmann, L., Romagnan, J.-B.,  
1791 Cawood, A., Pesant, S., García-Comas, C. and Prejger, F.: Digital zooplankton image  
1792 analysis using the ZooScan integrated system, *J Plankton Res*, 32(3), 285–303,  
1793 <https://doi.org/10.1093/plankt/fbp124>, 2010.

1794 Guieu, C. and Ridame, C.: Impact of atmospheric deposition on marine chemistry and  
1795 biogeochemistry, in *Atmospheric Chemistry in the Mediterranean Region: Comprehensive*

1796           Diagnosis and Impacts, edited by F. Dulac, S. Sauvage, and E. Hamonou, Springer, Cham,  
1797           Switzerland, , 2020.

1798   Guieu, C., Dulac, F., Desboeufs, K., Wagener, T., Pulido-Villena, E., Grisoni, J.-M., Louis, F.,  
1799           Ridame, C., Blain, S., Brunet, C., Bon Nguyen, E., Tran, S., Labiadh, M. and Dominici, J.-  
1800           M.: Large clean mesocosms and simulated dust deposition: a new methodology to  
1801           investigate responses of marine oligotrophic ecosystems to atmospheric inputs,  
1802           *Biogeosciences*, 7(9), 2765–2784, <https://doi.org/10.5194/bg-7-2765-2010>, 2010a.

1803   Guieu, C., Loye-Pilot, M. D., Benyahya, L. and Dufour, A.: Spatial variability of atmospheric  
1804           fluxes of metals (Al, Fe, Cd, Zn and Pb) and phosphorus over the whole Mediterranean  
1805           from a one-year monitoring experiment: Biogeochemical implications, *Marine Chemistry*,  
1806           120(1–4), 164–178, <https://doi.org/10.1016/j.marchem.2009.02.004>, 2010b.

1807   Guieu, C., Ridame, C., Pulido-Villena, E., Bressac, M., Desboeufs, K. and Dulac, F.: Impact of  
1808           dust deposition on carbon budget: a tentative assessment from a mesocosm approach,  
1809           *Biogeosciences*, 11(19), 5621–5635, 2014a.

1810   Guieu, C., Aumont, O., Paytan, A., Bopp, L., Law, C. S., Mahowald, N., Achterberg, E. P.,  
1811           Marañón, E., Salihoglu, B., Crise, A., Wagener, T., Herut, B., Desboeufs, K., Kanakidou,  
1812           M., Olgun, N., Peters, F., Pulido-Villena, E., Tovar-Sanchez, A. and Völker, C.: The  
1813           significance of the episodic nature of atmospheric deposition to Low Nutrient Low  
1814           Chlorophyll regions, *Global Biogeochemical Cycles*, 28(11), 1179–1198,  
1815           <https://doi.org/10.1002/2014GB004852>, 2014b.

1816   Guieu, C., D’Ortenzio, F., Dulac, F., Taillandier, V., Doglioli, A., Petrenko, A., Barrillon, S.,  
1817           Mallet, M., Nabat, P. and Desboeufs, K.: Process studies at the air-sea interface after  
1818           atmospheric deposition in the Mediterranean Sea: objectives and strategy of the  
1819           PEACETIME oceanographic campaign (May–June 2017), *Biogeosciences*, 2020(17),  
1820           5563–5585, <https://doi.org/10.5194/bg-17-5563-2020>, 2020.

1821 Herut, B., Zohary, T., Krom, M. D., Mantoura, R. F. C., Pitta, P., Psarra, S., Rassoulzadegan, F.,  
1822 Tanaka, T. and Frede Thingstad, T.: Response of East Mediterranean surface water to  
1823 Saharan dust: On-board microcosm experiment and field observations, *Deep Sea Research*  
1824 Part II: Topical Studies in Oceanography, 52(22), 3024–3040,  
1825 <https://doi.org/10.1016/j.dsr2.2005.09.003>, 2005.

1826 Holmes, R. M., Aminot, A., K rouel, R., Hooker, B. A. and Peterson, B. J.: A simple and precise  
1827 method for measuring ammonium in marine and freshwater ecosystems, *Can. J. Fish.*  
1828 *Aquat. Sci.*, 56(10), 1801–1808, <https://doi.org/10.1139/f99-128>, 1999.

1829 IPCC: *Climate Change, The Physical Science Basis.*, 2013.

1830 IPCC: *IPCC Special Report on the Ocean and Cryosphere in a Changing Climate*, edited by H.  
1831 O. P rtner, D. C. Roberts, V. Masson-Delmotte, P. Zhai, M. Tignor, E. Poloczanska, K.  
1832 Mintenbeck, A. Alegria, M. Nicolai, A. Okem, J. Petzold, B. Rama, and N. M. Weyer.,  
1833 2019.

1834 Irwin, A. J. and Oliver, M. J.: Are ocean deserts getting larger?, *Geophysical Research Letters*,  
1835 36, <https://doi.org/10.1029/2009gl039883>, 2009.

1836 Jickells, T. D., An, Z. S., Andersen, K. K., Baker, A. R., Bergametti, G., Brooks, N., Cao, J. J.,  
1837 Boyd, P. W., Duce, R. A., Hunter, K. A., Kawahata, H., Kubilay, N., laRoche, J., Liss, P.  
1838 S., Mahowald, N., Prospero, J. M., Ridgwell, A. J., Tegen, I. and Torres, R.: Global Iron  
1839 Connections Between Desert Dust, Ocean Biogeochemistry, and Climate, *Science*,  
1840 308(5718), 67–71, <https://doi.org/10.1126/science.1105959>, 2005.

1841 Kana, T. M. and Glibert, P. M.: Effect of irradiances up to 2000  $\mu\text{E m}^{-2} \text{s}^{-1}$  on marine  
1842 *Synechococcus* WH7803—I. Growth, pigmentation, and cell composition, *Deep Sea*  
1843 *Research Part A. Oceanographic Research Papers*, 34(4), 479–495,  
1844 [https://doi.org/10.1016/0198-0149\(87\)90001-X](https://doi.org/10.1016/0198-0149(87)90001-X), 1987.



1845 Kapsenberg, L., Alliouane, S., Gazeau, F., Mousseau, L. and Gattuso, J.-P.: Coastal ocean  
1846 acidification and increasing total alkalinity in the northwestern Mediterranean Sea, *Ocean*  
1847 *Science*, 13, 411–426, <https://doi.org/10.5194/os-13-411-2017>, 2017.

1848 Kouvarakis, G., Mihalopoulos, N., Tselepidis, A. and Stavrakakis, S.: On the importance of  
1849 atmospheric inputs of inorganic nitrogen species on the productivity of the Eastern  
1850 Mediterranean Sea, *Global Biogeochemical Cycles*, 15(4), 805–817,  
1851 <https://doi.org/10.1029/2001GB001399>, 2001.

1852 Lagaria, A., Mandalakis, M., Mara, P., Papageorgiou, N., Pitta, P., Tsiola, A., Kagiorgi, M. and  
1853 Psarra, S.: Phytoplankton response to Saharan dust depositions in the Eastern  
1854 Mediterranean Sea: A mesocosm study, *Front. Mar. Sci.*, 3,  
1855 <https://doi.org/10.3389/fmars.2016.00287>, 2017.

1856 Law, C. S., Brévière, E., de Leeuw, G., Garçon, V., Guieu, C., Kieber, D. J., Konradowitz, S.,  
1857 Paulmier, A., Quinn, P. K., Saltzman, E. S., Stefels, J. and von Glasow, R.: Evolving  
1858 research directions in Surface Ocean - Lower Atmosphere (SOLAS) science, *Environ.*  
1859 *Chem.*, 10(1), 1, <https://doi.org/10.1071/EN12159>, 2013.

1860 Lee, S. and Fuhrman, J. A.: Relationships between Biovolume and Biomass of Naturally Derived  
1861 Marine Bacterioplankton, *Appl Environ Microbiol*, 53(6), 1298–1303, 1987.

1862 Lekunberri, I., Lefort, T., Romero, E., Vázquez-Domínguez, E., Romera-Castillo, C., Marrasé,  
1863 C., Peters, F., Weinbauer, M. and Gasol, J. M.: Effects of a dust deposition event on  
1864 coastal marine microbial abundance and activity, bacterial community structure and  
1865 ecosystem function, *J Plankton Res*, 32(4), 381–396,  
1866 <https://doi.org/10.1093/plankt/fbp137>, 2010.

1867 Liu, X., Patsavas, M. C. and Byrne, R. H.: Purification and Characterization of meta-Cresol  
1868 Purple for Spectrophotometric Seawater pH Measurements, *Environ. Sci. Technol.*, 45(11),  
1869 4862–4868, <https://doi.org/10.1021/es200665d>, 2011.

1870 Longhurst, A., Sathyendranath, S., Platt, T. and Caverhill, C.: An estimate of global primary  
1871 production in the ocean from satellite radiometer data, *Journal of Plankton Research*, 17(6),  
1872 1245–1271, <https://doi.org/10.1093/plankt/17.6.1245>, 1995.

1873 López-Urrutia, A. and Morán, X. A. G.: Resource limitation of bacterial production distorts the  
1874 temperature dependence of oceanic carbon cycling, *Ecology*, 88(4), 817–822,  
1875 <https://doi.org/10.1890/06-1641>, 2007.

1876 Louis, J., Pedrotti, M. L., Gazeau, F. and Guieu, C.: Experimental evidence of formation of  
1877 transparent exopolymer particles (TEP) and POC export provoked by dust addition under  
1878 current and high  $p\text{CO}_2$  conditions, *PLOS ONE*, 12(2), e0171980,  
1879 <https://doi.org/10.1371/journal.pone.0171980>, 2017a.

1880 Louis, J., Guieu, C. and Gazeau, F.: Nutrient dynamics under different ocean acidification  
1881 scenarios in a low nutrient low chlorophyll system: The Northwestern Mediterranean Sea,  
1882 *Estuarine, Coastal and Shelf Science*, 186, 30–44,  
1883 <https://doi.org/10.1016/j.ecss.2016.01.015>, 2017b.

1884 Louis, J., Gazeau, F. and Guieu, C.: Atmospheric nutrients in seawater under current and high  
1885  $p\text{CO}_2$  conditions after Saharan dust deposition: Results from three minicosm experiments,  
1886 *Progress in Oceanography*, 163, 40–49, <https://doi.org/10.1016/j.pocean.2017.10.011>,  
1887 2018.

1888 Loye-Pilot, M. D. and Martin, J. M.: Saharan Dust Input to the Western Mediterranean: An  
1889 Eleven Years Record in Corsica, in *The Impact of Desert Dust Across the Mediterranean*,  
1890 edited by S. Guerzoni and R. Chester, pp. 191–199, Springer Netherlands, Dordrecht,  
1891 [https://doi.org/10.1007/978-94-017-3354-0\\_18](https://doi.org/10.1007/978-94-017-3354-0_18), , 1996.

1892 Manca, B., Burca, M., Giorgetti, A., Coatanoan, C., Garcia, M.-J. and Iona, A.: Physical and  
1893 biochemical averaged vertical profiles in the Mediterranean regions: an important tool to  
1894 trace the climatology of water masses and to validate incoming data from operational

1895 oceanography, *Journal of Marine Systems*, 48(1), 83–116,  
1896 <https://doi.org/10.1016/j.jmarsys.2003.11.025>, 2004.

1897 Marañón, E., Fernández, A., Mouriño-Carballido, B., Martínez-García, S., Teira, E., Cermeño,  
1898 P., Chouciño, P., Huete-Ortega, M., Fernández, E., Calvo-Díaz, A., Morán, X. A. G.,  
1899 Bode, A., Moreno-Ostos, E., Varela, M. M., Patey, M. D. and Achterberg, E. P.: Degree of  
1900 oligotrophy controls the response of microbial plankton to Saharan dust, *Limnology and*  
1901 *Oceanography*, 55(6), 2339–2352, <https://doi.org/10.4319/lo.2010.55.6.2339>, 2010.

1902 Marañón, E., Lorenzo, M. P., Cermeño, P. and Mouriño-Carballido, B.: Nutrient limitation  
1903 suppresses the temperature dependence of phytoplankton metabolic rates, *The ISME*  
1904 *Journal*, 12(7), 1836–1845, <https://doi.org/10.1038/s41396-018-0105-1>, 2018.

1905 Marie, D., Simon, N., Guillou, L., Partensky, F. and Vaultot, D.: Flow cytometry analysis of  
1906 marine picoplankton, in *living color: protocols in flow cytometry and cell sorting*, edited  
1907 by R. A. Diamond and S. DeMaggio, pp. 421–454, Springer, Berlin, , 2010.

1908 Markaki, Z., Oikonomou, K., Kocak, M., Kouvarakis, G., Chaniotaki, A., Kubilay, N. and  
1909 Mihalopoulos, N.: Atmospheric deposition of inorganic phosphorus in the Levantine Basin,  
1910 eastern Mediterranean: Spatial and temporal variability and its role in seawater  
1911 productivity, *Limnology and Oceanography*, 48(4), 1557–1568,  
1912 <https://doi.org/10.4319/lo.2003.48.4.1557>, 2003.

1913 Maugendre, L., Gattuso, J.-P., Louis, J., de Kluijver, A., Marro, S., Soetaert, K. and Gazeau, F.:  
1914 Effect of ocean warming and acidification on a plankton community in the NW  
1915 Mediterranean Sea, *ICES Journal of Marine Science*, 72(6), 1744–1755,  
1916 <https://doi.org/10.1093/icesjms/fsu161>, 2015.

1917 Maugendre, L., Guieu, C., Gattuso, J.-P. and Gazeau, F.: Ocean acidification in the  
1918 Mediterranean Sea: Pelagic mesocosm experiments. A synthesis, *Estuarine, Coastal and*  
1919 *Shelf Science*, 186, 1–10, <https://doi.org/10.1016/j.ecss.2017.01.006>, 2017.

1920 Mayot, N., D'Ortenzio, F., Ribera d'Alcalà, M., Lavigne, H. and Claustre, H.: Interannual  
1921 variability of the Mediterranean trophic regimes from ocean color satellites,  
1922 *Biogeosciences*, 13(6), 1901–1917, <https://doi.org/10.5194/bg-13-1901-2016>, 2016.

1923 Mélançon, J., Levasseur, M., Lizotte, M., Scarratt, M., Tremblay, J.-É., Tortell, P., Yang, G.-P.,  
1924 Shi, G.-Y., Gao, H., Semeniuk, D., Robert, M., Arychuk, M., Johnson, K., Sutherland, N.,  
1925 Davelaar, M., Nemcek, N., Peña, A. and Richardson, W.: Impact of ocean acidification on  
1926 phytoplankton assemblage, growth, and DMS production following Fe-dust additions in  
1927 the NE Pacific high-nutrient, low-chlorophyll waters, *Biogeosciences*, 13(5), 1677–1692,  
1928 <https://doi.org/10.5194/bg-13-1677-2016>, 2016.

1929 Moore, C. M., Mills, M. M., Arrigo, K. R., Berman-Frank, I., Bopp, L., Boyd, P. W., Galbraith,  
1930 E. D., Geider, R. J., Guieu, C., Jaccard, S. L., Jickells, T. D., La Roche, J., Lenton, T. M.,  
1931 Mahowald, N. M., Marañón, E., Marinov, I., Moore, J. K., Nakatsuka, T., Oschlies, A.,  
1932 Saito, M. A., Thingstad, T. F., Tsuda, A. and Ulloa, O.: Processes and patterns of oceanic  
1933 nutrient limitation, *Nature Geoscience*, 6(9), 701–710, <https://doi.org/10.1038/ngeo1765>,  
1934 2013.

1935 Morán, X. A. G., López-Urrutia, Á., Calvo-Díaz, A. and Li, W. K. W.: Increasing importance of  
1936 small phytoplankton in a warmer ocean, *Global Change Biology*, 16(3), 1137–1144,  
1937 <https://doi.org/10.1111/j.1365-2486.2009.01960.x>, 2010.

1938 Neale, P. J., Sobrino, C., Segovia, M., Mercado, J. M., Leon, P., Cortés, M. D., Tuite, P., Picazo,  
1939 A., Salles, S., Cabrerizo, M. J., Prasil, O., Montecino, V., Reul, A. and Fuentes-Lema, A.:  
1940 Effect of CO<sub>2</sub>, nutrients and light on coastal plankton. I. Abiotic conditions and biological  
1941 responses, *Aquatic Biology*, 22, 25–41, <https://doi.org/10.3354/ab00587>, 2014.

1942 Obernosterer, I., Kawasaki, N. and Benner, R.: P-limitation of respiration in the Sargasso Sea  
1943 and uncoupling of bacteria from P-regeneration in size-fractionation experiments, *Aquatic  
1944 Microbial Ecology*, 32(3), 229–237, <https://doi.org/10.3354/ame032229>, 2003.

1945 Orr, J. C., Epitalon, J.-M., Dickson, A. G. and Gattuso, J.-P.: Routine uncertainty propagation for  
1946 the marine carbon dioxide system, *Marine Chemistry*, 207, 84–107,  
1947 <https://doi.org/10.1016/j.marchem.2018.10.006>, 2018.

1948 Paytan, A., Mackey, K. R. M., Chen, Y., Lima, I. D., Doney, S. C., Mahowald, N., Labiosa, R.  
1949 and Post, A. F.: Toxicity of atmospheric aerosols on marine phytoplankton, *Proceedings of*  
1950 *the National Academy of Sciences*, 106(12), 4601–4605,  
1951 <https://doi.org/10.1073/pnas.0811486106>, 2009.

1952 Pitta, P., Kanakidou, M., Mihalopoulos, N., Christodoulaki, S., Dimitriou, P. D., Frangoulis, C.,  
1953 Giannakourou, A., Kagiorgi, M., Lagaria, A., Nikolaou, P., Papageorgiou, N., Psarra, S.,  
1954 Santi, I., Tsapakis, M., Tsiola, A., Violaki, K. and Petihakis, G.: Saharan Dust Deposition  
1955 Effects on the Microbial Food Web in the Eastern Mediterranean: A Study Based on a  
1956 Mesocosm Experiment, *Front. Mar. Sci.*, 4, <https://doi.org/10.3389/fmars.2017.00117>,  
1957 2017.

1958 Polovina, J. J., Howell, E. A. and Abecassis, M.: Ocean's least productive waters are expanding,  
1959 *Geophysical Research Letters*, 35(3), <https://doi.org/10.1029/2007gl031745>, 2008.

1960 Powley, H. R., Krom, M. D. and Cappellen, P. V.: Understanding the unique biogeochemistry of  
1961 the Mediterranean Sea: Insights from a coupled phosphorus and nitrogen model, *Global*  
1962 *Biogeochemical Cycles*, 31(6), 1010–1031, <https://doi.org/10.1002/2017GB005648>, 2017.

1963 Pulido-Villena, E., Wagener, T. and Guieu, C.: Bacterial response to dust pulses in the western  
1964 Mediterranean: Implications for carbon cycling in the oligotrophic ocean, *Global*  
1965 *Biogeochemical Cycles*, 22(1), <https://doi.org/10.1029/2007gb003091>, 2008.

1966 Pulido-Villena, E., Rerolle, V. and Guieu, C.: Transient fertilizing effect of dust in P-deficient  
1967 LNLC surface ocean, *Geophysical Research Letters*, 37,  
1968 <https://doi.org/10.1029/2009gl041415>, 2010.

1969 Pulido-Villena, E., Baudoux, A.-C., Obernosterer, I., Landa, M., Caparros, J., Catala, P.,  
1970 Georges, C., Harmand, J. and Guieu, C.: Microbial food web dynamics in response to a

1971 Saharan dust event: results from a mesocosm study in the oligotrophic Mediterranean Sea,  
1972 *Biogeosciences*, 11(19), 5607–5619, 2014.

1973 Putaud, J.-P., Dingenen, R. V., Dell’Acqua, A., Raes, F., Matta, E., Decesari, S., Facchini, M. C.  
1974 and Fuzzi, S.: Size-segregated aerosol mass closure and chemical composition in Monte  
1975 Cimone (I) during MINATROC, *Atmospheric Chemistry and Physics*, 4(4), 889–902,  
1976 <https://doi.org/10.5194/acp-4-889-2004>, 2004.

1977 Ras, J., Claustre, H. and Uitz, J.: Spatial variability of phytoplankton pigment distributions in the  
1978 Subtropical South Pacific Ocean: comparison between in situ and predicted data,  
1979 *Biogeosciences*, 5(2), 353–369, <https://doi.org/10.5194/bg-5-353-2008>, 2008.

1980 Regaudie-de-Gioux, A., Vaquer-Sunyer, R. and Duarte, C. M.: Patterns in planktonic  
1981 metabolism in the Mediterranean Sea, *Biogeosciences*, 6(12), 3081–3089,  
1982 <https://doi.org/10.5194/bg-6-3081-2009>, 2009.

1983 Richon, C., Dutay, J.-C., Dulac, F., Wang, R., Balkanski, Y., Nabat, P., Aumont, O., Desboeufs,  
1984 K., Laurent, B., Guieu, C., Raimbault, P. and Beuvier, J.: Modeling the impacts of  
1985 atmospheric deposition of nitrogen and desert dust-derived phosphorus on nutrients and  
1986 biological budgets of the Mediterranean Sea, *Progress in Oceanography*, 163, 21–39,  
1987 <https://doi.org/10.1016/j.pocean.2017.04.009>, 2018.

1988 Ridame, C. and Guieu, C.: Saharan input of phosphate to the oligotrophic water of the open  
1989 western Mediterranean Sea, *Limnology and Oceanography*, 47(3), 856–869, 2002.

1990 Ridame, C., Guieu, C. and L’Helguen, S.: Strong stimulation of N<sub>2</sub> fixation in oligotrophic  
1991 Mediterranean Sea: results from dust addition in large in situ mesocosms, *Biogeosciences*,  
1992 10(11), 7333–7346, 2013.

1993 Ridame, C., Dekaezemacker, J., Guieu, C., Bonnet, S., L’Helguen, S. and Malien, F.: Contrasted  
1994 Saharan dust events in LNLC environments: impact on nutrient dynamics and primary  
1995 production, *Biogeosciences (BG)*, 11(17), 4783–4800, 2014.

1996 Romero, E., Peters, F., Marrasé, C., Guadayol, Ò., Gasol, J. M. and Weinbauer, M. G.: Coastal  
1997 Mediterranean plankton stimulation dynamics through a dust storm event: An experimental  
1998 simulation, *Estuarine, Coastal and Shelf Science*, 93(1), 27–39,  
1999 <https://doi.org/10.1016/j.ecss.2011.03.019>, 2011.

2000 Roy-Barman, M., Folio, L., Douville, E., Leblond, N., Gazeau, F., Bressac, M., Wagener, T.,  
2001 Ridame, C., Desboeufs, K. and Guieu, C.: Contrasted release of insoluble elements (Fe, Al,  
2002 REE, Th, Pa) after dust deposition in seawater: a tank experiment approach,  
2003 *Biogeosciences Discussions*, 1–27, <https://doi.org/10.5194/bg-2020-247>, 2020.

2004 Sala, M. M., Aparicio, F. L., Balagué, V., Boras, J. A., Borrull, E., Cardelús, C., Cros, L.,  
2005 Gomes, A., López-Sanz, A., Malits, A., Martínez, R. A., Mestre, M., Movilla, J., Sarmiento,  
2006 H., Vázquez-Domínguez, E., Vaqué, D., Pinhassi, J., Calbet, A., Calvo, E., Gasol, J. M.,  
2007 Pelejero, C. and Marrasé, C.: Contrasting effects of ocean acidification on the microbial  
2008 food web under different trophic conditions, *ICES Journal of Marine Science*, 73(3), 670–  
2009 679, <https://doi.org/10.1093/icesjms/fsv130>, 2016.

2010 Sherr, E. B. and Sherr, B. F.: Bacterivory and herbivory: Key roles of phagotrophic protists in  
2011 pelagic food webs, *Microb Ecol*, 28(2), 223–235, <https://doi.org/10.1007/BF00166812>,  
2012 1994.

2013 Siokou-Frangou, I., Christaki, U., Mazzocchi, M. G., Montresor, M., Ribera d'Alcalá, M.,  
2014 Vaqué, D. and Zingone, A.: Plankton in the open Mediterranean Sea: a review,  
2015 *Biogeosciences*, 7(5), 1543–1586, <https://doi.org/10.5194/bg-7-1543-2010>, 2010.

2016 Tanaka, T., Thingstad, T. F., Christaki, U., Colombet, J., Cornet-Barthaux, V., Courties, C.,  
2017 Grattepanche, J.-D., Lagaria, A., Nedoma, J., Oriol, L., Psarra, S., Pujo-Pay, M. and  
2018 Wambeke, F. V.: Lack of P-limitation of phytoplankton and heterotrophic prokaryotes in  
2019 surface waters of three anticyclonic eddies in the stratified Mediterranean Sea,  
2020 *Biogeosciences*, 8(2), 525–538, <https://doi.org/10.5194/bg-8-525-2011>, 2011.

2021 Ternon, E., Guieu, C., Loÿe-Pilot, M.-D., Leblond, N., Bosc, E., Gasser, B., Miquel, J.-C. and  
2022 Martín, J.: The impact of Saharan dust on the particulate export in the water column of the  
2023 North Western Mediterranean Sea, *Biogeosciences*, 7(3), 809–826,  
2024 <https://doi.org/10.5194/bg-7-809-2010>, 2010.

2025 The Mermex group: Marine ecosystems' responses to climatic and anthropogenic forcings in the  
2026 Mediterranean, *Progress in Oceanography*, 91(2), 97–166,  
2027 <https://doi.org/10.1016/j.pocean.2011.02.003>, 2011.

2028 Theodosi, C., Markaki, Z., Tselepidis, A. and Mihalopoulos, N.: The significance of atmospheric  
2029 inputs of soluble and particulate major and trace metals to the eastern Mediterranean  
2030 seawater, *Marine Chemistry*, 120(1), 154–163,  
2031 <https://doi.org/10.1016/j.marchem.2010.02.003>, 2010.

2032 Van Wambeke, F., Goutx, M., Striby, L., Sempéré, R. and Vidussi, F.: Bacterial dynamics  
2033 during the transition from spring bloom to oligotrophy in the northwestern Mediterranean  
2034 Sea: relationships with particulate detritus and dissolved organic matter, *Marine Ecology  
2035 Progress Series*, 212, 89–105, 2001.

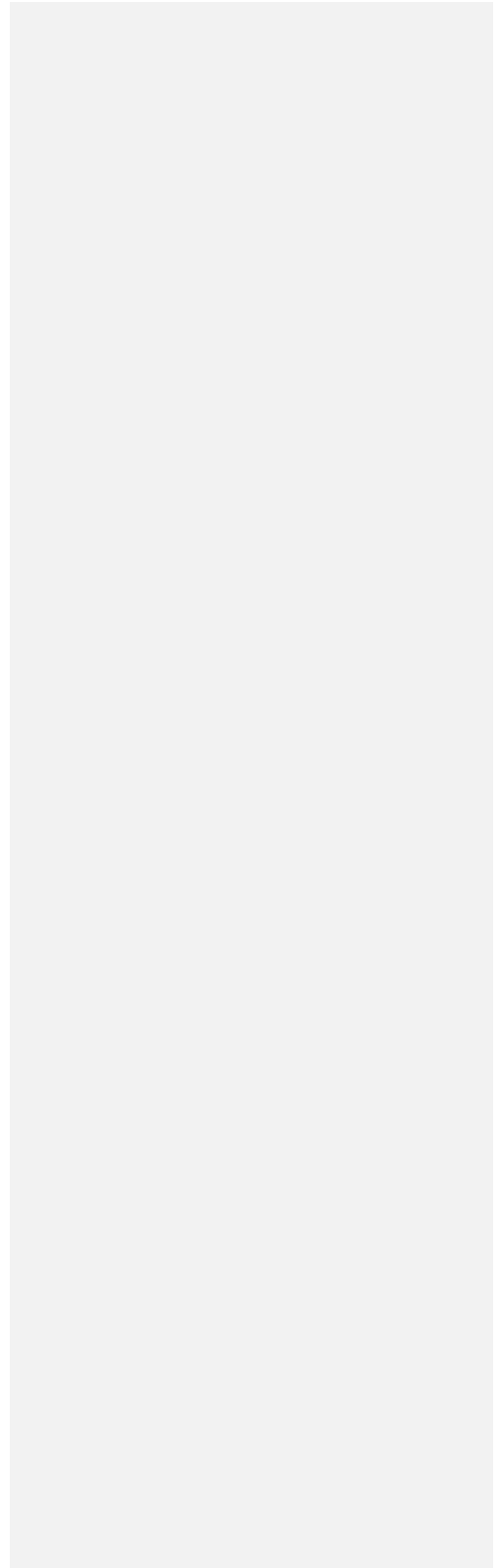
2036 Van Wambeke, F., Taillandier, V., Deboeufs, K., Pulido-Villena, E., Dinasquet, J., Engel, A.,  
2037 Marañón, E., Ridame, C. and Guieu, C.: Influence of atmospheric deposition on  
2038 biogeochemical cycles in an oligotrophic ocean system, *Biogeosciences Discussions*, 1–51,  
2039 <https://doi.org/10.5194/bg-2020-411>, 2020a.

2040 Van Wambeke, F., Pulido, E., Dinasquet, J., Djaoudi, K., Engel, A., Garel, M., Guasco, S.,  
2041 Nunige, S., Taillandier, V., Zäncker, B. and Tamburini, C.: Spatial patterns of biphasic  
2042 ectoenzymatic kinetics related to biogeochemical properties in the Mediterranean Sea,  
2043 *Biogeosciences Discussions*, 1–38, <https://doi.org/10.5194/bg-2020-253>, 2020b.

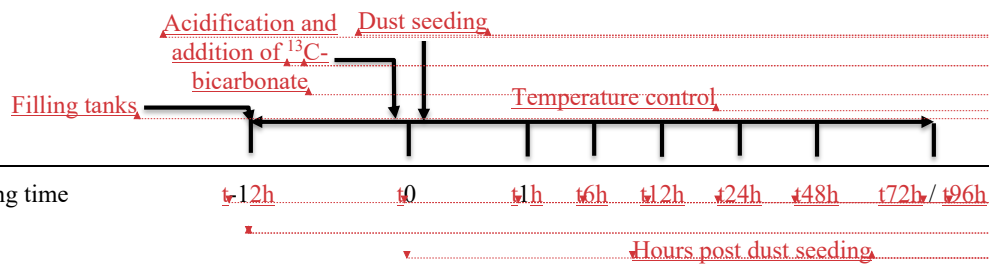
2044 Verity, P. G., Robertson, C. Y., Tronzo, C. R., Andrews, M. G., Nelson, J. R. and Sieracki, M.  
2045 E.: Relationships between cell volume and the carbon and nitrogen content of marine



2046 photosynthetic nanoplankton, *Limnology and Oceanography*, 37(7), 1434–1446,  
2047 <https://doi.org/10.4319/lo.1992.37.7.1434>, 1992.  
2048 Vidussi, F., Claustre, H., Manca, B. B., Luchetta, A. and Marty, J.-C.: Phytoplankton pigment  
2049 distribution in relation to upper thermocline circulation in the eastern Mediterranean Sea  
2050 during winter, *Journal of Geophysical Research: Oceans*, 106(C9), 19939–19956,  
2051 <https://doi.org/10.1029/1999JC000308>, 2001.  
2052



2053 Table 1. List of parameters and processes investigated during the three experiments at stations  
 2054 TYR, ION and FAST. Related manuscripts are indicated. pH<sub>T</sub>: pH on the total scale, A<sub>T</sub>: total  
 2055 alkalinity, <sup>13</sup>C-C<sub>T</sub>: <sup>13</sup>C signature of dissolved inorganic carbon, NO<sub>x</sub>: nitrate + nitrite, DIP:  
 2056 dissolved inorganic phosphorus, Si(OH)<sub>4</sub>: silicate, DFe: dissolved iron, DAL: dissolved  
 2057 aluminium, Th-REE-Pa: Thorium (<sup>230</sup>Th and <sup>232</sup>Th), Rare Earth elements and Protactinium  
 2058 (<sup>231</sup>Pa), POC: particulate organic carbon, DOC: dissolved organic carbon, <sup>13</sup>C-DOC: <sup>13</sup>C  
 2059 signature of dissolved organic carbon, TEP: transparent exopolymer particles, NCP/CR: net  
 2060 community production and community respiration (oxygen based), <sup>14</sup>C-PP: primary production  
 2061 based on <sup>14</sup>C incorporation.



		Related manuscript
Temperature	Continuous	This manuscript
Irradiance	Continuous	This manuscript

**Carbonate chemistry**

pH<sub>T</sub>

A<sub>T</sub>

δ<sup>13</sup>C-C<sub>T</sub>

**Macro-nutrients**

NO<sub>x</sub>

DIP

Si(OH)<sub>4</sub>

**Micro-nutrients**

DFe

DAI

Th-REE-Pa

**Biological stocks**

Pigments

Flow cytometry

This manuscript

This manuscript

Gazeau et al. (2021)

This manuscript

This manuscript

This manuscript

Roy-Barman et al. (2020)

Roy-Barman et al. (2020)

Roy-Barman et al. (2020)

This manuscript

This manuscript

Formatted: Font: 12 pt

Formatted: Font: 12 pt

Formatted: Font: 12 pt

Deleted: in preparation

Formatted: Font: 12 pt

Formatted: Font: 12 pt

Formatted: Font: 12 pt

Deleted: in preparation

Deleted: in preparation

Deleted: in preparation

Microscopy

Diazotroph abundance

Virus abundance

Meta-transcriptomics

Bacterial diversity

Micro-eukaryote diversity

Meso-zooplankton

POC (incl.  $\delta^{13}\text{C}$ )

POC sediment traps

DOC

$^{13}\text{C}$ -DOC

TEP

Amino acids

Carbohydrates

**Processes**

This manuscript

~~Céline Ridame (unpublished)~~

~~Dinasquet et al. (2021)~~

~~Dinasquet et al. (2021)~~

~~Dinasquet et al. (2021)~~

~~Dinasquet et al. (2021)~~

This manuscript

~~Gazeau et al. (2021)~~

~~Gazeau et al. (2021)~~

~~Gazeau et al. (2021)~~

~~Gazeau et al. (2021)~~

~~Gazeau et al. (2021)~~

~~Gazeau et al. (2021)~~

~~Gazeau et al. (2021)~~

**Deleted:** Ridame et al. (in preparation)

**Formatted:** French

**Deleted:** (in preparation)

**Deleted:** Dinasquet et al. (in preparation)

**Deleted:** Dinasquet et al. (in preparation)

**Deleted:** Dinasquet et al. (in preparation)

**Deleted:** in preparation

**Formatted:** Font: 12 pt

**Deleted:** Gazeau et al. (in preparation)

**Deleted:** Gazeau et al. (in preparation)

**Formatted:** Font: 12 pt

**Deleted:** Gazeau et al. (in preparation)

**Deleted:** Gazeau et al. (in preparation)

**Deleted:** Gazeau et al. (in preparation)

**Deleted:** Gazeau et al. (in preparation)

NCP/CR

<sup>14</sup>C-PP

~~Microtrophic~~

Ectoenzymatic activity

N<sub>2</sub> fixation

<sup>13</sup>CO<sub>2</sub>-fixation

Virus production,  
lysogeny

~~Gazeau et al. (2021)~~

~~Gazeau et al. (2021)~~

~~Gazeau et al. (2021)~~

~~Gazeau et al. (2021)~~

~~Céline Ridame (unpublished)~~

~~Céline Ridame (unpublished)~~ ~~Gazeau et al. (2021?)~~

~~Dinasquet et al. (2021)~~

**Deleted:** Gazeau et al. (in preparation)

**Formatted:** Font: 12 pt

**Deleted:** Gazeau et al. (in preparation)

**Deleted:** Gazeau et al. (in preparation)

**Deleted:** Gazeau et al. (in preparation)

**Formatted:** Font: 12 pt

**Deleted:** Ridame et al. (in preparation)

**Formatted:** French

**Deleted:** <sup>13</sup>

**Formatted:** Font: 12 pt

**Formatted:** Font: 12 pt

**Formatted:** English (US)

**Deleted:** Ridame et al. (in preparation)

**Deleted:** in preparation

**Deleted:** Dinasquet et al. (in preparation)

2117 Table 2. Initial conditions as measured while filling the tanks (initial conditions in pumped  
 2118 surface water; sampling time: t-12h). pH<sub>T</sub>: pH on the total scale, NO<sub>x</sub>: nitrate + nitrite, NH<sub>4</sub>:  
 2119 ammonium, DIP: dissolved inorganic phosphorus, Si(OH)<sub>4</sub>: silicate, TChl<sub>a</sub>: total chlorophyll *a*,  
 2120 HNF: heterotrophic nanoflagellates. The three most important pigments in terms of concentration  
 2121 are also presented (19'-hexanoyloxyfucoxanthin, Zeaxanthin and Divinyl Chlorophyll *a*).  
 2122 Biomasses of the different groups analyzed through flow cytometry were estimated based on  
 2123 conversion equations and/or factors found in the literature (see section 2.3). Autotrophic biomass  
 2124 was, as a first approximation, estimated only based on flow cytometry data and therefore  
 2125 corresponds to the fraction < 20 μm. Heterotrophic biomass was estimated as the sum of  
 2126 heterotrophic prokaryote and HNF biomasses (see section 2.3.2). Values below detection limits  
 2127 are indicated as < dl.

Sampling station	TYR	ION	FAST
Coordinates (decimal)	39.34 N, 12.60 E	35.49 N, 19.78 E	37.95 N, 2.90 N
Bottom depth (m)	3395	3054	2775
Day and time of sampling (local time)	17/05/2017 17:00	25/05/2017 17:00	02/06/2017 21:00
Temperature (°C)	20.6	21.2	21.5
Salinity	37.96	39.02	37.07
Carbonate pH <sub>T</sub>	8.04	8.07	8.03

Formatted: English (US)

chemistry	Total alkalinity ( $\mu\text{mol kg}^{-1}$ )	2529	2627	2443
Nutrients	$\text{NO}_x$ ( $\text{nmol L}^{-1}$ )	14.0	18.0	59.0
	$\text{NH}_4^+$ ( $\mu\text{mol L}^{-1}$ )	0.045	0.022	< dl
	DIP ( $\text{nmol L}^{-1}$ )	17.1	6.5	12.9
	$\text{Si(OH)}_4$ ( $\mu\text{mol L}^{-1}$ )	1.0	0.96	0.64
	$\text{NO}_x/\text{DIP}$ (molar ratio)	0.8	2.5	4.6
Pigments	TChla ( $\mu\text{g L}^{-1}$ )	0.063	0.066	0.072
	19'-hexanoyloxyfucoxanthin ( $\mu\text{g L}^{-1}$ )	0.017	0.021	0.016
	Zeaxanthin ( $\mu\text{g L}^{-1}$ )	0.009	0.006	0.036
	Divinyl Chlorophyll <i>a</i> ( $\mu\text{g L}^{-1}$ )	$\sim 0$	0	0.014
Flow cytometry	Pico-eukaryotes (abundance in cell $\text{mL}^{-1}$ ; biomass in $\mu\text{g C L}^{-1}$ )	347.8; 0.5	239.9; 0.4	701.0; 1.0
	Nano-eukaryotes (abundance in cell $\text{mL}^{-1}$ ; biomass in $\mu\text{g C L}^{-1}$ )	150.5; 3.9	188.8; 4.8	196.6; 5.0
	<i>Synechococcus</i> (abundance in cell $\text{mL}^{-1}$ ; biomass in $\mu\text{g C L}^{-1}$ )	4972; 1.2	3037; 0.8	6406; 1.6
	Autotrophic biomass ( $\mu\text{g C L}^{-1}$ )	5.6	6.0	7.7
	Heterotrophic prokaryotes abundance ( $\times 10^5$ cell $\text{mL}^{-1}$ )	4.79	2.14	6.15
	HNF (abundance in cell $\text{mL}^{-1}$ )	110.1	53.6	126.2
	Heterotrophic biomass ( $\mu\text{g C L}^{-1}$ )	9.9	4.5	12.7
Microscopy	Pennate diatoms (abundance in cell $\text{L}^{-1}$ )	140	520	880
	Centric diatoms (abundance in cell $\text{L}^{-1}$ )	200	380	580

Dinoflagellates (abundance in cell L <sup>-1</sup> )	2770	3000	3410
Autotrophic flagellates (abundance in cell L <sup>-1</sup> )	0	60	650
Ciliates (abundance in cell L <sup>-1</sup> )	270	380	770

---

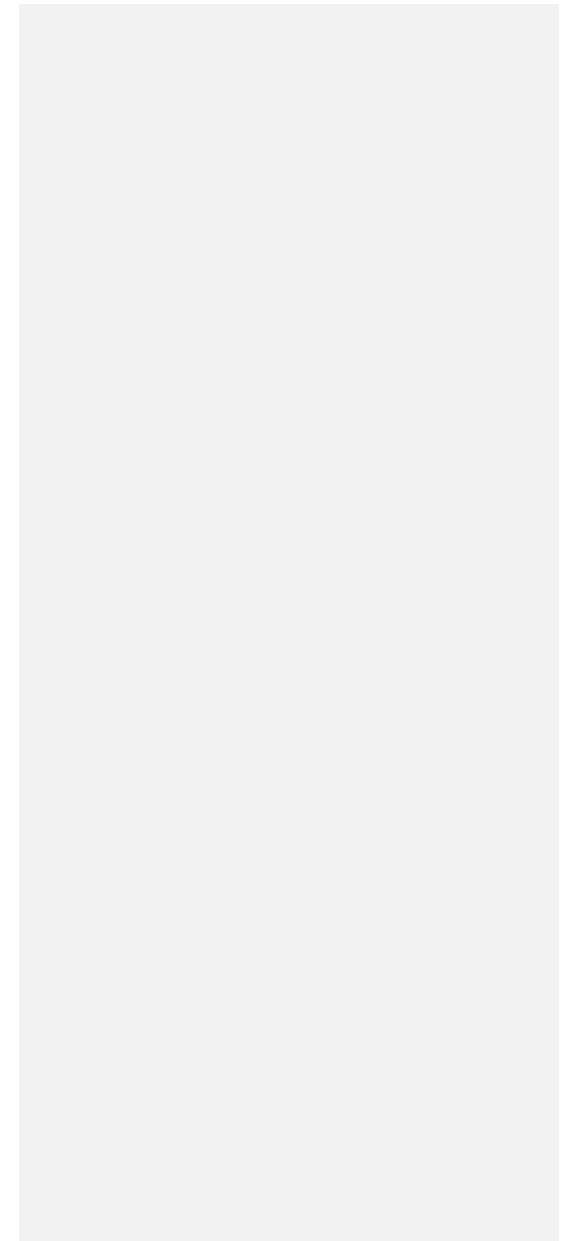




Table 3. Maximum input of nitrate + nitrite (NO<sub>x</sub>) and dissolved inorganic phosphorus (DIP) released from Saharan dust in tanks D and G as observed from the two discrete samplings performed over the first 6 h after seeding. The estimated maximal percentage of dissolution is also presented (see section 2.3.1 for details on the calculations).

	NO <sub>x</sub>				DIP			
	D1	D2	G1	G2	D1	D2	G1	G2
Maximum input	μmol L <sup>-1</sup>				nmol L <sup>-1</sup>			
TYR	11.0	11.1	11.1	11.0	24.6	20.4	24.6	23.9
ION	11.2	11.6	11.2	11.3	23.3	22.0	19.6	22.9
FAST	11.3	11.1	11.1	11.2	30.8	31.3	36.9	29.8
Percentage of dissolution (%)								
TYR	95	96	95	94	12	10	12	11
ION	96	99	96	97	11	10	9	11
FAST	97	97	95	97	15	15	17	14

Formatted: English (US)

1 Table 4. Removal rate of nitrate + nitrite (NO<sub>x</sub>) and dissolved inorganic phosphorus (DIP) in  
 2 tanks D and G during the three experiments (TYR, ION and FAST). For NO<sub>x</sub>, decreasing rates  
 3 were estimated based on linear regressions between maximal concentrations (i.e. after dust  
 4 enrichment, at t1h or t6h) and final concentrations (t72 h for TYR and ION and t96h for FAST).  
 5 For DIP, decreasing rates were estimated based on linear regressions between maximal  
 6 concentrations (i.e. after dust enrichment at t1h or t6h) and concentrations measured at sampling  
 7 times after which a stabilization was observed. This sampling time is shown in parentheses. All  
 8 rates are expressed in nmol L<sup>-1</sup> h<sup>-1</sup>.

	NO <sub>x</sub>			DIP		
	TYR	ION	FAST	TYR	ION	FAST
D1	-6.5	-8.6	-14.3	-0.4 (t72h)	-0.5 (t48h)	-0.2 (t96h)
D2	-1.0	-8.6	-13.5	-0.3 (t72h)	-0.8 (t24h)	-0.2 (t96h)
G1	-6.7	-13.1	-21.6	-1.3 (t24h)	-0.8 (t24h)	-1.5 (t24h)
G2	-0.8	-1.6	-25.2	-1.3 (t24h)	-1.6 (t24h)	-1.1 (t24h)

10 Table 5. Maximum relative changes in tanks D and G as compared to controls (average between  
 11 C1 and C2), expressed as a %, for the three experiments (TYR, ION and FAST). The sampling  
 12 time at which these maximum relative changes were observed is shown in brackets. Tchl $a$  refers  
 13 to the concentration of total chlorophyll  $a$  and B $_{micro}$  to the biomass proxy of micro-  
 14 phytoplankton (sum of Fucoxanthin and Peridinin, see Material and Methods) based on high  
 15 performance liquid chromatography (HPLC). HP and HNF refer to heterotrophic prokaryote and  
 16 heterotrophic nanoflagellate abundances, respectively, as measured by flow cytometry.

Experiment	Tank	HPLC			Flow cytometry			
		TChl $a$	B $_{micro}$	Pico-eukaryotes	Nano-eukaryotes	<i>Synechococcus</i>	HP	HNF
TYR	D1	-35 (t24h)	-33 (t12h)	-75 (t72h)	-80 (t1h)	-71 (t48h)	68 (t72h)	352 (t72h)
TYR	D2	-38 (t12h)	-39 (t24h)	-75 (t72h)	-80 (t1h)	-72 (t48h)	53 (t72h)	100 (t72h)
TYR	G1	60 (t72h)	52 (t72h)	-75 (t1h)	89 (t72h)	76 (t72h)	67 (t72h)	1095 (t72h)
TYR	G2	359 (t72h)	392 (t72h)	323 (t72h)	119 (t72h)	700 (t72h)	68 (t48h)	298 (t72h)
ION	D1	183 (t72h)	157 (t72h)	126 (t72h)	89 (t72h)	317 (t72h)	128 (t72h)	44 (t72h)
ION	D2	109 (t72h)	156 (t72h)	117 (t72h)	-59 (t1h)	390 (t72h)	133 (t72h)	27 (t72h)
ION	G1	399 (t72h)	454 (t72h)	458 (t72h)	256 (t72h)	805 (t72h)	176 (t72h)	175 (t72h)

ION	G2	426 (t72h)	612 (t72h)	510 (t72h)	292 (t72h)	1425 (t72h)	161 (t72h)	129 (t72h)
FAST	D1	318 (t96h)	356 (t96h)	113 (t96h)	208 (t72h)	348 (t96h)	27 (t96h)	-38 (t96h)
FAST	D2	237 (t96h)	322 (t96h)	91 (t96h)	219 (t72h)	197 (t96h)	40 (t48h)	-49 (t96h)
FAST	G1	399 (t96h)	415 (t96h)	198 (t72h)	274 (t72h)	357 (t48h)	61 (t48h)	243 (t24h)
FAST	G2	395 (t96h)	421 (t96h)	129 (t72h)	202 (t96h)	344 (t48h)	67 (t48h)	74 (t24h)

---

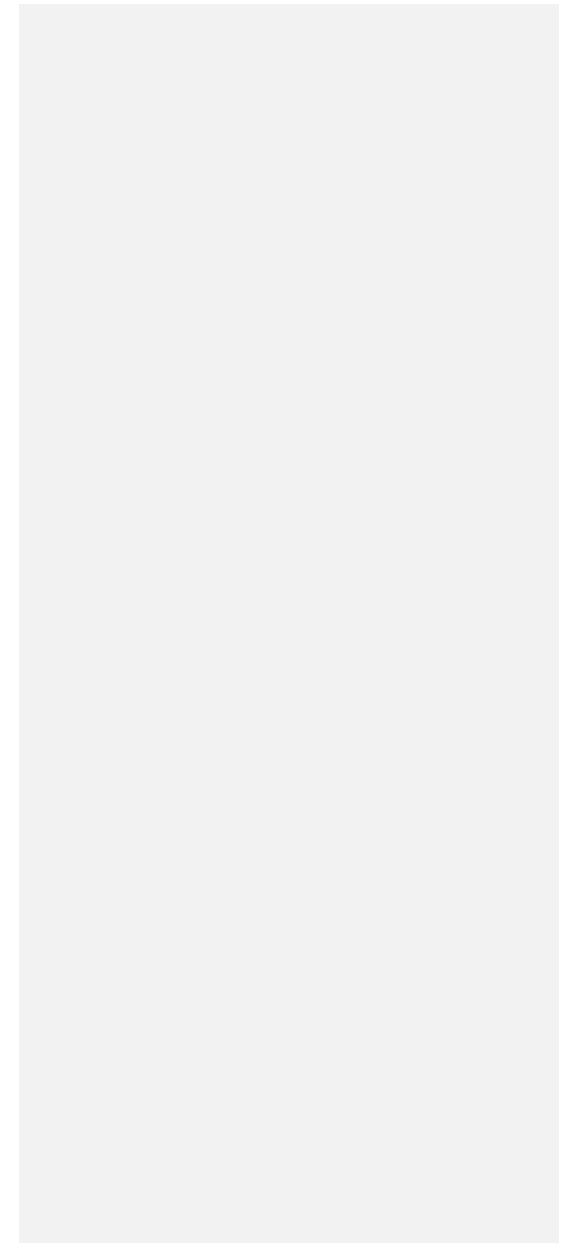


## Figure captions

Fig. 1. ~~Location of the sampling stations in the Mediterranean Sea onboard the R/V “Pourquoi Pas ?” during the PEACETIME cruise, on map of satellite-derived surface chlorophyll *a* concentration averaged over the entire duration of the cruise (Courtesy of Louise Rousselet).~~

**Deleted:** Location of

**Deleted:** , on a

**Formatted:** Font colour: Black

Fig. 2. Scheme of an experimental tank (climate reactor).

**Deleted:** Map showing the sampling stations in the Mediterranean Sea along the transect performed onboard the R/V “Pourquoi Pas ?” during the PEACETIME cruise.

Fig. 3. Proportion of the different pigments, as measured by high performance liquid chromatography (HPLC) in pumped surface seawater for the three experiments (t-12h).

Fig. 4. Continuous measurements of temperature and irradiance level (PAR) in the six tanks during the three experiments. The dashed vertical line indicates the time of dust seeding (after t<sub>0</sub>).

Fig. 5. pH on the total scale (pH<sub>T</sub>) and total alkalinity (A<sub>T</sub>) measured in the six tanks during the three experiments. The dashed vertical line indicates the time of dust seeding (after t<sub>0</sub>). Error bars correspond to the standard deviation based on analytical triplicates.

Fig. 6. Nutrients (nitrate + nitrite: NO<sub>x</sub>, dissolved inorganic phosphorus: DIP, silicate: Si(OH)<sub>4</sub> as well as the molar ratio between NO<sub>x</sub> and DIP, measured in the six tanks during the three experiments. The dashed vertical line indicates the time of seeding (after t<sub>0</sub>).

Fig. 7. Concentrations of total chlorophyll *a* and major pigments, measured by high performance liquid chromatography (HPLC), in the six tanks during the three experiments. The dashed vertical line indicates the time of seeding (after t<sub>0</sub>).

Fig. 8. Abundance of **autotrophic** pico-eukaryotes, **autotrophic** nano-eukaryotes, *Synechococcus*, heterotrophic prokaryotes (HP), and heterotrophic nano-flagellates (HNF), measured by flow cytometry, in the six tanks during the three experiments. The evolution of autotrophic biomass

(see Material and Methods for details on the calculation) is also shown. The dashed vertical line indicates the time of seeding (after  $t_0$ ).

Fig. 9. Abundances of meso-zooplankton species as measured at the end of each experiment.

Fig. 10. Maximal relative change (%) of main biological stocks (TCH1a: total chlorophyll  $a$ , HP: heterotrophic prokaryotes) and processes (BP: bacterial production; PP:  $^{14}\text{C}$ -based primary production; see Gazeau et al., 2021; BR: bacterial respiration (no data from this study); and  $\text{N}_2$  fixation, Céline Ridame, unpublished results) as obtained during the present study at the 3 stations (TYR, ION and FAST) under ambient conditions of pH and temperature (open red squares) and future conditions (full green squares). Squares are delimited by the range of responses observed among the duplicates for each treatment. The dotted green squares for station TYR denote the large variability observed between duplicates for some parameters and processes that prevented drawing solid conclusions. Box-plots represent the distribution of responses observed from studies conducted in the Mediterranean Sea, as compiled by Guieu and Ridame (2020).

**Deleted:** in preparation, this issue

**Formatted:** English (US)

**Deleted:** see

**Formatted:** English (US)

**Formatted:** English (US)

**Deleted:** et al., in preparation, this issue

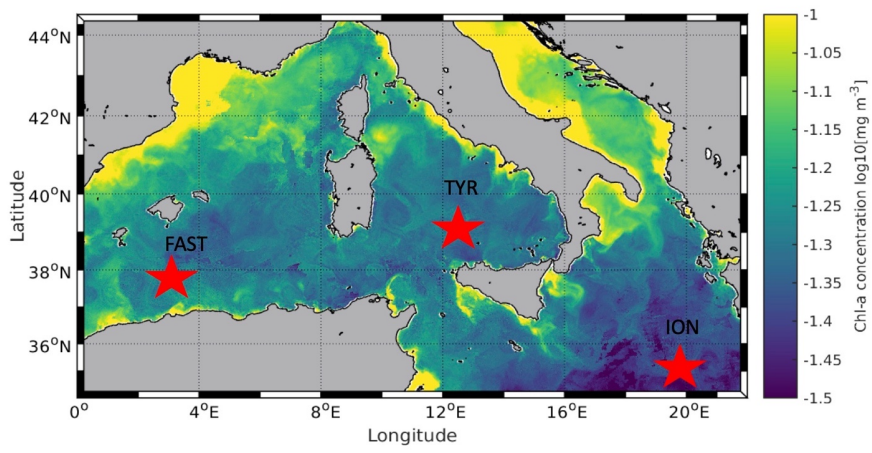


Fig. 1.

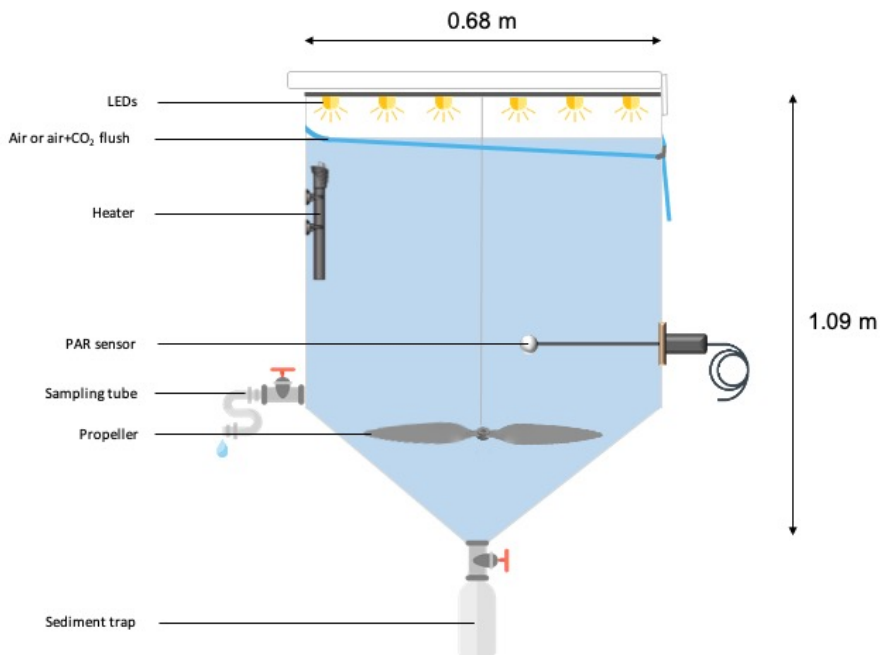
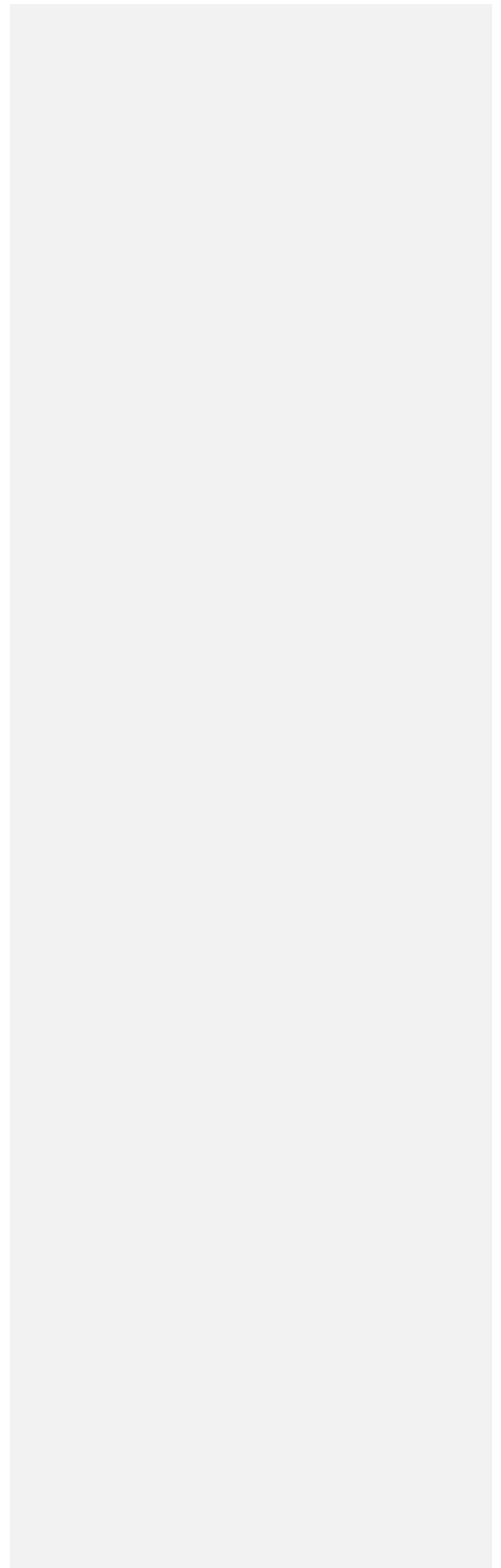


Fig. 2.





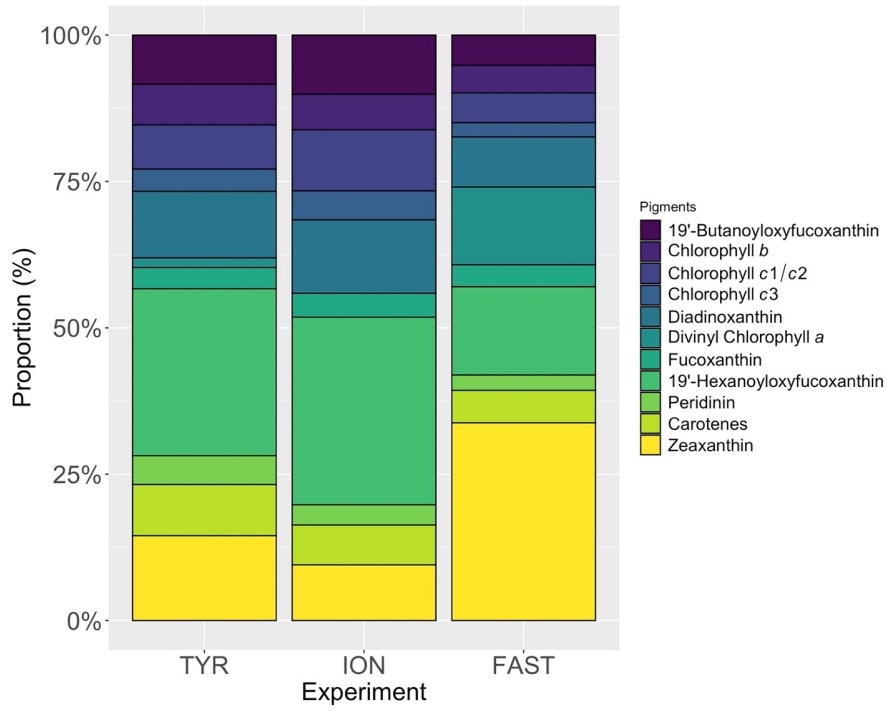


Fig. 3.

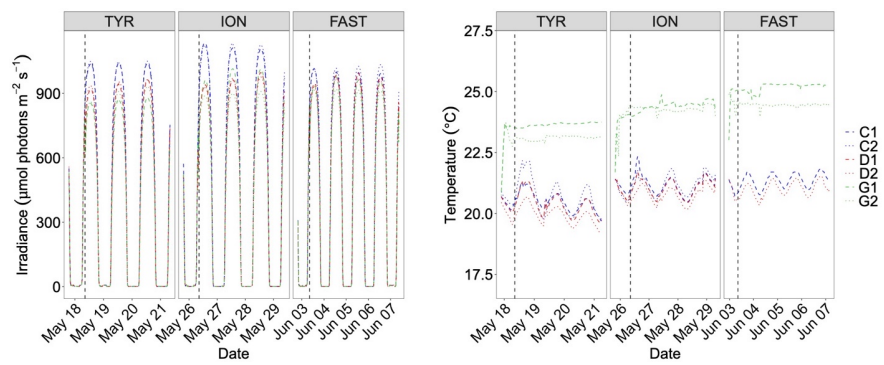


Fig. 4.

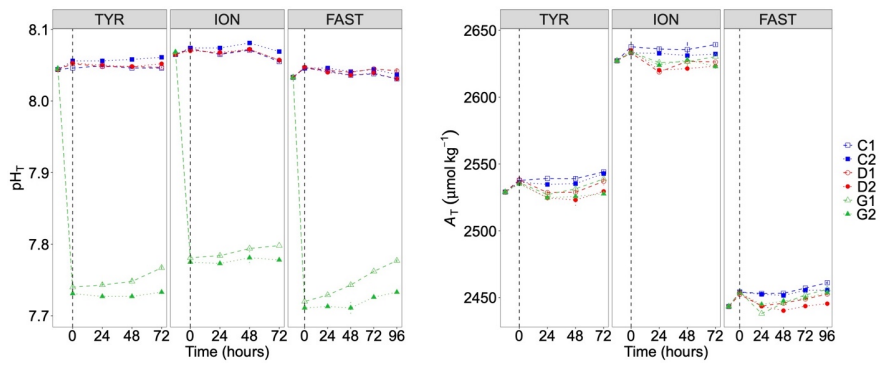
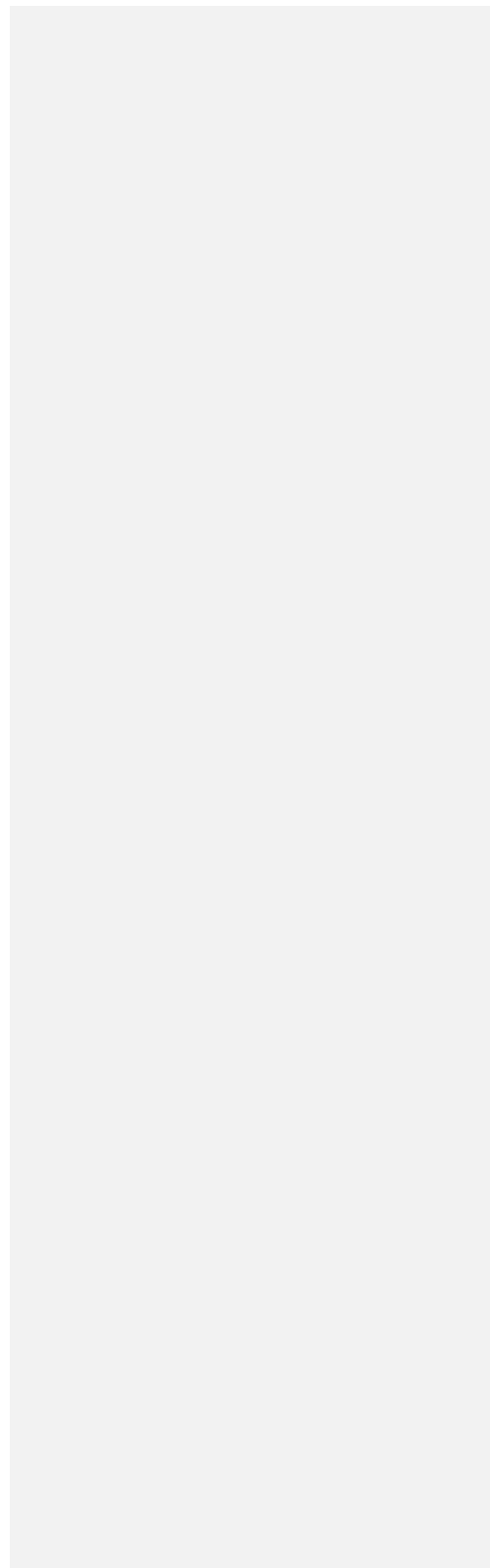


Fig. 5.



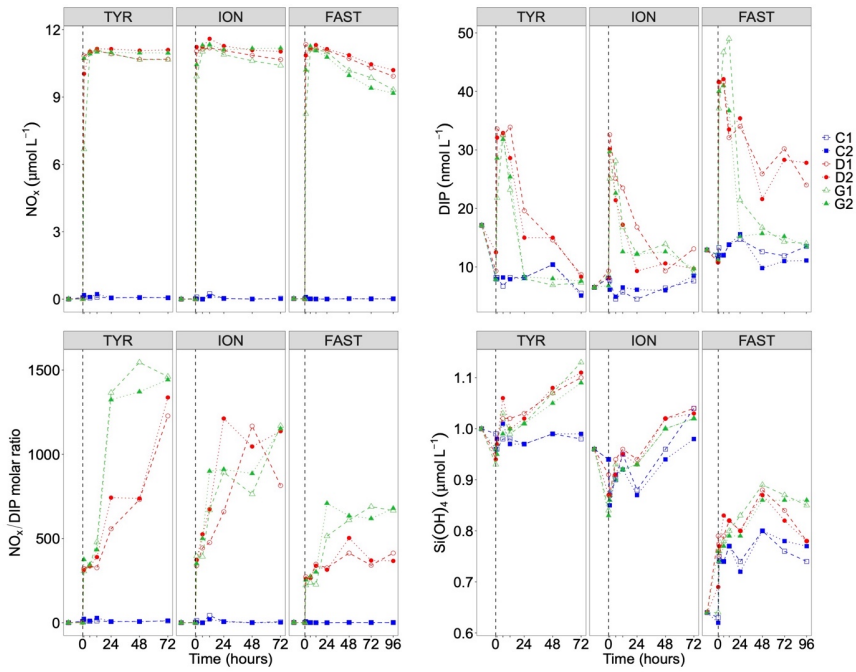


Fig. 6.

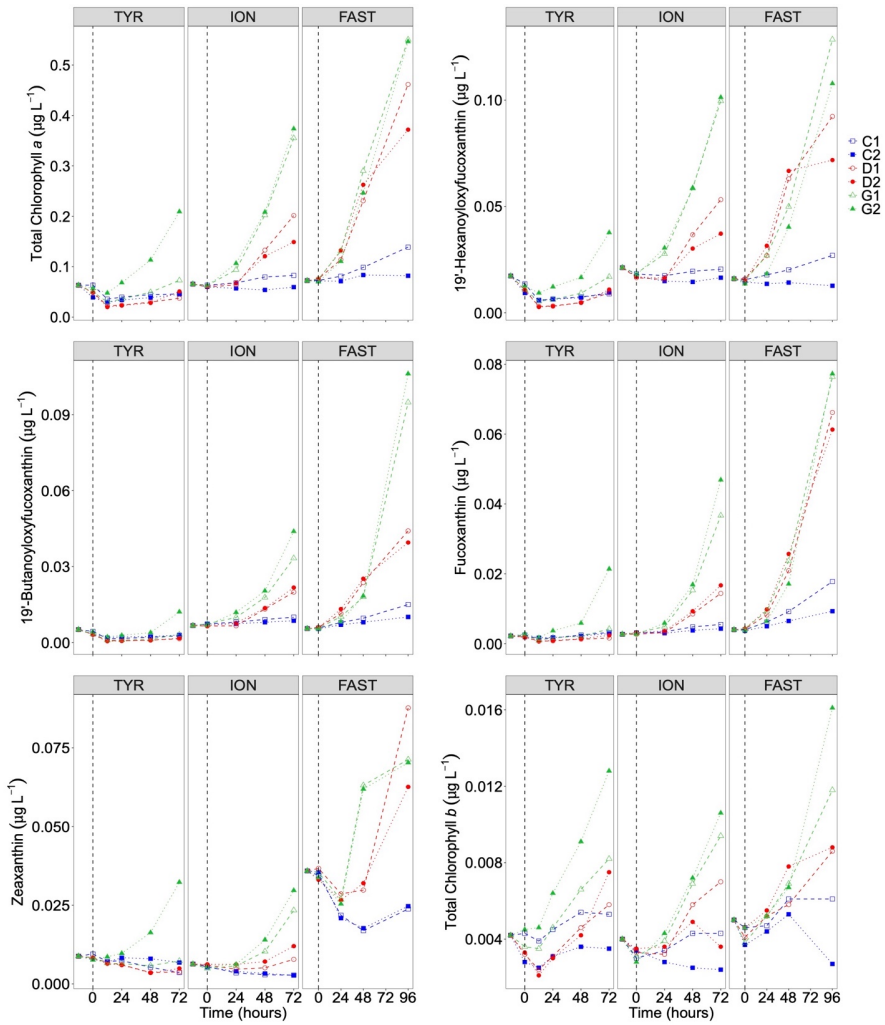


Fig. 7.

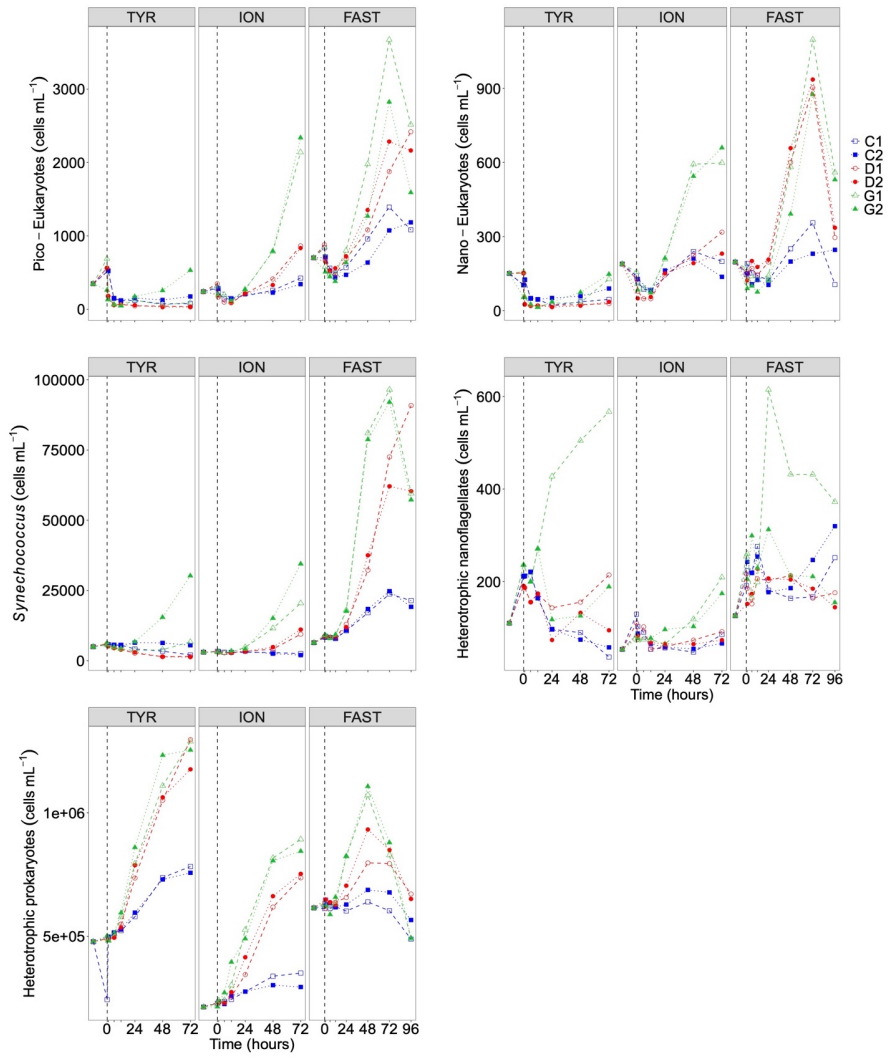


Fig. 8.

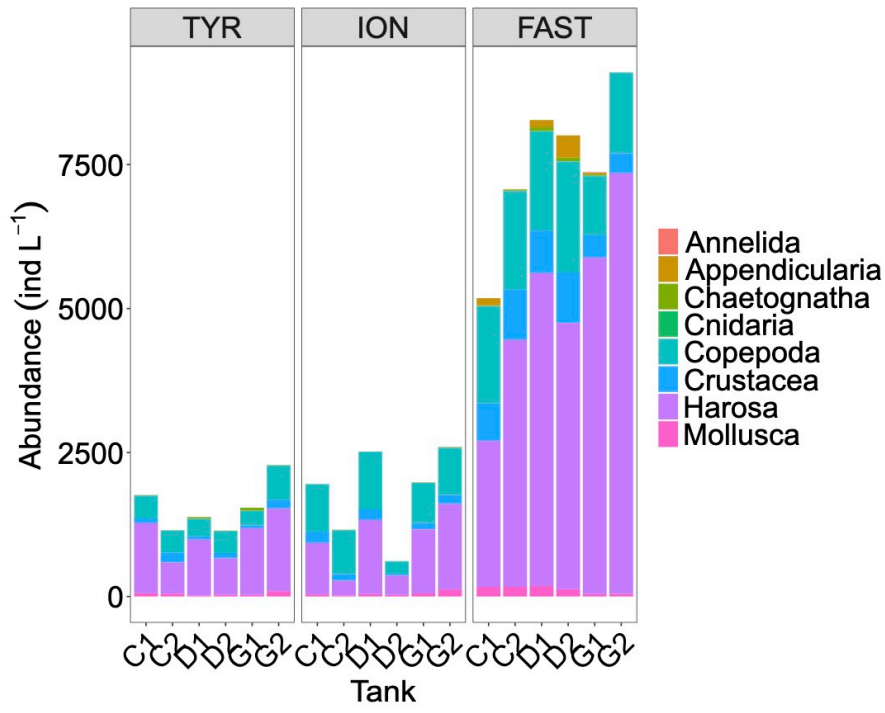
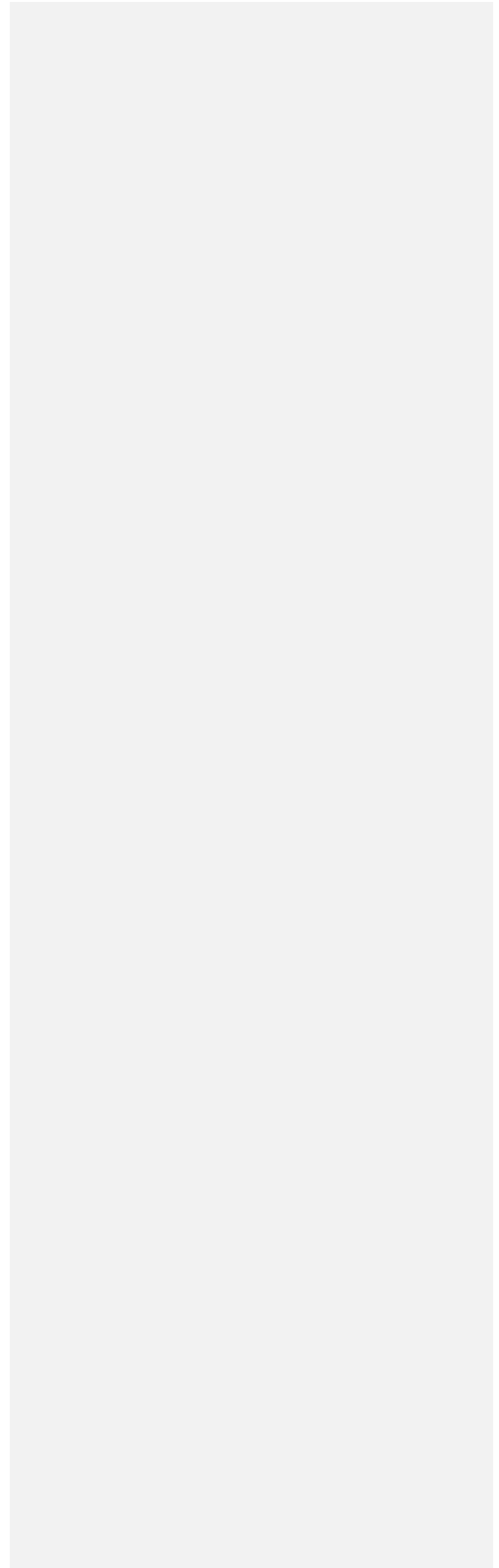


Fig. 9.



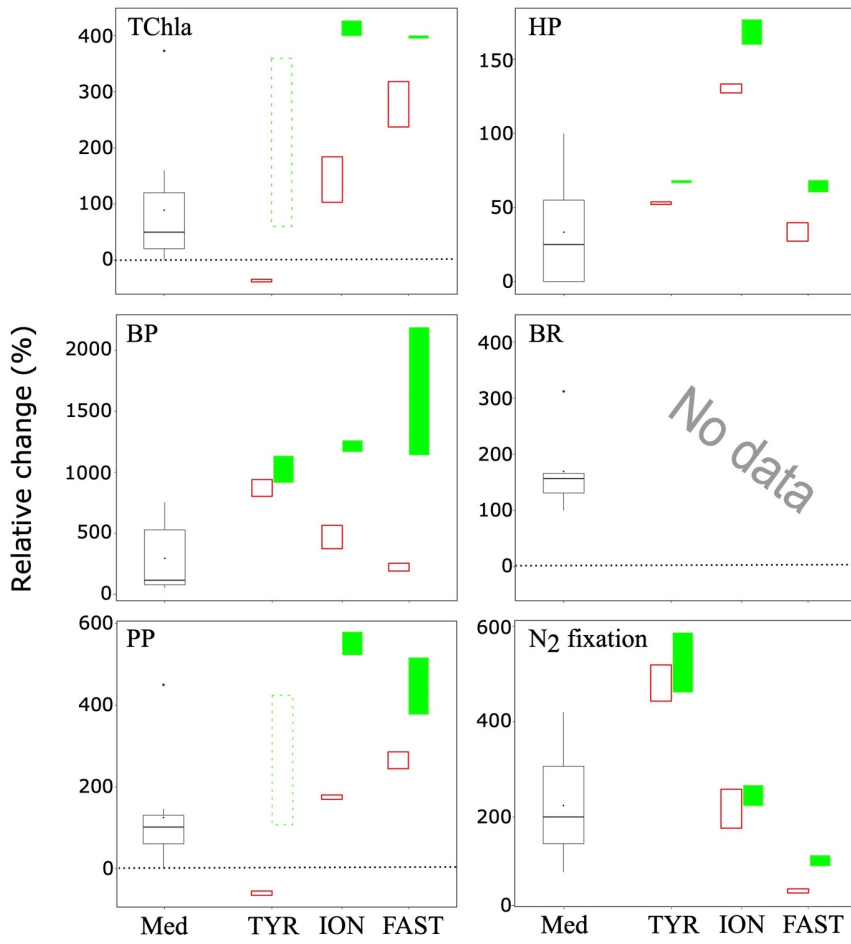


Fig. 10.



Page 26: [1] Formatted	Frederic GAZEAU	12/02/2021 11:57:00
English (US)		
Page 26: [1] Formatted	Frederic GAZEAU	12/02/2021 11:57:00
English (US)		
Page 26: [1] Formatted	Frederic GAZEAU	12/02/2021 11:57:00
English (US)		
Page 26: [1] Formatted	Frederic GAZEAU	12/02/2021 11:57:00
English (US)		
Page 26: [1] Formatted	Frederic GAZEAU	12/02/2021 11:57:00
English (US)		
Page 26: [2] Formatted	Frederic GAZEAU	12/02/2021 11:58:00
English (US)		
Page 26: [2] Formatted	Frederic GAZEAU	12/02/2021 11:58:00
English (US)		
Page 26: [2] Formatted	Frederic GAZEAU	12/02/2021 11:58:00
English (US)		
Page 26: [2] Formatted	Frederic GAZEAU	12/02/2021 11:58:00
English (US)		
Page 26: [2] Formatted	Frederic GAZEAU	12/02/2021 11:58:00
English (US)		
Page 26: [2] Formatted	Frederic GAZEAU	12/02/2021 11:58:00
English (US)		
Page 26: [3] Formatted	Frederic GAZEAU	12/02/2021 15:52:00
English (US)		
Page 26: [3] Formatted	Frederic GAZEAU	12/02/2021 15:52:00
English (US)		
Page 26: [4] Formatted	Frederic GAZEAU	11/02/2021 11:24:00
English (US)		
Page 26: [4] Formatted	Frederic GAZEAU	11/02/2021 11:24:00
English (US)		
Page 26: [5] Formatted	Frederic GAZEAU	11/02/2021 11:24:00
English (US)		
Page 26: [5] Formatted	Frederic GAZEAU	11/02/2021 11:24:00
English (US)		
Page 26: [6] Formatted	Frederic GAZEAU	11/02/2021 11:24:00
English (US)		
Page 26: [6] Formatted	Frederic GAZEAU	11/02/2021 11:24:00
English (US)		

▲ **Page 26: [6] Formatted** Frederic GAZEAU 11/02/2021 11:24:00  
English (US)

▲ **Page 26: [6] Formatted** Frederic GAZEAU 11/02/2021 11:24:00  
English (US)

▲ **Page 26: [6] Formatted** Frederic GAZEAU 11/02/2021 11:24:00  
English (US)

▲ **Page 26: [7] Deleted** Frederic GAZEAU 10/02/2021 14:33:00

▲ **Page 26: [8] Formatted** Frederic GAZEAU 12/02/2021 12:03:00  
English (US)

▲ **Page 26: [8] Formatted** Frederic GAZEAU 12/02/2021 12:03:00  
English (US)

▲ **Page 26: [8] Formatted** Frederic GAZEAU 12/02/2021 12:03:00  
English (US)

▲ **Page 26: [8] Formatted** Frederic GAZEAU 12/02/2021 12:03:00  
English (US)

▲ **Page 26: [8] Formatted** Frederic GAZEAU 12/02/2021 12:03:00  
English (US)

▲ **Page 26: [8] Formatted** Frederic GAZEAU 12/02/2021 12:03:00  
English (US)

▲ **Page 26: [8] Formatted** Frederic GAZEAU 12/02/2021 12:03:00  
English (US)

▲ **Page 26: [8] Formatted** Frederic GAZEAU 12/02/2021 12:03:00  
English (US)

▲ **Page 26: [8] Formatted** Frederic GAZEAU 12/02/2021 12:03:00  
English (US)

▲ **Page 26: [9] Deleted** Frederic GAZEAU 02/02/2021 12:10:00

▲ **Page 26: [10] Formatted** Frederic GAZEAU 11/02/2021 11:24:00  
Font colour: Text 1

▲ **Page 26: [10] Formatted** Frederic GAZEAU 11/02/2021 11:24:00  
Font colour: Text 1

▲ **Page 26: [10] Formatted** Frederic GAZEAU 11/02/2021 11:24:00  
Font colour: Text 1

▲ **Page 26: [10] Formatted** Frederic GAZEAU 11/02/2021 11:24:00  
Font colour: Text 1

▲ **Page 26: [11] Formatted** Frederic GAZEAU 11/02/2021 11:24:00

English (US)

▲ **Page 26: [11] Formatted** Frederic GAZEAU 11/02/2021 11:24:00

English (US)

▲ **Page 26: [12] Deleted** Frederic GAZEAU 10/02/2021 14:31:00

▼

▲

**Page 26: [12] Deleted** Frederic GAZEAU 10/02/2021 14:31:00

▼

▲

**Page 26: [13] Deleted** Frederic GAZEAU 11/02/2021 11:15:00

▼

▲

**Page 26: [13] Deleted** Frederic GAZEAU 11/02/2021 11:15:00

▼

▲

**Page 26: [13] Deleted** Frederic GAZEAU 11/02/2021 11:15:00

▼

▲

**Page 26: [14] Deleted** Frederic GAZEAU 11/02/2021 11:15:00

▼

▲

**Page 26: [15] Formatted** Frederic GAZEAU 11/02/2021 16:38:00

English (US)

▲ **Page 26: [15] Formatted** Frederic GAZEAU 11/02/2021 16:38:00

English (US)

▲ **Page 27: [16] Formatted** Frederic GAZEAU 10/02/2021 15:09:00

English (US)

▲ **Page 27: [17] Formatted** Frederic GAZEAU 10/02/2021 15:09:00

English (US)

▲ **Page 27: [18] Formatted** Frederic GAZEAU 12/02/2021 12:05:00

English (US)

▲ **Page 27: [19] Formatted** Frederic GAZEAU 12/02/2021 12:06:00

English (US)

▲ **Page 27: [20] Formatted** Frederic GAZEAU 12/02/2021 12:06:00

English (US)

▲ **Page 27: [21] Deleted** Frederic GAZEAU 12/02/2021 12:05:00

▼

▲

Page 27: [22] Formatted Frederic GAZEAU 12/02/2021 12:06:00  
English (US)

Page 27: [23] Formatted Frederic GAZEAU 03/02/2021 15:53:00  
English (US)

Page 27: [23] Formatted Frederic GAZEAU 03/02/2021 15:53:00  
English (US)

Page 27: [24] Deleted Frederic GAZEAU 03/02/2021 15:53:00

Page 27: [24] Deleted Frederic GAZEAU 03/02/2021 15:53:00

Page 27: [25] Formatted Frederic GAZEAU 03/02/2021 15:54:00  
English (US)

Page 27: [25] Formatted Frederic GAZEAU 03/02/2021 15:54:00  
English (US)

Page 27: [26] Deleted Frederic GAZEAU 03/02/2021 15:54:00

Page 27: [26] Deleted Frederic GAZEAU 03/02/2021 15:54:00

Page 27: [27] Formatted Frederic GAZEAU 10/02/2021 15:51:00  
English (US)

Page 27: [27] Formatted Frederic GAZEAU 10/02/2021 15:51:00  
English (US)

Page 27: [28] Formatted Frederic GAZEAU 10/02/2021 15:51:00  
English (US)

Page 27: [29] Deleted Frederic GAZEAU 10/02/2021 15:10:00

Page 27: [29] Deleted Frederic GAZEAU 10/02/2021 15:10:00

Page 27: [29] Deleted Frederic GAZEAU 10/02/2021 15:10:00

**Page 27: [30] Formatted**                      **Frederic GAZEAU**                      **10/02/2021 15:30:00**

English (US)

**Page 27: [31] Deleted**                      **Frederic GAZEAU**                      **10/02/2021 15:10:00**



**Page 27: [32] Formatted**                      **Frederic GAZEAU**                      **10/02/2021 15:31:00**

English (US)

**Page 27: [33] Formatted**                      **Frederic GAZEAU**                      **10/02/2021 15:11:00**

English (US)

**Page 27: [34] Formatted**                      **Frederic GAZEAU**                      **10/02/2021 15:11:00**

English (US)

**Page 27: [35] Deleted**                      **Frederic GAZEAU**                      **10/02/2021 15:11:00**



**Page 27: [35] Deleted**                      **Frederic GAZEAU**                      **10/02/2021 15:11:00**



**Page 27: [36] Formatted**                      **Frederic GAZEAU**                      **10/02/2021 15:35:00**

English (US)

**Page 27: [36] Formatted**                      **Frederic GAZEAU**                      **10/02/2021 15:35:00**

English (US)

**Page 27: [37] Formatted**                      **Frederic GAZEAU**                      **10/02/2021 15:35:00**

English (US)

**Page 27: [38] Deleted**                      **Frederic GAZEAU**                      **10/02/2021 15:35:00**



**Page 27: [38] Deleted**                      **Frederic GAZEAU**                      **10/02/2021 15:35:00**



**Page 27: [38] Deleted**                      **Frederic GAZEAU**                      **10/02/2021 15:35:00**



**Page 27: [39] Formatted**                      **Frederic GAZEAU**                      **12/02/2021 12:07:00**

English (US)

**Page 27: [39] Formatted**                      **Frederic GAZEAU**                      **12/02/2021 12:07:00**

English (US)

**Page 27: [39] Formatted**                      **Frederic GAZEAU**                      **12/02/2021 12:07:00**

English (US)

▲ **Page 27: [40] Formatted** Frederic GAZEAU 03/02/2021 15:58:00

English (US)

▲ **Page 27: [41] Deleted** Frederic GAZEAU 10/02/2021 15:36:00

▼

▲

**Page 27: [42] Formatted** Frederic GAZEAU 12/02/2021 09:33:00

English (US)

▲ **Page 27: [43] Formatted** Frederic GAZEAU 10/02/2021 15:37:00

English (US)

▲ **Page 27: [44] Formatted** Frederic GAZEAU 10/02/2021 15:17:00

English (US)

▲ **Page 27: [45] Deleted** Frederic GAZEAU 10/02/2021 15:37:00

▼

▲

**Page 27: [45] Deleted** Frederic GAZEAU 10/02/2021 15:37:00

▼

▲

**Page 27: [45] Deleted** Frederic GAZEAU 10/02/2021 15:37:00

▼

▲

**Page 27: [46] Formatted** Frederic GAZEAU 10/02/2021 15:16:00

English (US)

▲ **Page 27: [46] Formatted** Frederic GAZEAU 10/02/2021 15:16:00

English (US)

▲ **Page 27: [47] Deleted** Frederic GAZEAU 12/02/2021 12:07:00

▼

▲

**Page 27: [47] Deleted** Frederic GAZEAU 12/02/2021 12:07:00

▼

▲

**Page 27: [48] Formatted** Frederic GAZEAU 10/02/2021 15:15:00

English (US)

▲ **Page 27: [49] Formatted** Frederic GAZEAU 10/02/2021 15:52:00

English (US)

▲ **Page 28: [50] Formatted** Frederic GAZEAU 03/02/2021 16:02:00

English (US)

▲ **Page 28: [50] Formatted** Frederic GAZEAU 03/02/2021 16:02:00

English (US)

▲ **Page 28: [51] Deleted** Frederic GAZEAU 03/02/2021 16:09:00

▼ ▲ **Page 28: [51] Deleted** Frederic GAZEAU 03/02/2021 16:09:00

▲ **Page 28: [52] Formatted** Frederic GAZEAU 03/02/2021 16:08:00

English (US)

▲ **Page 28: [52] Formatted** Frederic GAZEAU 03/02/2021 16:08:00

English (US)

▲ **Page 28: [52] Formatted** Frederic GAZEAU 03/02/2021 16:08:00

English (US)

▲ **Page 28: [52] Formatted** Frederic GAZEAU 03/02/2021 16:08:00

English (US)

▲ **Page 28: [53] Deleted** Frederic GAZEAU 03/02/2021 16:10:00

▼ ▲ **Page 28: [53] Deleted** Frederic GAZEAU 03/02/2021 16:10:00

▲ **Page 28: [54] Deleted** Frederic GAZEAU 03/02/2021 16:11:00

▼ ▲ **Page 28: [54] Deleted** Frederic GAZEAU 03/02/2021 16:11:00

▲ **Page 28: [55] Deleted** Frederic GAZEAU 03/02/2021 16:11:00

▼ ▲ **Page 28: [55] Deleted** Frederic GAZEAU 03/02/2021 16:11:00

▲ **Page 28: [55] Deleted** Frederic GAZEAU 03/02/2021 16:11:00

▲  
**Page 28: [56] Formatted** Frederic GAZEAU 03/02/2021 16:11:00  
English (US)

▲  
**Page 28: [56] Formatted** Frederic GAZEAU 03/02/2021 16:11:00  
English (US)

▲  
**Page 28: [56] Formatted** Frederic GAZEAU 03/02/2021 16:11:00  
English (US)

▲  
**Page 28: [56] Formatted** Frederic GAZEAU 03/02/2021 16:11:00  
English (US)

▲  
**Page 28: [57] Deleted** Frederic GAZEAU 03/02/2021 16:12:00  
▼

▲  
**Page 28: [57] Deleted** Frederic GAZEAU 03/02/2021 16:12:00  
▼

▲  
**Page 28: [58] Formatted** Frederic GAZEAU 03/02/2021 16:12:00  
English (US)

▲  
**Page 28: [58] Formatted** Frederic GAZEAU 03/02/2021 16:12:00  
English (US)

▲  
**Page 28: [58] Formatted** Frederic GAZEAU 03/02/2021 16:12:00  
English (US)

▲  
**Page 28: [59] Formatted** Frederic GAZEAU 10/02/2021 17:04:00  
English (US), Not Highlight

▲  
**Page 28: [59] Formatted** Frederic GAZEAU 10/02/2021 17:04:00  
English (US), Not Highlight

▲  
**Page 28: [59] Formatted** Frederic GAZEAU 10/02/2021 17:04:00  
English (US), Not Highlight

▲  
**Page 29: [60] Formatted** Frederic GAZEAU 10/02/2021 18:13:00  
English (US)

▲  
**Page 29: [60] Formatted** Frederic GAZEAU 10/02/2021 18:13:00  
English (US)

▲  
**Page 29: [60] Formatted** Frederic GAZEAU 10/02/2021 18:13:00  
English (US)

▲  
**Page 29: [61] Deleted** Frederic GAZEAU 10/02/2021 17:08:00  
▼

▲  
**Page 29: [61] Deleted** Frederic GAZEAU 10/02/2021 17:08:00  
▼



▲ .....  
**Page 29: [61] Deleted**                      **Frederic GAZEAU**                      **10/02/2021 17:08:00**

▼ ..... ◀

▲ .....  
**Page 29: [62] Formatted**                      **Frederic GAZEAU**                      **10/02/2021 16:43:00**

English (US)

▲ .....  
**Page 29: [62] Formatted**                      **Frederic GAZEAU**                      **10/02/2021 16:43:00**

English (US)

▲ .....  
**Page 29: [63] Deleted**                      **Frederic GAZEAU**                      **10/02/2021 17:08:00**

▼ ..... ◀

▲ .....  
**Page 29: [63] Deleted**                      **Frederic GAZEAU**                      **10/02/2021 17:08:00**

▼ ..... ◀

▲ .....  
**Page 29: [64] Deleted**                      **Frederic GAZEAU**                      **10/02/2021 18:18:00**

▼ ..... ◀

▲ .....  
**Page 29: [64] Deleted**                      **Frederic GAZEAU**                      **10/02/2021 18:18:00**

▼ ..... ◀

▲ .....  
**Page 29: [65] Formatted**                      **Frederic GAZEAU**                      **10/02/2021 18:19:00**

English (US)

▲ .....  
**Page 29: [65] Formatted**                      **Frederic GAZEAU**                      **10/02/2021 18:19:00**

English (US)

▲ .....  
**Page 29: [66] Formatted**                      **Frederic GAZEAU**                      **10/02/2021 16:45:00**

English (US)

▲ .....  
**Page 29: [66] Formatted**                      **Frederic GAZEAU**                      **10/02/2021 16:45:00**

English (US)

▲ .....  
**Page 29: [67] Formatted**                      **Frederic GAZEAU**                      **10/02/2021 16:45:00**

English (US)

▲ .....  
**Page 29: [67] Formatted**                      **Frederic GAZEAU**                      **10/02/2021 16:45:00**

English (US)

▲ .....  
**Page 29: [68] Formatted**                      **Frederic GAZEAU**                      **10/02/2021 16:45:00**

English (US)

▲ .....  
**Page 29: [68] Formatted**                      **Frederic GAZEAU**                      **10/02/2021 16:45:00**

English (US)

▲ .....  
**Page 29: [69] Deleted**                      **Frederic GAZEAU**                      **10/02/2021 16:46:00**

▼ ..... ◀

▲ ..... ◀

<b>Page 29: [69] Deleted</b>	<b>Frederic GAZEAU</b>	<b>10/02/2021 16:46:00</b>
------------------------------	------------------------	----------------------------

▼ ..... ◀

▲ ..... ◀

<b>Page 29: [70] Formatted</b>	<b>Frederic GAZEAU</b>	<b>11/02/2021 17:06:00</b>
--------------------------------	------------------------	----------------------------

English (US)

▲ ..... ◀

<b>Page 29: [70] Formatted</b>	<b>Frederic GAZEAU</b>	<b>11/02/2021 17:06:00</b>
--------------------------------	------------------------	----------------------------

English (US)

▲ ..... ◀

<b>Page 29: [70] Formatted</b>	<b>Frederic GAZEAU</b>	<b>11/02/2021 17:06:00</b>
--------------------------------	------------------------	----------------------------

English (US)

▲ ..... ◀

<b>Page 29: [71] Formatted</b>	<b>Frederic GAZEAU</b>	<b>11/02/2021 11:41:00</b>
--------------------------------	------------------------	----------------------------

English (US), Not Highlight

▲ ..... ◀

<b>Page 29: [71] Formatted</b>	<b>Frederic GAZEAU</b>	<b>11/02/2021 11:41:00</b>
--------------------------------	------------------------	----------------------------

English (US), Not Highlight

▲ ..... ◀

<b>Page 29: [71] Formatted</b>	<b>Frederic GAZEAU</b>	<b>11/02/2021 11:41:00</b>
--------------------------------	------------------------	----------------------------

English (US), Not Highlight

▲ ..... ◀

<b>Page 29: [71] Formatted</b>	<b>Frederic GAZEAU</b>	<b>11/02/2021 11:41:00</b>
--------------------------------	------------------------	----------------------------

English (US), Not Highlight

▲ ..... ◀

<b>Page 29: [72] Deleted</b>	<b>Frederic GAZEAU</b>	<b>10/02/2021 17:11:00</b>
------------------------------	------------------------	----------------------------

▼ ..... ◀

▲ ..... ◀

<b>Page 29: [73] Deleted</b>	<b>Frederic GAZEAU</b>	<b>10/02/2021 17:13:00</b>
------------------------------	------------------------	----------------------------

▼ ..... ◀

▲ ..... ◀

<b>Page 29: [73] Deleted</b>	<b>Frederic GAZEAU</b>	<b>10/02/2021 17:13:00</b>
------------------------------	------------------------	----------------------------

▼ ..... ◀

▲ ..... ◀

<b>Page 29: [74] Deleted</b>	<b>Frederic GAZEAU</b>	<b>10/02/2021 17:22:00</b>
------------------------------	------------------------	----------------------------

▼ ..... ◀

▲ ..... ◀

<b>Page 31: [75] Deleted</b>	<b>Frederic GAZEAU</b>	<b>11/02/2021 15:20:00</b>
------------------------------	------------------------	----------------------------

▼ ..... ◀

▲ ..... ◀

<b>Page 33: [76] Deleted</b>	<b>Frederic GAZEAU</b>	<b>11/02/2021 15:41:00</b>
------------------------------	------------------------	----------------------------

<b>Page 33: [77] Formatted</b>	<b>Frederic GAZEAU</b>	<b>11/02/2021 16:10:00</b>
English (US)		
<b>Page 33: [78] Formatted</b>	<b>Frederic GAZEAU</b>	<b>11/02/2021 16:50:00</b>
Indent: First line: 0 cm		
<b>Page 33: [79] Deleted</b>	<b>Frederic GAZEAU</b>	<b>11/02/2021 16:50:00</b>
<b>Page 33: [80] Formatted</b>	<b>Frederic GAZEAU</b>	<b>11/02/2021 16:30:00</b>
English (US)		
<b>Page 33: [81] Formatted</b>	<b>Frederic GAZEAU</b>	<b>11/02/2021 16:32:00</b>
English (US)		
<b>Page 33: [82] Formatted</b>	<b>Frederic GAZEAU</b>	<b>17/02/2021 10:17:00</b>
English (US)		
<b>Page 58: [83] Formatted Table</b>	<b>Frederic GAZEAU</b>	<b>12/02/2021 17:11:00</b>
Formatted Table		
<b>Page 58: [84] Formatted</b>	<b>Frederic GAZEAU</b>	<b>12/02/2021 17:05:00</b>
French		
<b>Page 58: [85] Deleted</b>	<b>Frederic GAZEAU</b>	<b>12/02/2021 17:02:00</b>
<b>Page 58: [86] Deleted</b>	<b>Frederic GAZEAU</b>	<b>12/02/2021 16:56:00</b>
<b>Page 58: [87] Formatted</b>	<b>Frederic GAZEAU</b>	<b>12/02/2021 16:56:00</b>
French		
<b>Page 58: [88] Formatted</b>	<b>Frederic GAZEAU</b>	<b>15/02/2021 14:01:00</b>
English (US)		
<b>Page 58: [89] Formatted</b>	<b>Frederic GAZEAU</b>	<b>12/02/2021 17:05:00</b>
Centred		
<b>Page 58: [90] Formatted</b>	<b>Frederic GAZEAU</b>	<b>15/02/2021 14:02:00</b>
English (US), Superscript		
<b>Page 58: [91] Formatted</b>	<b>Frederic GAZEAU</b>	<b>15/02/2021 14:01:00</b>
English (US)		
<b>Page 58: [92] Formatted</b>	<b>Frederic GAZEAU</b>	<b>15/02/2021 14:01:00</b>
Font colour: Text 1		
<b>Page 58: [93] Formatted</b>	<b>Frederic GAZEAU</b>	<b>12/02/2021 16:51:00</b>
Font colour: Text 1		
<b>Page 58: [94] Formatted</b>	<b>Frederic GAZEAU</b>	<b>12/02/2021 16:51:00</b>
Centred		
<b>Page 58: [95] Formatted</b>	<b>Frederic GAZEAU</b>	<b>12/02/2021 16:51:00</b>
Font colour: Text 1, French		
<b>Page 58: [96] Formatted</b>	<b>Frederic GAZEAU</b>	<b>12/02/2021 17:05:00</b>
Centred		

<b>Page 58: [97] Formatted</b>	<b>Frederic GAZEAU</b>	<b>12/02/2021 16:51:00</b>
--------------------------------	------------------------	----------------------------

Font colour: Text 1, French

<b>Page 58: [98] Formatted</b>	<b>Frederic GAZEAU</b>	<b>12/02/2021 16:51:00</b>
--------------------------------	------------------------	----------------------------

Centred

<b>Page 58: [99] Formatted</b>	<b>Frederic GAZEAU</b>	<b>12/02/2021 16:51:00</b>
--------------------------------	------------------------	----------------------------

Font colour: Text 1, French